New Approaches to Composite Reliability Assessment of Smart Power Systems

by

Badr Lami

A thesis
presented to the University of Waterloo
in fulfillment of the
thesis requirement for the degree of
Doctor of Philosophy
in
Electrical and Computer Engineering

Waterloo, Ontario, Canada, 2017

Examining Committee Membership

The following served on the Examining Committee for this thesis. The decision of the Examining Committee is by majority vote.

External Examiner	Xiao-Ping Zhang Professor
Supervisor	Kankar Bhattacharya Professor
Internal Member	Guang Gong Professor
Internal Member	Ramadan El-Shatshat Lecturer
Internal-external Member	Kaamran Raahemifar Professor

Author's Declaration

I hereby declare that I am the sole author of this thesis. This is a true copy of the thesis, including any required final revisions, as accepted by my examiners.

I understand that my thesis may be made electronically available to the public.

Abstract

Electric power networks are complex systems because of their geographic spread and the consequent need for interconnections and integration of different components such as generators, transformers, lines, reactors, relays, and loads. Therefore, power utilities seek to ensure an acceptable degree of reliability in planning and operations, and accordingly, need information on component outages while satisfying the growing demand in order to ensure the availability of the system and prevent downtimes. Power systems of today are facing major challenges because of the rapid increase in penetration of energy resources (ERs) and plug-in electric vehicles (PEV).

This thesis focuses on the evaluation of composite system reliability using direct probabilistic analysis techniques. The research presents the mathematical foundations, evaluation procedures, and reliability and risk indices associated with composite power system reliability evaluation using the minimal cut set calculations. The concept of minimal cut sets is applied to evaluate two sets of reliability and risk indices, system indices and nodal indices. System indices are essential for system planners and operators to determine the likelihood of interruption of supply, while nodal indices provide useful information on significant load points. The performance of the system under outage condition of generators, transmission lines, or both, is examined by conducting an appropriate power flow study. An optimal power flow (OPF) model is solved to find the system and nodal minimal cut sets and the associated indices.

The thesis presents a novel composite system reliability based planning for ERs with clustering techniques based approaches to determine the optimal location, size and year of installation of ERs in the system. The K-means clustering and Fuzzy C-means clustering techniques are applied to the set of reliability indices, Load Not Served per Interruption (LNSI), which are determined using nodal minimal cut sets. The nodal minimal cut sets are obtained using an OPF based approach. Once the optimal sizes and locations of ERs

are obtained, the earliest year of their penetration into the system is determined using an adequacy check algorithm.

The thesis further presents a novel method to detect the critical components of composite power systems under steady-state conditions and short-term operations in order to help planners make economic decisions on new investments in generation capacities and transmission lines upgrades, and also to help operators maintain the delivery of electricity during system failure and disturbance events. Each component is ranked based on minimal cut set outage probability and the consequent loss of load arising from the outages of components belonging to a minimal cut set.

Finally, the thesis presents a novel framework to evaluate the impact of PEV charging loads on composite power system reliability. A Smart-OPF model combined with a minimum cut set approach is proposed to evaluate the system reliability indices. Demand response (DR) is included in the proposed procedure and its impact on system reliability indices is studied. The procedure to determine the critical components of the power system in the presence of PEV loads and DR is also proposed.

Acknowledgements

First and foremost, all praises to Allah the Almighty for His blessing in completing this thesis.

Then I would like to express my sincere gratitude to my supervisor Professor Kankar Bhattacharya for his guidance, encouragement, support and patience throughout my PhD studies. It was my privilege to complete my studies under his supervision.

I would like to acknowledge my PhD committee members for their valuable support: Professor Xiao-Ping Zhang from the Department of Electronic, Electrical and Systems Engineering, University of Birmingham, United Kingdom; Professor Kaamran Raahemifar from the Department of Electrical and Computer Engineering, Ryerson University, Canada; Professor Guang Gong and Dr. Ramadan El-Shatshat from the Department of Electrical and Computer Engineering, University of Waterloo.

I gratefully acknowledge the Saudi Arabian Ministry of Higher Education represented by Taibah University, Medina, Saudi Arabia for sponsoring my studies and providing the funding necessary to carry out this research.

Finally, I would like to thank my family and friends for their support and love.

Dedication

TO MY DEAR PARENTS

My Lord! Have mercy upon them, as they cherished me when I was little and as they still care for me when I am grown up.

Table of Contents

List of Tables

List of Figures

List of Abbreviations

AER	All Electric Range
ARMA	Auto Regression Moving Average
BEV	Battery Electric Vehicle
CR	Criticality Index
DG	Distributed Generation
DOD	Depth of Discharge
DR	Demand Response
DSM	Demand-Side Management
ECLL	Expected Cost of Load Loss
EDNS	Expected Demand Not Supplied
EENS	Expected Energy Not Supplied
ER	Energy Resource
EV	Electric Vehicle
FOR	Forced Outage Rate
HEV	Hybrid Electric Vehicles
HL	Hierarchical Level
LNSI	Load Not Supplied per Interruption
LOLE	Loss of Load Expectation
LOLP	Loss of Load Probability
ME	Means Vector
MTTF	Mean Time to Failure
MTTR	Mean Time to Repair
NERC	North American Electric Reliability Corporation

OMS	Outage Management System
OPF	Optimal Power Flow
PEV	Plug-in Electric Vehicle
PHEV	Plug-in Hybrid Electric Vehicle
RBTS	Roy Billinton Test System
RTS	Reliability Test System
SOC	State of Charge
SSF	Sum of Squares Function
TOU	Time of Use
WCSSE	Within Cluster Sum of Squared Error

Nomenclature

A. Indices and Sets

a	Cluster
h, l, m, w	Member of cut set
c	Index for PEV class
C_h	Cut set h
cl	Index for charging level
cm	Component of a power system
hr	Hour
i, j	Bus
K, C	Number of clusters
N	Number of buses
NG	Number of generator buses
NL	Number of load buses
M	Order of minimal cut set
TY	Terminal year

B. Parameters

AER	All electric range, km
B^{Cap}	Battery capacity, p.u.
B_{UP}, B_{DN}	Maximum upward or downward shiftable demand, p.u.
$\bar{C}_h$	Minimal cut set
$(\bar{C}_h)_{cm}$	Component cm associated to $\bar{C}_h$

$(\bar{C}_h)_i$	Nodal minimal cut set
CR_{cm}	Component cm criticality index, p.u.
CR^t_{cm}	Component cm criticality index at time t, p.u.
D^{km}	Mileage driven data, km
DOD	Depth of discharge of a PEV, p.u.
E_c	Average energy needed to charge PEVs of class c, p.u.
$EDNS$	Expected Demand Not Supplied, p.u.
$EDNS^t_{a,i}$	Expected Demand Not Supplied of cluster a, at bus i, at time t, p.u.
$EENS$	Expected Energy Not Supplied, p.u./day
f_{cm}	Frequency of occurrence of component cm in minimal cut sets
G_{ij}	Conductance of line i-j, p.u.
$LNSI_{\bar{C}_h}$	Load Not Supplied per Interruption when cut set $\bar{C}_h$ causes a system failure, p.u.
$LNSI_{\bar{C}_h,cm}$	Load Not Supplied per Interruption, with cm on outage, when cut set $\bar{C}_h$ causes a system failure, p.u.
$LNSI_{\bar{C}_h,i}$	Load Not Supplied per Interruption at bus i when cut set $\bar{C}_h$ causes a system failure, p.u.
$LNSI^{(a)}_{\bar{C}_h,i}$	Load Not Supplied per Interruption of cluster a, at bus i when cut set $\bar{C}_h$ causes a system failure, p.u.
$LOLE$	Loss of Load Expectation, hour/day
$LOLP_i$	Nodal Loss of Load Probability
$LOLP_{Sys}$	System Loss of Load Probability
me^t_a	The mean value of cluster a at time t
$N^{EV}_{i,c,cl}$	Number of PEVs at bus i of class c and charging level cl
$p(\bar{C}_h)$	Probability of failure of $\bar{C}_h$
P_{cl}	Power drawn by PEV at given charging level
p^t_{cm}	Probability of failure of component cm, at time t
p^t_i	Probability of load not served at bus i, at time t
p^t_{sys}	Probability of system failure at time t

p_{ER}^{st}	Probability of failure of an ER to start up
$p(\bar{C}_h)^t$	Probability of failure of cut set $\bar{C}_h$ at time t
$p(\bar{C}_h)_i^t$	Probability of failure of cut set $\bar{C}_h$, at bus i, at time t
$p(\bar{C}_h)_{cm}^t$	Probability of failure of cut set $\bar{C}_h$, at time t, with cm on outage
$[p(\bar{C}_h)_i^t]^{(a)}$	Probability of failure of cut set $\bar{C}_h$, at cluster a, at bus i, at time t
$P_{ER_i}^{Min}, P_{ER_i}^{Max}$	Lower and upper limit of real power from ER at bus i, p.u.
$P_{i,hr}^{PEV\_Unc}$	Uncontrolled charging demand at hour hr and bus i, p.u.
P_{Loss}	Real power loss, p.u.
Pd_i, Qd_i	Real and reactive power demand at bus i, p.u.
$Pd_{i,hr}, Qd_{i,hr}$	Real and reactive power demand at bus i and hour hr, p.u.
${Pg_i}^{Min}, {Pg_i}^{Max}$	Lower and upper limit of active power generation, p.u.
$Pg_{i,hr}^{Min}, Pg_{i,hr}^{Max}$	Lower and upper limit of active power generation from generator, p.u.
$Q_{ER_i}^{Min}, Q_{ER_i}^{Max}$	Lower and upper limit of reactive power from ER at bus i, p.u.
Qg_i^{Min}, Qg_i^{Max}	Lower and upper limit of reactive power from generator i, p.u.
$Qg_{i,hr}^{Min}, Qg_{i,hr}^{Max}$	Lower and upper limit of reactive power from generator, p.u.
S_{ij}^{Max}	Maximum capacity of line i-j, p.u.
SOC	State of charge, p.u.
t	Outage time, hour
t_{in}	ER response time, hour
T	Lead time, hour
T^D	Charging duration of a PEV, hour
V_i^{Min}, V_i^{Max}	Lower and upper limits of voltage magnitude at bus i, p.u.
$V_{i,hr}^{Min}, V_{i,hr}^{Max}$	Lower and upper limits of voltage magnitude at bus i, p.u.
Y_{ij}	Magnitude of bus admittance matrix element i-j, p.u.
β	Share of PEV fleet using smart charging, %
λ_{cm}	Failure rate of component cm, yr^{-1}
μ_{cm}	Repair rate of component cm, yr^{-1}
η	Charging efficiency, %

γ	Charging delay, hour
δ_i	Voltage angle at bus i, rad
θ_{ij}	Angle of bus admittance element i-j, rad

C. Variables

J, J_1, J_2	Objective functions
$P^{EV\_S}_{i,hr,c,cl}$	Smart charging demand by PEV of class c and level cl at bus i and hour hr, p.u.
P_{ER_i}, Q_{ER_i}	Real and reactive power from ER at bus i, p.u.
Pg_i, Qg_i	Real and reactive power generation at bus i, p.u.
$Pd^{UNM}_{i,hr}$	Real power load curtailment at bus i, p.u.
$Qd^{UNM}_{i,hr}$	Reactive power relief at bus i associated with real power interruption, p.u.
$\Delta PD^{UP}_{i,hr}$	Upward load DR at bus i and hour hr, p.u.
$\Delta PD^{DN}_{i,hr}$	Downward load DR at bus i and hour hr, p.u.
S_{ij}	Complex power on line i-j, p.u.
V_i	Voltage magnitude at bus i, p.u.

Chapter 1

Introduction

1.1 Motivation

Electric power systems can be very complex due to their geographic spread and the consequent need for interconnections, and integration of different components such as transformers, transmission lines, cables, generators, and loads. The electricity grid is designed and operated to withstand any single and double contingencies by its protection and control system [1]. Therefore, power utilities seek to ensure an acceptable degree of system reliability in the planning and operation of their systems. The power system, however, is often subjected to abnormal effects, such as weather conditions, animals, human errors, overload, and ageing, that can cause failure of a component.

Table 1.1 presents a fourteen-year historical outage statistics based on an eastern U.S. utility's Outage Management System (OMS) Report for some causes that led components to fail [2]. Power system planners and operators need to carry out reliability analysis considering component outage and repair rates in order to ensure system availability and prevent downtimes. Therefore, maintaining continuity and quality of supply, plays an important role in power systems design and operation.

In recent years, energy resources (ER), demand response (DR), and plug-in electric vehicles (PEV) are receiving considerable interest in the context of smart grids, and are

Table 1.1: Failure Cause Statistics [2]

	Overall System	Transmission system	Distribution System		
			Overall System	Overhead System	Underground System
Animal	40	3	37	35	2
Tree Contact	8260	29	8231	8224	7
Overload	14	2	12	11	1
Work Error	6	0	6	6	0
Equipment Failure	1472	23	1449	1312	137
Lightning	2845	147	2968	2575	123
Accident	140	19	121	89	32
Prearranged	7	1	6	4	2
Customer Problem	122	9	113	109	4
Other	355	10	345	330	15
Total Number of Outages	13261	243	13288	12695	323

expected to play a significant role in system reliability, in the future. Therefore, it becomes extremely important to develop tools that consider these options and can evaluate and ensure the required degree of system reliability and continuity of service.

With the ever increasing demand for electricity, system planners are faced with a difficult task of identifying the exact size, location and year when ERs may be allowed to penetrate the system over a planning horizon. Because of the multitudes of complex factors influencing the decisions, it would be pertinent to adopt a top-down approach, where system reliability is considered as the primary determinant to identify the appropriate sites, sizes and years when ERs can be deployed.

ERs have gained attention as a practical option that can significantly improve the power system operation and system reliability without introducing undesirable effects on the environment. ERs also contribute to reducing transmission and distribution congestion, provide spinning reserves, assist in demand-supply balance provisions, and reduce the need for additional system generation, transmission and distribution capacity. The system and nodal reliability indices can be improved by proper siting and sizing of ERs. There is a need to investigate the impact of ERs on power system reliability and risk by identifying the buses that suffer the highest loss of load. Clustering algorithms are unsupervised learning

methods which structure a group of unclassified data with similar characteristics. There methods can be applied on the data set of nodal reliability indices to arrive at the optimal sizing and siting of ERs.

Identifying critical components in power systems play an important role in enhancing the system reliability and reducing investment costs. Although over-investments in the power sector can improve the system reliability, it often leads to high operational costs. On the other hand, under-investments can lead to high maintenance costs in addition to increasing the risk of power system outages and failures. Therefore, power system planners and operators need a systematic method to identify the components, such as generators, lines, transformers, *etc.*, that are critical to the system, and target their investment plans accordingly, instead of undertaking investments in a general manner.

The purchase of PEVs is rapidly increasing, thanks to the incentives offered by various governments and the growing awareness of the contribution of PEVs to emissions reduction from the transport sector. As of 2017, there are more than 28,000 PEVs on the road in Canada, and counting [3]. With the complex charging behaviour of PEVs and the tendency of charging loads to cluster within certain neighbourhoods or to occur at the same time during the day, the electricity grid can be at risk, and need be investigated, given that the grids are not inherently designed to accommodate PEV charging loads. Therefore, it is necessary to accurately assess and quantify the impact of PEV charging loads on system reliability in order to decide on the right actions such as developing the associated infrastructure, upgrading the local equipment, and developing an appropriate scheduling model that coordinates the charging of PEVs.

1.2 Literature Review

1.2.1 Impact of ERs on Power System Reliability

Power system planners and operators need information on component outages and repair rates in order to ensure the availability of the system and prevent downtimes. Maintaining

the continuity and quality of supply plays an important role in power system design and operation. For decades, heuristic methods based on experimentation and rule-of-thumb method were used in determining the reliability of power systems.

The concept of nodal minimal cut sets is proposed in [4] to understand the reliability of serving customers at a specific load bus. The outage states of generators, transmission lines, or both, are considered within a dc optimal power flow (OPF) model to determine the minimal cut sets. Thereafter, Markov process is applied to the components of the determined minimal cut sets instead of the entire system. In [5], a Markov cut set method is developed to evaluate the reliability of a simple system comprising five components, where the minimal cut sets are determined by using enumeration technique and connectivity analysis. The methodology aims to evaluate the impact of failures from generation and transmission systems on the distribution systems.

In [6], a random fuzzy model is presented to evaluate the failure probability of system components due to weather, environment and other operating conditions. A system operational risk assessment method based on credibility theory is developed to accommodate the two-fold uncertainty combining randomness and fuzziness in power system operations.

In [7], a combined fuzzy and probabilistic method is developed to calculate system risk indices considering system component outage and load uncertainties. The fuzzy membership functions of system component outages are developed using statistical records whereas the system load is modeled using the hybrid method of fuzzy set and Monte Carlo simulation.

In [8], several aspects of operational risk assessment of transmission systems are discussed. The operational risk during different timelines of adverse weather condition is estimated once the component failure rates are calculated. The effect of weather parameters on the momentary failure rate and operational risk is discussed.

In [9], a methodology using particle swarm optimization and genetic algorithm-based optimization techniques is developed for autonomous microgrids to determine the optimal sizing and siting of distributed generation (DG) units. Ranking the candidate buses for DGs is carried out based on maximum loading limits, without causing voltage violations,

to identify the optimal sites.

A dynamic programming based method is used to determine the optimal location and size of ERs in [10]. The method considers the energy index of reliability in designing microgrids to determine the optimal mix of resource types such as micro-turbines, solar PVs and battery storages to satisfy electrical and thermal loads. The energy index reflects the transmission adequacy of the system by considering transmission capacities, time varying loads, and time varying capacities of the ERs.

The impact of ERs on distribution system reliability is discussed in [11]. A method based on minimal cut sets and chronological Monte Carlo simulation is proposed to assess the capacity transferred to other feeders and hence the impact on reliability indices of load points taking into account DG penetrations.

The effect of natural disasters on microgrids is discussed in [12] wherein different microgrid models and two aspects that can affect their availability during natural disasters, the lifeline performance and local energy storage, are studied. The availability of microgrid components such as micro-turbines, engine generators, DGs, converters, *etc.*, are determined using Markov state-space models via minimal cut set approximations.

In [13], a comprehensive evaluation model of reliability and cost for small isolated systems containing renewable energy sources is presented. Simulation models are used to generate reasonable atmospheric data, evaluate chronological renewable power outputs and combine total energy and load to provide useful system indices.

In [12] different ER models study the effect of natural disasters on microgrid availability. A method based on Markov state-space models is used to calculate the system availability via minimal cut set approximations. In [14], a methodology based on the concept of chronological power flow and a set of performance indices that minimize wind energy spillage is used to determine the network reinforcements and possible integration of ERs. In the same context, an iterative method based on the analysis of power flow continuation is presented in [15] to determine the most sensitive buses to voltage collapse for optimally allocating ERs. The work in [16] presents an optimization model to determine the optimal set of decisions including siting, sizing, and time of investment for solar PV based ERs.

The optimization model helps investors in their decision making by maximizing the net present value of the profit. In [17], an expansion planning model is presented to optimally design incentive rates for renewable ERs integration, and simultaneously considering sizing, siting, and timing of new ER capacities to achieve a target renewable penetration level.

However, the ER planning models proposed in [12, 14–17] do not explicitly consider reliability aspects, nor the uncertainty of outages of generation and transmission lines. In [18], reliability is included in a stochastic programming model as an Expected Cost of Load Loss (ECLL) for planning of multi-area power generation and transmission system. The ECLL is approximated by considering only sample scenarios and then evaluated in the optimization problem. In [19], a multi-area reliability-planning model is proposed, based on convolution technique, to include generation Loss of Load Probability (LOLP), expected unserved energy and covering the entire set of possible outage events. In [20], the generation expansion planning problem takes into account the cost of Expected Energy Not Supplied (EENS) to determine the optimal number of generators and their locations in order to improve power system reliability. In [21], an OPF based technique is proposed to evaluate the maximum feasible load levels and hence the load point reliabilities considering the effect of ERs. The work in [22] studies the reliability level at each load bus resulting from optimal generation planning. A stochastic programming with sample-average approximation technique is proposed for the optimal placement incorporating some reliability indices such as expected unserved energy and expected power loss.

In order to determine the candidate locations for ER installation, it is important to understand how the resource will impact the adequacy of the location. Nodal adequacy indices, such as Load Not Supplied per Interruption (LNSI) and Expected Demand Not Supplied (EDNS) have been developed for this purpose [23]. The concept of nodal minimal cut sets, proposed in [4], and calculated using a dc-OPF, helps understand the reliability of serving customers at a load bus. In [11] the minimal cut sets are determined using an enumeration technique and connectivity analysis. However, for a better understanding of the adequacy needs at a location, it is important to consider both the active and reactive power balance and voltage related factors. Thus a dc optimal power flow may not be sufficient and there is a need for a full ac OPF based method to determine the nodal

minimal cut sets.

A simplified method for reliability evaluation of power systems with wind generation is presented in [24]. A wind speed model for different locations is developed first, then the method is simplified by determining the minimum multi-state representation of a wind farm model in reliability evaluation. The method requires historical wind speed data over many years, in order to determine the necessary parameters of the wind speed models for a specific wind farm location.

1.2.2 Critical Components

Power systems comprise generators, transformers, transmission lines, busses, and loads. These components are scattered to cover a large geographical area; together, they are built to maintain the continuity of generation, transmission, and consumption of energy. In abnormal operating conditions, such as severe weather, component breakdown, human error, *etc.*, the overall system may be affected, if an action is not taking. Therefore, power system components should be prioritized as to which component outage may contribute more to the violation of system stability or loading limits. Detecting critical components can help system planners to make economic decisions on new investments in generation capacities and transmission lines upgrades, also this information can help operators maintain the delivery of electricity during system failure and disturbance events.

One of the indices used to measure the importance or criticality of a system component is the traditional sensitivity analysis based Birnbaum's measure, first introduced in 1969 [25]. It basically measures the maximum loss of the system when a component fails. Mathematically, it is the partial derivative of system reliability at a specific time with respect to failure rate of a component. In [26, 27], *reliability importance indices* of power system components have been studied, where the classical component *reliability importance indices*, such as the Birnbaum's and Fussell-Vesely's measure, are presented and compared to indices that identify components as critical with respect to their impact on system interruption cost.

In [28], a method for quantifying and ranking of power system components with respect to the system security margin, loss of load, and loss of energy, is presented. The method is based on simulating outage events which causes the system to fail, and hence identifying components associated with the interruptions. Different criticality indices are proposed and assigned to each component based on their risk to power system security margin.

Reliability importance measures are applied to bulk power systems to mainly identify weak-links [29]. The proposed measures are extended from popular importance measures, such as Birnbaum, Fussell-Vesely, and Reliability Achievement Worth (RAW) measures to make them compatible with electricity transmission systems. The work in [29] is based on minimal cut sets pertaining to components outage rates and repair rates, instead of the probability of failure for a specified time interval.

In [30], an *importance index* for power system generators is proposed adopting the concept of game theory, namely Shapely Value Criterion. The proposed methodology aims to prioritize generation units based on their failure impacts on bulk power system reliability. The reliability index is first calculated by multiplying the probability and consequence of a generator outage occurrence that result from Monte Carlo simulations and state enumeration, respectively. After that, the cost due to a generator outage is calculated using the concept of Shapley Value where each generator's contribution to the total cost of an outage is used as an *importance index*.

In [31], the importance of components of a power substation such as bars, cables, switches, transformers, and disconnector, is evaluated using time sequential Monte Carlo simulation which is based on the mean time to failure (MTTF) and mean time to repair (MTTR) parameters. The calculated indices rank the components in terms of which the component failure causes a system failure, as well as, which component ensures a better system reliability.

1.2.3 Impact of PEV Loads

Electrification of transportation is gaining trust nowadays as an alternative to the conventional internal combustion engine (ICE) based vehicles. This transition will undoubtedly

impact power systems in various aspects from increasing the system peak load, increasing losses, and deterioration in voltage profile, to weakening the system reliability, despite their numerous benefits such as reducing CO_2 emissions and lowering transport costs. Numerous studies have investigated the impact of PEVs on power systems, from different perspectives.

In the context of distribution systems, a condition-dependent outage model is used in [32] to determine the outage rate of transformers, which is then included in system adequacy assessment considering PEV charging loads. A PEV smart charging strategy to enhance the distribution adequacy while minimizing cost is hence proposed.

The impact of residential electric vehicle (EV) charging on distribution system voltages, taking into account different factors such as EV load location, size, and percentage of penetration, is presented in [33]. An optimization based model using dynamic programming successive approximation method is carried out for each vehicle charging profile. It is noted that the voltage drops decrease when the EV loads are closer to the service transformer, decrease when the size of EV chargers are doubled, and increase at the secondary customer locations when the penetration of EV is increased.

At the generation level, the impact of PEV charging demand on generation adequacy is studied in [34] and [35] considering a coordinated bidirectional charging power control in grid-to-vehicle (G2V) and vehicle-to-grid (V2G) modes. These studies conclude that the risk of integration of PEVs to power systems can be reduced by charging power control within the control capability of vehicles. It is noted that considering the EVs as conventional load only may have a severe impact on power system reliability.

In [36], a stochastic unit commitment model is used to study the impact of PEVs on power system operation and scheduling. The proposed model considers coordination of thermal generators, wind generations, PEV charging loads, and ancillary services provided by V2G modes. It is noted that smart charging PEV loads can reduce the operating cost of the power system and compensate for the fluctuations in wind generation.

From the composite power system point of view, the reliability of an EV integrated system in the battery exchange mode is studied in [37]. It is noted that the investment

in battery exchange stations and its charging and discharging strategies should be coordinated to achieve improved reliability performances of the system. The proposed method uses information on travel and refuelling pattern data, adopted from the (U.S) National Households Travel Survey (NHTS) [38] and the General Motor Refueling Pattern Survey [39], respectively.

In [40], a Monte Carlo simulation based approach is presented to determine the reliability of composite power systems in the presence of PEV loads, but only considering uncontrolled charging of the EVs. It is noted that the system LOLP is not significantly affected when considering transmission lines outages. However, the penetration of PEVs, even at nominal load levels, negativity impacts the system reliability, although smart charging impacts are not investigated.

In [41], several optimization models that minimize reliability indices, such as loss of load expectation (LOLE) and EENS, in the presence of EVs are presented. Monte Carlo simulation is carried out to produce sets of driving patterns and energy consumption data that are applied in the optimization models. The work concludes that choosing a proper charging/discharging strategy of EVs can improve system reliability, as well as EVs can efficiently provide some system reserve.

1.3 Research Objectives

The main objectives of the research presented in this thesis are as follows:

- Develop a mathematical optimization model for composite power system planning to identify the optimal site, size and year of installation of ERs. A reliability analysis based framework will be proposed to obtain the *nodal minimal cut sets* and the respective nodal adequacy indices, LNSIs. The nodal LNSI indices with their outage probabilities need be clustered using the principle of classical K-means and Fuzzy C-means clustering techniques, and the EDNS for each cluster will be obtained, based on which the sizing and siting of ERs will be determined. Finally, an adequacy check

algorithm to determine the earliest year of penetration of ERs will be applied to maintain the system adequacy constraints.

- Develop an OPF based procedure combined with determining the *system minimum cut sets* to identify the *critical components* in composite power systems, under steady-state conditions and short-term operations. The objective is to rank each component based on the minimal cut set outage probability and the consequent loss of load arising from outages of components belonging to a minimal cut set.

- Examine the impact of uncontrolled *vis-à-vis* smart charging PEV loads on composite power systems reliability, by developing a Smart-OPF model to determine the system minimal cut sets, and hence the system reliability indices, taking into account various degrees of smart charging penetration. The uncontrolled PEV charging load profile at the system buses will be obtained using a data analysis technique with real mobility data. Thereafter, the contribution of DR on damping the adverse impact of PEV charging loads on system reliability will be investigated, and the critical components of the system in the presence of PEV charging loads will be determined.

1.4 Outline of Thesis

The remainder of this thesis is organized as follows. Chapter 2 reviews the background on power system reliability, presents some basic definitions and basic approaches used in power system reliability analysis. The definitions and applications of ERs, DR, and PEVs are discussed. A brief background to clustering techniques is also presented. Chapter 3 presents a novel clustering technique based approach to determine the optimal location and size of ERs in power systems. Systematic approaches to apply the K-means and Fuzzy C-means clustering techniques on a set of reliability indices, which are determined using the *nodal minimal cut sets*, are presented to determine the location and size of ERs. Finally, using an adequacy check algorithm, the earliest year of penetration of each ER is obtained. Chapter 4 presents an OPF based method to determine the *system minimal cut sets* of a composite power system and hence identify the *critical components* of the system.

This chapter focuses on the evaluation of composite system reliability under steady state conditions, and assessing operational risks in real-time system operations. Each component is ranked based on minimal cut set outage probability and the consequent loss of load arising from outages of components belonging to a minimal cut set. Chapter 5 presents a novel Smart-OPF model combined with a minimum cut set approach to evaluate the impact of PEV charging loads on composite power system reliability. Thereafter, DR is included in the proposed procedure and its impact on system reliability indices is studied. Ranking of components by their criticality in the presence of PEV charging loads and DR is also presented. Finally, Chapter 6 presents the main conclusions and contributions of this thesis, and identifies some directions for future research work.

Chapter 2

Background

The electric power system is the most complex system to have ever been built by mankind. The basic function of a power system is to deliver electricity to customers as reliably and economically as possible [23]. A brief overview of power system reliability evaluation is presented in this chapter including some basic concepts of power system reliability. Thereafter, the definitions and applications of ERs, DR, and PEVs are discussed. Finally, a brief background to clustering techniques is presented.

2.1 Power System Reliability

Power system reliability is a measure of the ability of the system to meet the load requirements within acceptable standards over a period of several years. In other words, reliability can be defined as the probability that a system or component will perform a required function under stated conditions for a stated period of time [42]. According to the North American Electric Reliability Corporation (NERC), reliability is defined as "the degree to which the performance of the elements of the electrical system results in power being delivered to customers within accepted standards and in the amount desired" [43].

Power system reliability is based on the concepts of system adequacy and system security [42, 44], as shown in Fig. 2.1. Power system adequacy is the ability of the system to

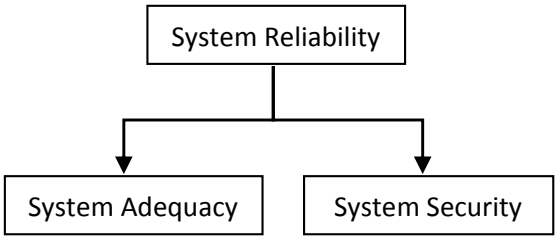

Figure 2.1: Explaining power system reliability [23].

supply all energy demand requirements at all times. System adequacy is associated with system steady-state conditions and offers information on future system behavior that can be used in system planning. Security, on the other hand, is the ability of the system to avoid service interruption under sudden disturbances. System security is associated with the dynamic and transient real-time system operations, such as generator and transmission line contingencies and generation uncertainties [23, 42].

Due to the large-scale and complexity of practical power systems, reliability evaluation can be divided into three zones, *i.e.*, generation, transmission, and distribution, organized into three hierarchical levels (HLs) as hierarchical level 1 (HL-I), hierarchical level 2 (HL-II) and hierarchical level 3 (HL-III) as shown in Fig. 2.2 [45]. Reliability studies can be applied to any zone alone, to the combined zones of generation and transmission (HL-II), or to the combined zones of generation, transmission and distribution (HL-III).

Reliability assessment at HL-I considers generating capacity adequacy evaluation to meet the total system demand. At HL-II, reliability evaluation of the composite system comprising generation and transmission is considered to examine the ability of the system to deliver electrical energy to all the load points within accepted standards and in the amount desired. Studies also include generation rescheduling and load shedding options.

In composite power system reliability assessment, it is challenging to quantify the indices as it is mandatory to include detailed modelling of generation units, transmission lines and their ancillary elements. The challenge of using analytical methods in such complex

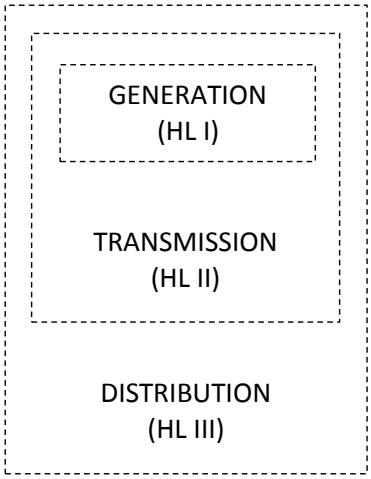

Figure 2.2: Reliability assessment hierarchical levels [23].

systems is the large computational burden involved to determine most significant indices which are related to load curtailment and expected outage events. Components considered in a composite power system reliability study comprise among others, generators, transformers, lines, reactors, relays, and loads. The research presented in this thesis focuses on HL-II analysis.

An overall reliability assessment, HL-III, considers all the three zones simultaneously, and is an extremely problem because of the large-scale modeling and computation involved. Thus, distribution system reliability studies are usually performed separately, which is beyond the scope of this thesis.

Independent outages are those outages of different components which does not affect the probability of outage of the others. Single or multiple independent outages or overlapping outages are the easiest to evaluate and many evaluation methods are available assuming that all the component outages are independent [23]. The research described in this thesis concentrates on independent outages.

The conventional two-state model, shown in Fig. 2.3, represents the probabilistic behavior of most generators and lines, and the basic data required for this model are failure

rates and repair rates. For multiple independent outages, the model adopted for reliability assessment can be found by combining the two-state models of each component.

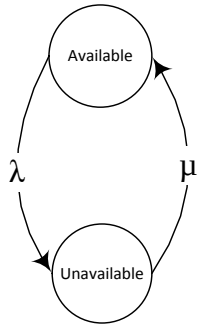

Figure 2.3: Two-state model.

2.1.1 Reliability Measures

Failure Rate (λ) and Mean Time to Failure (MTTF)

Failure rate is the probability that a component is online during a time interval F. In other words, it is the number of failures of a component per unit measurement of time. Failure rate, as one of the important reliability indices, specifies the rate of system aging. It is generally expressed in failures per hour and often denoted by λ. A failure occurs if any component causes power interruption or abnormal voltage profile.

MTTF is the expected or average time of a component to fail. MTTF is the inverse of the failure rate. From Fig. 2.4, we have,

$$F = MTTF = 1/\lambda \tag{2.1}$$

Repair Rate (μ) and Mean Time to Repair (MTTR)

The repair rate is the probability that a component is recovered and restored to service in time R that is less than time F. The repair time represents the time taken to locate

the failed component, diagnose, repair or replace, test, and resume to the system. It is generally expressed in repairs per hour and often denoted by μ.

MTTR is the expected time taken to repair a failed component. MTTR is the inverse of the repair rate. From Fig. 2.4, we have,

$$R = MTTR = 1/\mu \tag{2.2}$$

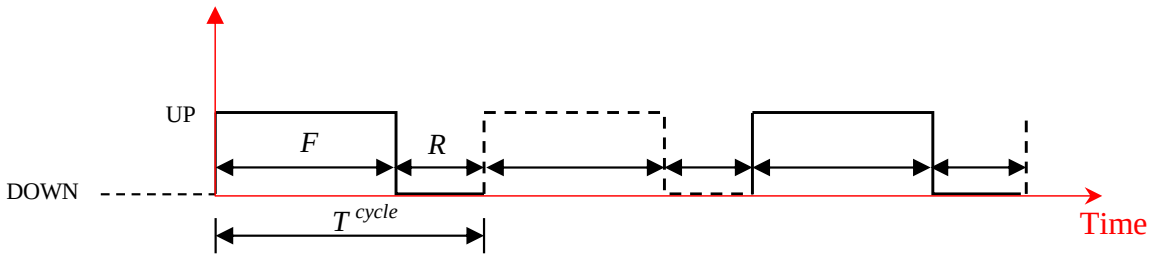

Figure 2.4: System operation and breakdown.

System/Component Availability

Availability is the probability of a system or a component being in service and operating. By modeling the system components in series and parallel as interconnections, system availability can be determined.

In order to determine the component availability, let us assume that a component has two states: available and unavailable. The conventional two-state model, shown in Fig. 2.3 is adopted for reliability assessment.

Figure 2.3 indicates the state transition diagram for a two-state device. The model includes an UP (In Service /Available) state and a DOWN (Outage/Unavailable) state. If failures and repairs are exponentially distributed, the probability of a component cm on outage at a time t, *i.e.*, unavailability of cm, given that it was operating successfully at $t = 0$ [23], is:

$$p_{cm}^{t} = \frac{\lambda_{cm}}{\lambda_{cm} + \mu_{cm}} - \frac{\lambda_{cm}}{\lambda_{cm} + \mu_{cm}} e^{-(\lambda_{cm}+\mu_{cm})t} \tag{2.3}$$

In steady-state condition, *i.e.*, $t = \infty$, the unavailability or the Forced Outage Rate (FOR) of component cm is given as,

$$FOR_{cm} = p_{cm}^{\infty} = (\frac{\lambda_{cm}}{\lambda_{cm} + \mu_{cm}}) \tag{2.4}$$

Minimal Cut Sets

The reliability indices are used by planners and operators to determine the likelihood of interruption of supply and are often defined using the concept of minimal cut sets [42]. A *cut set* in the context of power systems, is a set of system components such as generators, loads, transformers, lines, *etc.*, which, when fails, causes failure of the system. The *minimal cut set*, a subset of the cut set, is one, which when fails, causes system failure but when any one of its components has not failed, does not cause system failure. This implies that all components of a minimal cut set must be in the failure state to cause a system failure. The research presented in this work is based on determining the minimal cut sets for the system or for a certain load bus.

Adequacy Indices

The calculation of reliability and risk indices involve determining which combination of component outages result in interruptions and then calculating the probability of these contingencies occurring.

Two sets of adequacy indices– system indices and nodal indices, are used in composite power systems. They are complementary rather than alternative [23]. System indices are necessary for both planners and operators to determine the likelihood of interruption of supply, while nodal indices provide information on the most important nodes during system disturbances. Both sets can be categorized as annualized and annual indices. Annualized

indices are calculated considering the system load as a constant load; the annual peak load is normally used. Annual indices are calculated considering the time-varying load on a year. The indices of interest, for both system and buses, in this work are the following [23]:

- **Loss of Load Probability** ($LOLP$): calculated by adding the probabilities of all states that cause load curtailment. The calculation of reliability and risk indices involve determining which combination of component outages result in interruptions and then calculating the probability of these contingencies occurring. The LOLP of a power system can be calculated using cut sets, as follows:

  – Step-1: Calculate the probability of failure of a given component at time t, using (2.3) for operational risk assessment and at time $t = \infty$ (steady-state) using (2.4) for determination of unavailability or FOR.

  – Step-2: Multiply the probability of failure of each individual component that construct a cut set and obtain $p(\bar{C}_h)^t$, as given below:

$$p(\bar{C}_h) = \prod_{cm \in \bar{C}_h} FOR_{cm} \tag{2.5}$$

  – Step-3: Use cut set probabilities, as given below [46],to determine the system $LOLP_{Sys}$, as follows:

$$\begin{aligned} LOLP^t_{Sys} = \sum_h p(\bar{C}_h)^t - \sum_{h<l} p(\bar{C}_h \cap \bar{C}_l)^t \\ - \sum_{h<l<m} p(\bar{C}_h \cap \bar{C}_l \cap \bar{C}_m)^t ... (-1)^{w-1} p(\bar{C}_1 \cap \bar{C}_2 \cap ... \bar{C}_w)^t \end{aligned} \tag{2.6}$$

  However, determining cut set probabilities is a difficult and time-consuming exercise for large and complex systems which needs to consider all the cut sets. To overcome the computational complexity of $LOLP^t_{Sys}$ in (2.6), approximations can be made in the evaluation by using the upper bound approximation (first term of (2.6)) by summing the minimal cut set probabilities of system failure as discussed in [42], and

accordingly, the system $LOLP^t_{Sys}$ is obtained as:

$$LOLP^t_{Sys} \cong \sum_h p(\bar{C}_h)^t \tag{2.7}$$

The results obtained with this approximation, although not very accurate, allows fast calculation of system reliability and risk. The degree of inaccuracy introduced, is usually negligible and often within the tolerance associated with the data of the component reliabilities for a system with high values of component reliability.

The LOLP and operational risk of nodes that suffer loss of load can now be calculated in the same way as discussed before where (2.6) of Step-3 is modified to consider the node index i. The nodal minimal cut sets obtained are subsets of the system minimal cut sets.

$$\begin{aligned} LOLP^t_i = \sum_h p(\bar{C}_h)^t_i - \sum_{h<l} p(\bar{C}_h \cap \bar{C}_l)^t_i \\ - \sum_{h<l<m} p(\bar{C}_h \cap \bar{C}_l \cap \bar{C}_m)^t_i ... (-1)^{w-1} p(\bar{C}_1 \cap \bar{C}_2 \cap ... \bar{C}_w)^t_i \end{aligned} \tag{2.8}$$

The upper bound approximation can also be applied to speed up the nodal reliability and risk calculations, as follows:

$$LOLP^t_i \cong \sum_h p(\bar{C}_h)^t_i \tag{2.9}$$

- **Loss of Load Expectation** (LOLE): Summation of the probability of failure, associated with a minimal cut set, over the day, measured in hour/day.

$$LOLE = \sum_{hr} \sum_h p(\bar{C}_h) \qquad \forall \ \bar{C}_h. \tag{2.10}$$

- **Load Not Supplied per Interruption** ($\text{LNSI}_{\bar{C}_h}$): Denotes the real power load curtailment when a minimal cut set $\bar{C}_h$ causes a system failure, measured in MW per

disturbance; in a p.u. system as p.u. per disturbance.

- **Expected Demand Not Supplied** (EDNS): Summation of the products of the probability of failure associated with a minimal cut set and the corresponding $\text{LNSI}_{\bar{C}_h}$ for every hour of the day, measured in MW; ; in a p.u. system as p.u.

$$EDNS_{hr} = \sum_{h} p(\bar{C}_h).LNSI_{\bar{C}_h} \qquad \forall\ hr. \tag{2.11}$$

- **Expected Energy Not Supplied** (EENS): The sum of EDNS over 24 hours determines the daily EENS, measured in MWh/day; ; in a p.u. system as p.u./day.

$$EENS = \sum_{hr} EDNS_{hr}. \tag{2.12}$$

2.1.2 Operational Risk Assessment of Power Systems

Risk and reliability are the two aspects of measuring the ability of the electric power system to meet the load requirements within accepted standards and in the amount desired. Both, risk and reliability are associated with each other. Higher risk means lower reliability, and vice versa. Operational risk assessment is the probability that a system or component will perform a required function under stated conditions during a short period of time.

The first major operational risk assessment was published in 1963 by PJM Interconnection [47]. In this approach, the unit commitment risk is applied to the operational planning of generation units. A procedure is presented for determining operating reserve requirements to maintain a uniform level of risk in the day-to-day operation, taking into account the changing load level, the variability of the load, and the size of units scheduled, so that the spinning reserve capacity in any part of the system can be fully available in any other part of the system [48].

Risk assessment of power systems cover a time scale of hours (T), called a *lead time* with a known initial operational state [8]. The operating conditions of the system components are uncertain, which render the probability of outage of the components continuously

changing. For instance, during severe weather, the failure rate of overhead lines can increase significantly as T increases. The system operational risk can be determined in the same way, from (2.6) as follows:

$$LOLP_{sys}^{T} \cong \sum_{h} p(\bar{C}_h)^T \tag{2.13}$$

And the nodal operational risk is measured as:

$$LOLP_{i}^{T} \cong \sum_{h} p(\bar{C}_h)_i^T \tag{2.14}$$

2.1.3 Basic Approaches to Reliability Evaluation

Several techniques are reported in the literture dealing with reliability evaluation of power systems. The criteria applied to assess the composite system reliability can be categorized as deterministic or probabilistic [49].

The Deterministic Approach

The deterministic approach is an old and simple method used by system planners to evaluate the system performance and maintain system security in different scenarios based on past experience. The most common deterministic method is the N-1 criterion. Based on this criterion, if a system is able to operate, supply load and remain stable after any single unplanned outage (one line or one generator) that may occur, the system will be considered reliable. The main advantage of the deterministic approach is its straightforwardness to implement and the easiness to understand. However, the difficulty to determine the degree of system unreliability, which fails under more than one scenario, limits the applications of this method [49].

The Probabilistic Approach

The probabilistic approach provides a better understanding of system behavior and allocation of resources. The benefit of using the probabilistic approach is in incorporating

uncertain events in the system. The most common types of uncertainties are the components state, the weather, and the load. Stochastic models are used to represent these uncertainties.

The probabilistic approach is categorized as analytical methods and simulation (Monte Carlo simulation) methods [23]. The analytical methods represent the system behavior by mathematical models and evaluate the system reliability using direct numerical solutions. Some of the analytical methods in use are cut set, Markov, and equivalent method. The simulation methods, on the other hand, estimate the system reliability based on simulating a series of random sampling of scenarios, such as Monte Carlo simulations.

In the reliability evaluation of power systems, the states of power system components are usually assumed to be independent and the methods used to calculate the system reliability are based on the multiplication rule of probabilities [4, 50]. The application of probability techniques based on a series of approximate equations to calculate failure rates and component unavailabilities of simple systems is presented in [51,52]. The mathematical expressions to calculate various measures of reliability are based on series and parallel connections criteria employing probability theory.

2.2 Energy Resources (ERs) and Demand Response (DR)

Reliability improvements can be achieved by implementing ERs and DR in power systems which also contribute to reducing transmission and distribution congestion, provide spinning reserve, assist in demand-supply balance provisions, and reduce the need for additional system generation, transmission and distribution capacity.

ERs are on-site small-scale power sources or storage technologies that can be managed and coordinated to provide power where it is needed, and has been defined over a broad range of capacities, ranging from 3 kW to 50 MW [53]. In other words, any distributed generation (DG) resource or demand-side management (DSM) measure is referred to as an ER.

Outage probability for a component in the system is discussed in Section 2.1.1; in the same way, the probability of failure of an ER can be obtained as follows:

1. Time-dependent probability of failure:

   It is assumed that the ER is only available when needed, which means, the ER serves as a supplemental reserve with a response time of t_{in} hours and a start-up failure probability of p_{ER}^{st}, where before an instant takes effect the unavailability has been taken equal to zero. This is a generic representation, and for $t_{in} = 0$, the ER can be considered to be in continuous service.

$$p_{ER}^{t} = p_{ER}^{st} + [\frac{\lambda_{ER}}{\lambda_{ER} + \mu_{ER}} - \frac{\lambda_{ER}}{\lambda_{ER} + \mu_{ER}} e^{-(\lambda_{ER}+\mu_{ER})(t-t_{in})}] \tag{2.15}$$

2. Steady-state probability of failure:

   From (2.15), the FOR of a ER can be stated for $t = \infty$, as follows:

$$FOR_{ER} = p_{ER}^{\infty} = (\frac{\lambda_{ER}}{\lambda_{ER} + \mu_{ER}}) \tag{2.16}$$

Furthermore, DR refers to various programs that engage customers to reduce or shift their electricity usage from peak hours in response to incentive payments or time-based tariffs. Two types of DR are currently available: incentive-based and time-based rates [54]. Incentive-based DR programs can be categorized into four types, as given in Table 2.1:

Table 2.1: Categories of Incentive-Based DR [54]

Program	Definition	Target
Direct load control	Cycling of end-use devices, such as smart thermostat	Residential and small commercial
Demand buy back	Customers respond to curtail upon request for a specified period and price	Commercial and industrial
Demand bidding	Customers bid load reduction into utility or market on advance	Commercial and industrial
Interruptible rate	Offering discounted rates or credits for customers willing to curtail operations or power up the grid using DGs	Commercial and industrial
Ancillary-services market	On contract customers receive payment for agreeing to reduce load when called to ensure power system reliability	Commercial and industrial

On the other hand, time-based DR programs can be classified to three types, as given in Table 2.2:

Table 2.2: Categories of Time-Based DR [54]

Program	Definition
Time of use (TOU) pricing	Prices set for a specific time period on a forward basis, usually not changing more than two times a year
Critical peak	Established TOU prices in effect except for critical peak load days or hours, on which a critical peak price is in effect
Real-time pricing	Prices vary based on the market

Most of the work on DR examines the system impact at the distribution level or develops DR market design frameworks [55, 56]. No work is reported on how DR can impact the reliability of a composite power system.

2.3 Electric Vehicles (EVs)

The innovation of EVs goes back to the 1830s, however, with the revolution of fuel-powered ICE, alongside cheap supply of abundant oil in the early 1900s led to successful improve-

ments and wide availability of motor-fuel cars; therefore, the interest in EVs had mostly died down.

With the current growing interest in EVs and soaring gas prices, driven by a foreseeable fossil fuel depletion in the future, with the developments in the automotive sector and driven by environmental concerns, penetration of EV loads is increasing. In 2010, the Electric Vehicle Incentive Program (EVIP) was introduced by the government of Ontario, Canada, offering up to $14,000 rebate on the purchase of an EV, encouraging Ontarians to shift to low- or zero-emission vehicles as part of an overall government strategy to cut greenhouse gas emissions [3, 57].

2.3.1 Types of Electric Vehicles

Battery Electric Vehicle (BEV):

This type of EVs is powered by electric motors fed by batteries and the traditional ICE is not used. The BEV batteries can be recharged by plugging in to an external electric power source. Charging time varies from half an hour to overnight depending on the level of charging (Level-1 or Level-2). The typical driving range of BEVs is between $135 \sim 425$ km. Example of BEVs are Tesla Model S, Ford Focus EV, Nissan Leaf, Chevrolet Bolt, Chevrolet Spark, Hyundai IONIQ, Kia Soul EV, Mitsubishi i-MiEV, and Smart Fortwo.

Hybrid Electric Vehicle (HEV):

HEVs have two complementary drive systems, powered by electric and fuel motors, combining the benefits of low emissions and high fuel economy. These type of EVs are not manufactured to be plugged in to an external electrical source to recharge the battery; instead, the battery is recharged through the regenerative braking and the ICE during driving. Typically, in the electric power mode, the driving range is less than 10 km. Example of HEVs are Chevrolet Volt Hybrid, Hyundai Sonata Plug-in Hybrid, Honda Civic Hybrid, and Toyota Prius Plug-in Hybrid.

Plug-in Hybrid Electric Vehicle (PHEV):

The mechanical process of the PHEVs are similar to the HEVs. In addition, the PHEVs can be plugged in to an electric power source to recharge the battery unlike HEVs. With the larger battery capacity, PHEVs can offer up to 60 km to drive using the electric mode until the state of charge (SOC) of the battery is very depleted. This is commonly referred to as an AER (all electric range). Example of PHEVs are Audi A3 Sportback e-tron, BMW i8, Fiat Chrysler Pacifica, Ford C-Max, Mercedes-Benz S550E, Porsche Cayenne, and Volvo XC90.

2.3.2 Electric Vehicle Charging Levels

Battery charging of EVs that can be plugged in to the power grid is either carried out conveniently at home or publicly at a charging station. Majority of EV charging occurs overnight at homes when the electricity price is cheaper. Charging times vary, based on different factors, such as the level of charging, battery type, battery SOC, and battery capacity. Charging levels, available currently or still under development, are presented in Table 2.3 [33, 58]:

Table 2.3: EVs Charging Levels [33, 58]

	Primary Use	Current Type	Amperage (A)	Voltage (V)	Power (kW)	Kilometers of Range per Charging Time
Level 1	Residential charging	AC	12-16	110/120, 1ϕ	1.3-1.9	3.2 -8 km of range per hour of charging
Level 2	Residential and public charging	AC	Up tp 80	208/240, 1ϕ	Up to 19.2	16 -24 km of range per hour of charging
Level 3 (under development)	Public charging	AC	TBD	400/600, 3ϕ	TBD	96 -128 km of range in less than 30 minutes
DC Fast Chargers	Public charging	DC	Up tp 200	Up to 600	Up to 240	96 -128 km of range in less than 30 minutes

*TBD: to be determined

2.3.3 PEV Controlled Charging Schemes

Several PEV charging schemes may be adopted depending on the EV controllability. The charging profile is constructed based on charging duration and starting time of charging. The behaviour of PEV drivers has a direct impact on the starting time of charging and hence the charging profile. Therefore, controlled charging can be categorized as follows [59]:

- *Smart Charging* - this strategy envisions an active management system moving the PEV charging load from the on-peak to off-peak hours where the EV aggregating entity will monitor EVs usage controlling overload penetrations and excessive voltage drops.
- *Vehicle-to-Grid* (V2G) - is an extension of smart charging, and considers bidirectional power flow between the PEV and the grid. It assumes that during the on-peak hours, the excess battery power will be utilized to push excess power into the grid for the provision of ancillary services.

2.4 Clustering Technique

Clustering is an important unsupervised learning technique that structures a group of unclassified data with similar characteristics. Clustering analysis plays an important role in many applications of different fields including psychology, social sciences, biology, statistics, pattern recognition, information retrieval, machine learning, and data mining [60]. Different clustering techniques are available, and each may provide different grouping for a data set. Based on the output desired, a particular method can be selected.

Popular clustering techniques such as Fuzzy C-means, self-organizing map, K-means, extreme learning machine, *etc.*, are studied in [61–67] in the context of power engineering applications, although these studies are not used for the purpose of reliability assessment. The use of clustering techniques in load profiling is to partition the initial data sample and group them into classes according to their load characteristics to develop load patterns,

which is significant for load control [61], tariff purposes [62, 66], load forecasting [63], locational customer services [63, 67], power system analysis [63, 66, 67], and estimating non-technical losses affecting power utilities [64]. In the literature, various methods of clustering load curves have been proposed. In [61], the combination of Auto Regression Moving Average (ARMA) modeling technique and genetic based K-means algorithm is utilized to classify the direct load control curves of customer behavior pertaining to use of air conditioners. Different stages of data mining models based on unsupervised and supervised learning techniques is applied in [62] to create load patterns for tariff purposes. Classification of loads in terms of time-varying power consuming behavior is referred in [63]. Historical load curves are used to create a fuzzy relation matrix based approach to the clustering problem. Further, a data mining model is presented in [64], where the analysis is mainly applied to customer consumption behavior to detect non-technical losses.

K-Means Clustering Algorithm

K-means was first introduced by James MacQueen in 1967 [47]. It is one of the simplest unsupervised learning algorithm and easiest to implement in solving many practical clustering problems. The most common approach used to determine the cluster centers is based on minimizing the sum of squared distances from each data point to its cluster center. K-means is typically applied to objects in a continuous n-dimensional space [60], and data clustering is achieved by a simple K-means partitional clustering algorithm.

The main idea is to choose K initial means (centroids), where K is the number of clusters desired. Each data point is then assigned to the nearest mean. Each group of points assigned to the same mean forms a cluster. The algorithm updates cluster means, by minimizing the error of the *Sum of Squares Function* (SSF) considering the Euclidean distance from each data point to its mean, until no point changes clusters or until the means remain the same. The standard operation of the K-means clustering algorithm is demonstrated in Fig. 2.5.

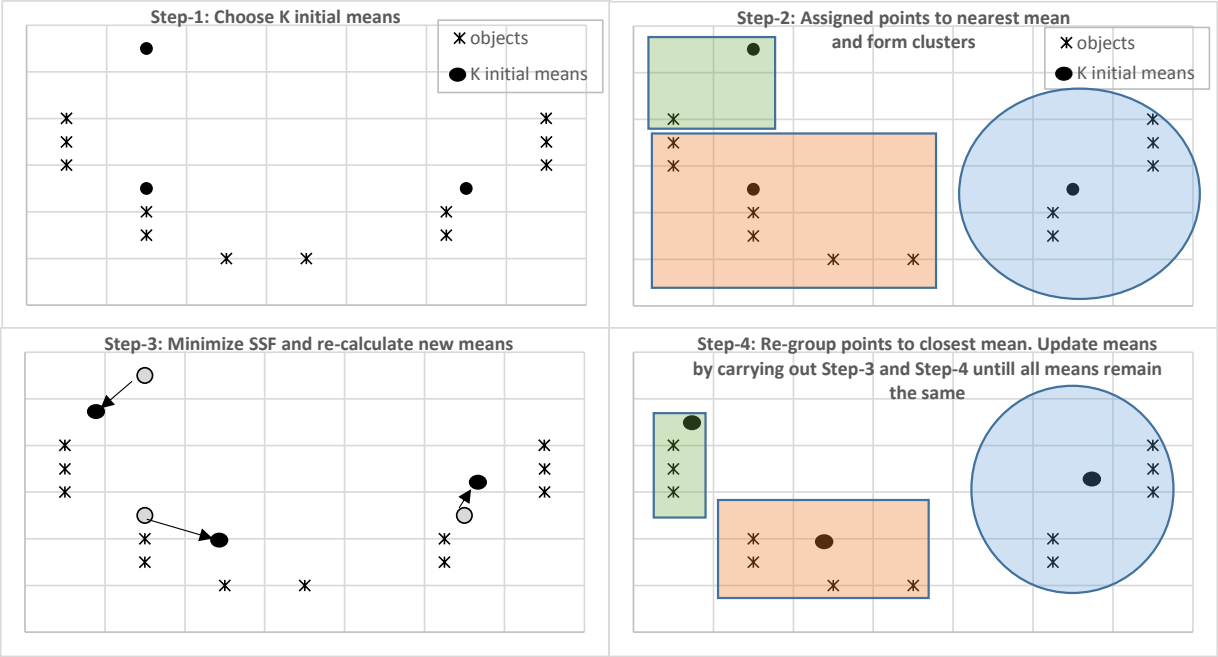

Figure 2.5: Demonstration of K-means clustering algorithm.

Fuzzy C-Means Clustering Algorithm

The Fuzzy C-means clustering algorithm was developed by Dunn in 1973 [68,69] then it was improved by Bezdek in 1981 [69,70]. In fuzzy clustering, each data point has a probability to belong to more than one cluster, unlike the K-means technique, with different degrees of membership based on its distance from the mean of a cluster. Each data point is only then assigned to the cluster with the highest degree of membership [60, 71]. The criterion of goodness is a modified version of the SSF. Both algorithms, K-means and Fuzzy C-means, are classified as partitional clustering algorithms and aim to find best partition of dataset into number of clusters.

2.5 Summary

In this chapter an attempt was made to present a brief background on power system reliability and some basic approaches used in power system reliability analysis. The definitions of power system reliability, adequacy and security, as well as reliability hierarchical levels were briefly discussed. This chapter also presented a brief description of operational risks in power system operation. Thereafter, the definitions and applications of ERs, DR, and PEVs were discussed. Finally, the concepts of K-means and Fuzzy C-means clustering techniques were discussed briefly.

Chapter 3

Clustering Technique Applied to Nodal Reliability Indices for Optimal Planning of Energy Resources[‡]

3.1 Introduction

Electric power systems are facing major challenges because of the increase in penetration of ERs. This chapter focuses on composite system reliability based planning for ERs, and presents novel clustering techniques based approaches to determine the optimal location, size and year of installation of ERs in the system. The K-means clustering and Fuzzy C-means clustering techniques are applied to the set of reliability indices, LNSI, which are determined using nodal minimal cut sets. The nodal minimal cutsets are obtained using an OPF based approach in this chapter. Once the optimal sizes and locations of ERs are

[‡]Parts of this chapter have been published in: B. Lami and K. Bhattacharya, Clustering technique based siting and sizing of distributed energy resources considering nodal reliability and risk, *IEEE Transactions on Power Systems*, vol. 31, no. 6, pp. 4679-4690, Nov. 2016.

[*]An earlier versions of this work was presented in: B. Lami and K. Bhattacharya, "Power system reliability and operational risk evaluation using minimal cut sets," *CIGRÉ Canada Conference-Modernizing the Grid to Better Serve Evolving Customer Needs, Calgary, Alberta, Canada* Sept 2013.

obtained, the earliest year of penetration is determined using an adequacy check algorithm. Detailed studies presented considering the IEEE RTS demonstrate the applicability of the proposed technique.

3.2 OPF Based Determination of Nodal Minimal Cut Sets

The concept of nodal minimal cut sets was first reported in [4] for reliability evaluation of composite power systems. In order to understand the reliability of serving load at a specific bus, it is necessary to determine location specific reliability indices. A select set of minimal cut sets, when are on outage, and if that results in the loss of load at a particular bus, this set of minimal cut sets is termed as the nodal minimal cut set for that bus.

A new method is developed in this chapter building upon the work in [4], to obtain the select set of nodal minimal cut sets that result in loss of load at a bus, $(\bar{C}_h)_i$, as described in Fig. 3.1 and in the following step-wise procedure:

- Step-1: Select a cut set of first order, *i.e.*, each generator or each line is considered individually as a first order cut set.
- Step-2: Execute the OPF with this cut set on outage.
- Step-3: If there is a loss of load at any bus ($Pd_i^{UNM} \neq 0$) then this cut set is a first order minimal cut set. Then,
    1. Calculate the probability of failure of this minimal cut set, $p(\bar{C}_h)$, by multiplying the probability of failure of each individual component that construct this minimal cut set.
    2. Associate buses with unserved loads to this minimal cut set, $(\bar{C}_h)_i$, and to its probability, $p(\bar{C}_h)_i$.
    3. The load not supplied at bus i, because of this outage is denoted by $LNSI_{\bar{C}_h,i}$.

If there is no loss of load at any bus, then go to Step-2 with new first order cut set and check for loss of load at a bus. Continue until all first order cut sets are considered to be on outage and hence form the complete list of first order nodal minimal cut sets.

- Step-4: Select a second order cut set, *i.e.*, a combination of two elements, which may be a generator-generator, generator-line, or line-line pair. Carry out Step-2 and Step-3 to determine the complete list of second order nodal minimal cut sets.

- Step-5: Continue Step-1 to Step-4 to determine higher order combinations of outages of system components, and hence higher order nodal minimal cut sets.

It should be noted that, since the unserved load at a bus need be modelled as a variable, so as to determine the nodal minimal cut sets, a simple power flow analysis is inadequate, and an OPF becomes necessary. Two objective functions are considered for the OPF, loss and load curtailment minimization (J_1), and minimization of load curtailment (J_2), as given below:

$$J_1 = \frac{1}{2}\sum_{i=1}^{N}\sum_{j=1}^{N} G_{ij}[V_i^2 + V_j^2 - 2V_iV_jCos(\delta_{ji})] + \varphi(Pd_i^{UNM} + Qd_i^{UNM}) \tag{3.1}$$

where φ is a large weighting factor; and,

$$J_2 = \sum_{i=1}^{N}\sqrt{(Pd_i^{UNM})^2 + (Qd_i^{UNM})^2}. \tag{3.2}$$

The above objectives are subjected to the following equality and inequality constraints:

1. Nodal active and reactive power balance: is ensured by the power flow equations which also include PD^{UNM} and QD^{UNM}, the real and reactive power load curtailment variables, respectively, that may arise from the outages of various components.

$$Pg_i - Pd_i + Pd_i^{UNM} = \sum_{j=1}^{N}|V_i||V_j||Y_{ij}|cos(\theta_{ij} + \delta_j - \delta_i), \tag{3.3}$$

$$Qg_i - Qd_i + Qd_i^{UNM} = -\sum_{j=1}^{N}|V_i||V_j||Y_{ij}|sin(\theta_{ij} + \delta_j - \delta_i). \tag{3.4}$$

2. Limits on bus voltages:

$$V_i^{Min} \leq |V_i| \leq V_i^{Max}. \tag{3.5}$$

3. Limits on active and reactive power generation:

$$Pg_i^{Min} \leq Pg_i \leq Pg_i^{Max}, \tag{3.6}$$

$$Qg_i^{Min} \leq Qg_i \leq Qg_i^{Max}. \tag{3.7}$$

4. Power flow limits of transmission lines:

$$|S_{ij}| \leq S_{ij}^{Max}. \tag{3.8}$$

5. Limits on load curtailment:

$$0 \leq Pd_i^{UNM} \leq Pd_i, \tag{3.9}$$

$$0 \leq Qd_i^{UNM} \leq Qd_i. \tag{3.10}$$

3.3 Optimal Allocation of ERs Using Clustering Technique

The $LNSI_{\bar{C}_h,i}$ and their respective $p(\bar{C}_h)_i$ are determined considering the system under outage conditions, as discussed in the previous section. A suitable approach to organize the large number of $LNSI_{\bar{C}_h,i}$ data with their respective $p(\bar{C}_h)_i$ for a given bus, considering the large number of possible combinations of outages, is to use clustering algorithms for the terminal year, which are based on the nearest centroid sorting algorithm. In this chapter, two well known clustering approaches, the K-means clustering and the Fuzzy C-means

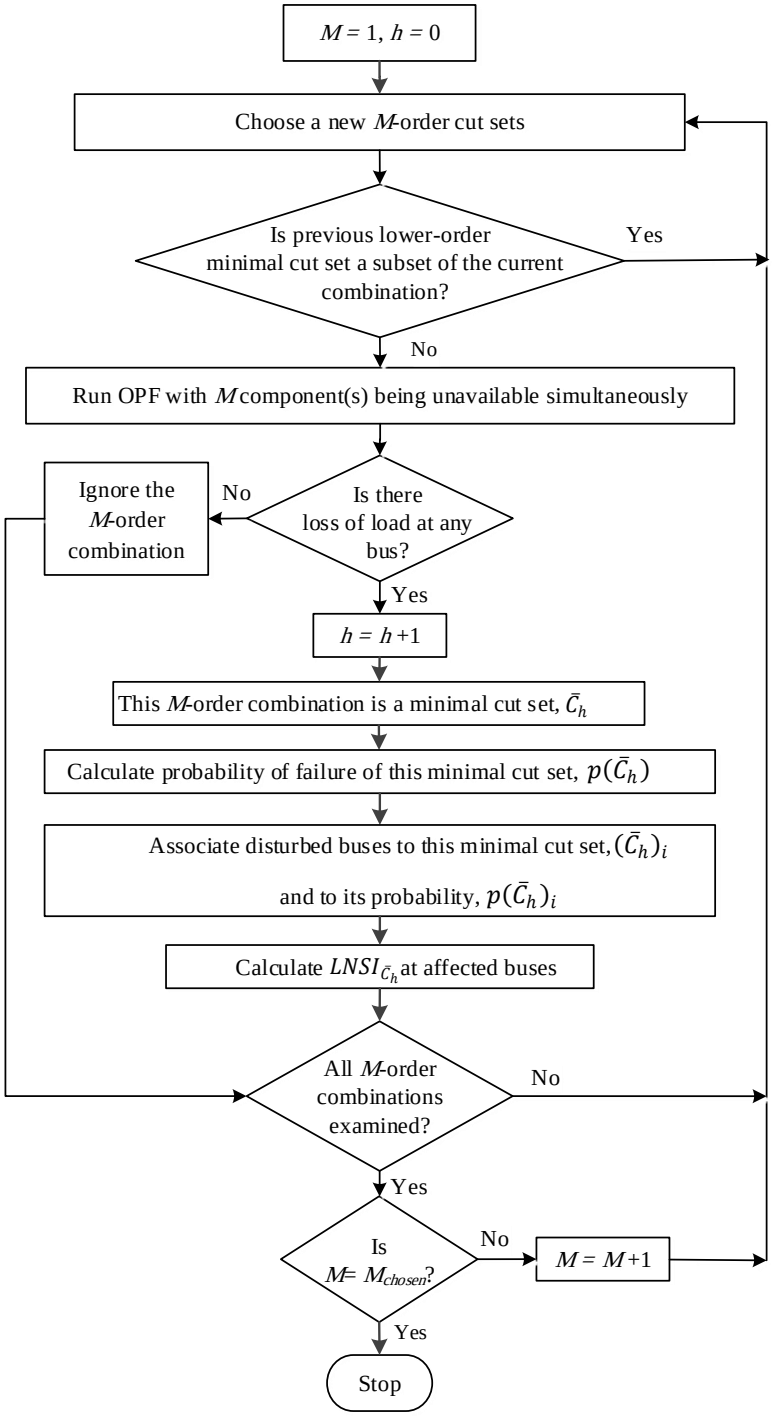

Figure 3.1. Schematic for determining nodal minimal cut sets and adequacy indices.

clustering are used for siting and sizing of ERs based on the calculation of $EDNS$, as discussed next.

3.3.1 Using K-Means Clustering

In the K-means clustering technique, data clustering is achieved by a simple K-means partitional clustering [60]. The main idea is to initiate K number of means (centroids), where K is the desired number of clusters. Each data point is then assigned to the nearest mean. Each group of points assigned to the same mean forms a cluster. The algorithm updates cluster means by minimizing the error of the *sum of squares function* considering the Euclidean distance from each data point to its mean. The proposed K-means clustering algorithm is described in Fig. 3.2, and the step-wise procedure is as follows:

- Step-1: Identify all nodal minimal cut sets associated with each bus, $(\bar{C}_h)_i$, their failure probabilities, $p(\bar{C}_h)_i$, and corresponding values of $LNSI_{\bar{C}_h,i}$, for the terminal year.
- Step-2: Construct a list of two-dimensional points b$\Big(p(\bar{C}_h)_i$,$LNSI_{\bar{C}_h,i}\Big)$.
- Step-3: Choose the desired number of clusters, K.
- Step-4: Choose initial values of cluster means (centroids), me_a, within the data domain.
- Step-5: Calculate Within Cluster Sum of Squared Error, $(WCSSE)$ considering the Euclidean distances from each b$\Big(p(\bar{C}_h)_i$, $LNSI_{\bar{C}_h,i}\Big)$ to its cluster mean, as follows [60]:

$$WCSSE = \sum_{a=1}^{K} \sum_{i=1}^{N} \sum_{h} ||b\Big(p(\bar{C}_h)_i, LNSI_{\bar{C}_h,i}\Big)^{(a)} - me_a||^2. \tag{3.11}$$

- Step-6: Re-group the data points of b$\Big(p(\bar{C}_h)_i$,$LNSI_{\bar{C}_h,i}\Big)$ to the closest cluster mean and re-calculate new cluster means:

$$me_a = \frac{1}{nu_a} \sum_{i=1}^{N} \sum_{h} b\Big(p(\bar{C}_h)_i, LNSI_{\bar{C}_h,i}\Big)^{(a)} \tag{3.12}$$

where nu_a is the number of data points, $\mathrm{b}\Big(p(\bar{C}_h)_i,\ LNSI_{\bar{C}_h,i}\Big)$, in the a^{th} cluster.

- Step-7: Update cluster means by carrying out Step-5 and Step-6 untill all cluster means retain the same value between iterations.
- Step-8: Reassign $\mathrm{b}\Big(p(\bar{C}_h)_i,\ LNSI_{\bar{C}_h,i}\Big)^{(a)}$ to their original buses and cluster those with the same me_a.
- Step-9: Calculate $EDNS$ of each cluster, at each bus, $EDNS_{a,i}$, using nodal minimal cut sets, as follows:

$$EDNS_{a,i} = \sum_{h} \left[p(\bar{C}_h)_i\right]^{(a)}.LNSI^{(a)}_{\bar{C}_h,i} \qquad \forall\ \bar{C}_h \in a, i. \tag{3.13}$$

- Step-10: For every bus, find the highest $EDNS_{a,i}$.
- Step-11: Identify buses with clusters that have $EDNS_{a,i}$ higher than system adequacy. Those are major sites that require ERs. A bus is considered a valid candidate for ER if its adequacy exceeds the plan criteria.
- Step-12: The y-coordinate of a cluster mean indicates the size of the ER.

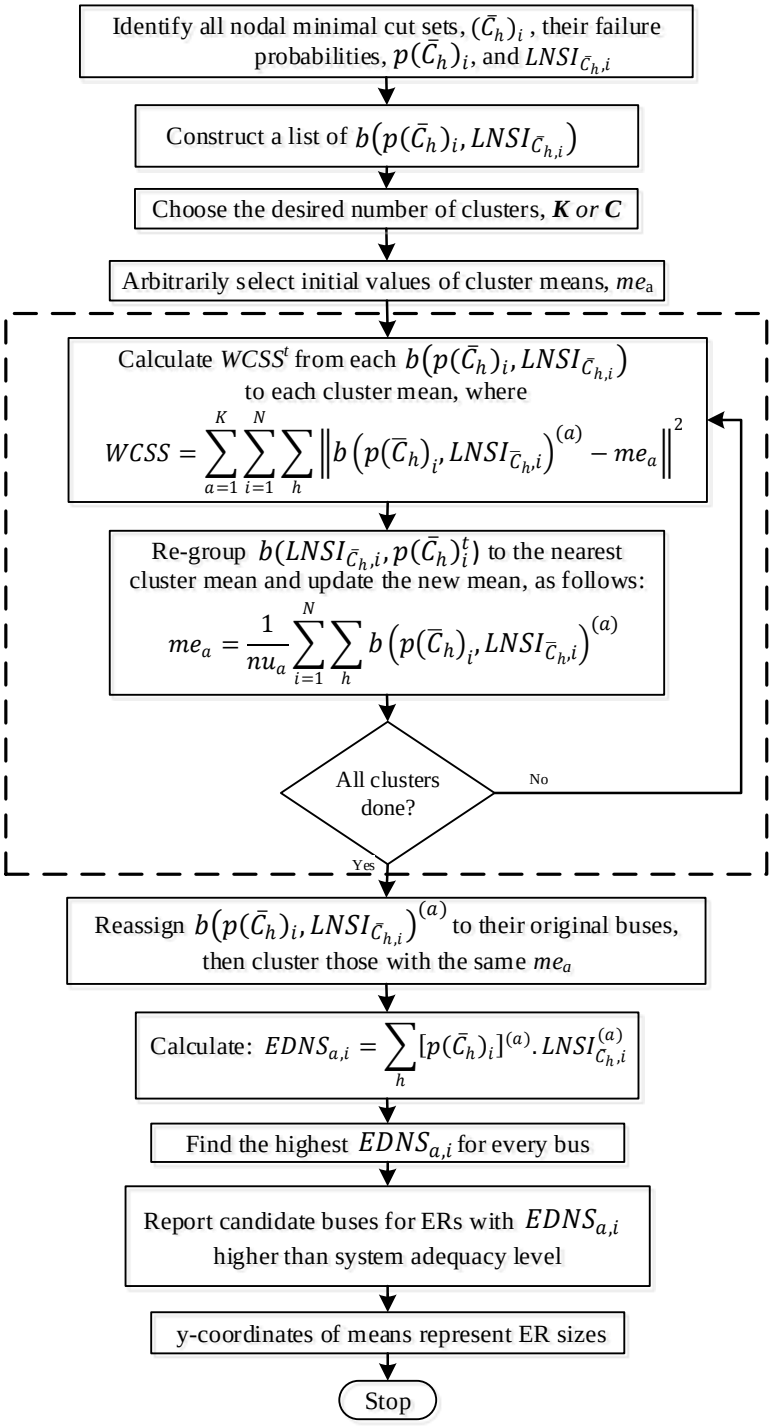

Figure 3.2. Optimal siting and sizing of ERs using K-means clustering technique.

3.3.2 Using Fuzzy C-Means Clustering

Fuzzy C-means is a clustering technique that allows every data point to belong to more than one cluster with different degrees of membership based on its distance from the mean of a cluster. Each data point is only then assigned to the cluster with the highest degree of membership [60, 71]. The criterion of goodness is a modified version of the WCSSE (3.11) [60]. Fuzzy clustering is carried out through an iterative optimization of the objective function $WCSSE_F$ shown below, updating both the memberships and cluster means [72].

$$WCSSE_F = \sum_{a=1}^{C}\sum_{i=1}^{N}\sum_{h} u_{\bar{C}_h,i,a}^{\alpha}||b\Big(p(\bar{C}_h)_i, LNSI_{\bar{C}_h,i}\Big)^{(a)} - me_a||^2 \tag{3.14}$$

where $u_{\bar{C}_h,i,a} \in [0,1]$ is the degree of membership of a data point and $\alpha > 1$ is the shape parameter of the membership function [60].

The application of the Fuzzy C-means clustering algorithm to determine the optimal sizing and siting of ERs is described in the step-wise procedure, as follows:

- Step-1: Carry out Step-1 to Step-4 from K-means clustering algorithm, discussed earlier.
- Step-2: Initialize $\mathbf{U} = [u_{\bar{C}_h,i,a}]_{(h,N)\times C}$ matrix, $\mathbf{U}^{(z=0)}$.
  where $\mathbf{U}$ is the fuzzy partition matrix and z is iteration steps.
- Step-3: Calculate cluster means vectors $\mathbf{ME}^{(z)} = [me_a]_{C\times 1}$ with $\mathbf{U}^{(z)}$

$$me_a = \frac{\sum_{i=1}^{N}\sum_{h} u_{\bar{C}_h,i,a}^{\alpha} b\Big(p(\bar{C}_h)_i, LNSI_{\bar{C}_h,i}\Big)}{\sum_{i=1}^{N}\sum_{h} u_{\bar{C}_h,i,a}^{\alpha}}. \tag{3.15}$$

- Step-4: Update $\mathbf{U}^{(z)}$, $\mathbf{U}^{(z+1)}$

$$u_{\bar{C}_h,i,a}^{(z)} = 1/\sum_{z=1}^{C}\left(\frac{||b\Big(p(\bar{C}_h)_i, LNSI_{\bar{C}_h,i}\Big)^{(a)} - me_a||}{||b\Big(p(\bar{C}_h)_i, LNSI_{\bar{C}_h,i}\Big)^{(z)} - me_z||}\right)^{\frac{2}{\alpha-1}}. \tag{3.16}$$

- Step-5: Repeat Step-3 and Step-4 until $||\mathbf{U}^{(z+1)} - \mathbf{U}^{(z)}|| < \epsilon$.
  where ϵ is a termination criterion $\in$ [0,1].
- Step-6: Assign each of $b\left(p(\bar{C}_h)_i, LNSI_{\bar{C}_h,i}\right)^{(a)}$ to the cluster with highest degree of membership.
- Step-7: Carry out Step-8 to Step-12 from K-means clustering algorithm, discussed earlier.

The core procedure of this clustering technique is shown in Fig. 3.3, essentially the steps within the dotted box in Fig. 3.2 are replaced by the dotted box in Fig. 3.3 to arrive at the complete Fuzzy C-means clustering technique.

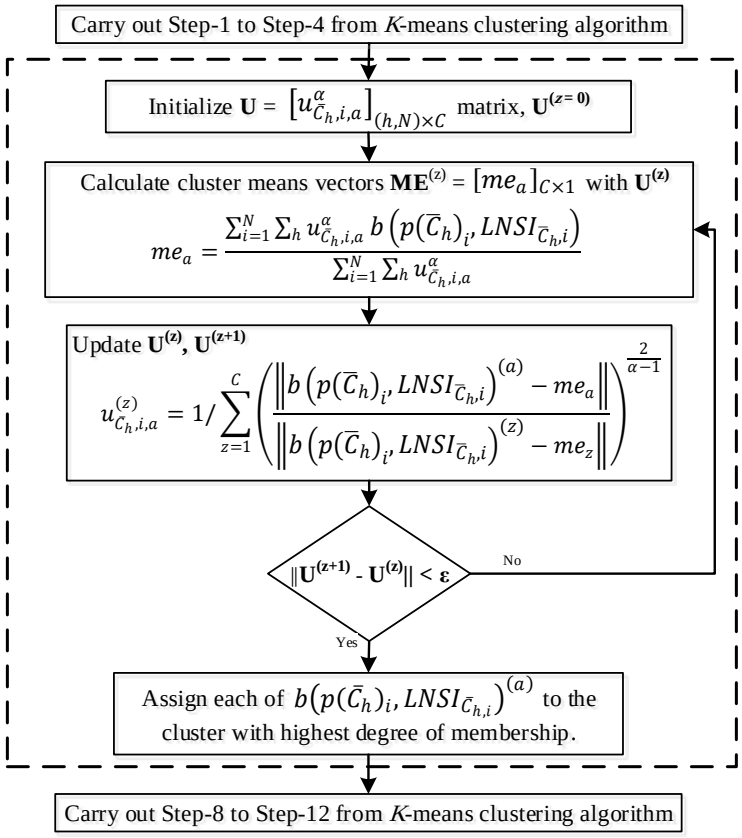

Figure 3.3. Optimal siting and sizing of ERs using Fuzzy C-means clustering technique.

3.3.3 Optimal Year of Allocations of ERs

The proper allocation of ERs over the plan period is an important issue and can significantly impact the system reliability. The two proposed clustering technique based methods determines the candidate buses for ERs along with their sizes, at the terminal year of planning. As described in Fig. 3.4, considering the list of ERs in decreasing order of their $EDNS$, with associated sizes and locations, the proposed algorithm examines $LOLP_{Sys}$ (2.7), starting from year-1. If the $LOLP_{Sys}$ at year-1 does not meet the desired reliability target ($LOLP_{targ}$) of the system, penetrate as much ERs to achieve the adequacy level. However, if the $LOLP_{Sys}$ at year-1 is met, examine the next year and so on, up until the terminal year.

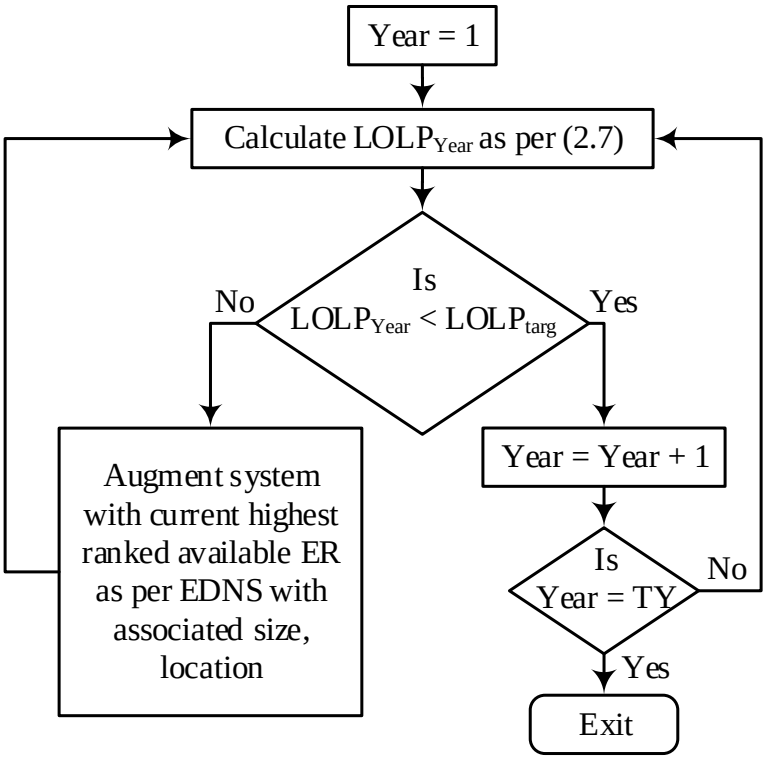

Figure 3.4. Schematic for optimal year of planning ERs.

3.4 Case Study: Analysis and Results

The proposed clustering technique based siting and sizing of ERs considering nodal reliability indices, determined using minimal cut sets, is tested on the IEEE RTS [73] shown in Fig. 3.5. This system is specially designed by the IEEE Task Force on Power System Reliability and provides all relevant data of lines, generators and outages. There are 32 generators ranging from 12 MW to 400 MW in capacity, 24 buses, and 38 transmission lines and transformers. The system has an annual peak load of 2,850 MW and 580 Mvar, and the annual peak load is assumed to increase 1% per year, over ten years. The system installed generation capacity is 3,405 MW. The transmission network comprises lines at 138 kV and 230 kV voltage levels. All per unit quantities refer to active power (MW), reactive power (Mvar) or complex power (MVA) with a base of 100 MVA. The $LNSI$ and $EDNS$ indices, both denote active power in per unit. Relevant data of the IEEE RTS is given in Appendix A.

3.4.1 Determine $(\bar{C}_h)_i$ and $LNSI_{\bar{C}_h,i}$ for Terminal Year

The nodal minimal cut sets, $(\bar{C}_h)_i$, are identified by using the method discussed in Section III. The minimal cut sets are determined up to the third-order, in this chapter, in order to keep the computational burden within reasonable limits, but without any loss of generality. It is to be noted that both the objective functions J_1 (3.1) and J_2 (3.2) are considered separately to determine the minimal cut sets and consequently parallel set of results are obtained. This is to examine how the choice of the OPF objective function impacts the selection of minimal cut sets and hence the optimal planning of ER. There are 1483 minimal cut sets up to the third order for the terminal year (year-10), for the IEEE RTS under study with J_1 objective while 1595 minimal cut sets with J_2 objective (Table 3.1).

The first-order minimal cut sets are determined considering a single component outage at a time, either a generator or a transmission line. For each outage case, if there is loss of load at a bus, the particular component on outage, becomes a first-order minimal cut set. As observed from Table 3.1, there are three first-order minimal cut sets of generator only,

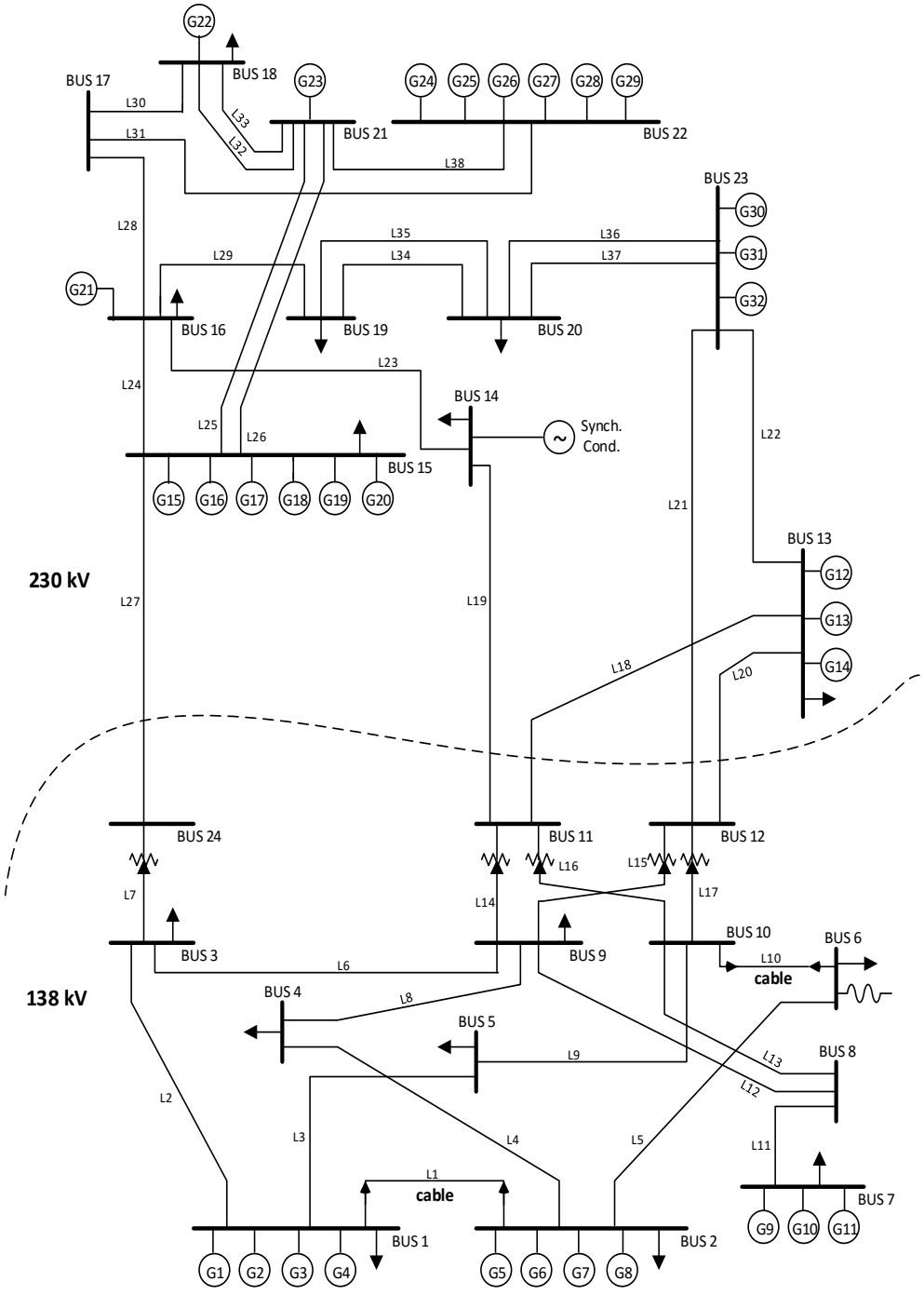

Figure 3.5. IEEE Reliability Test System [73].

in the IEEE RTS, with either objectives.

The second-order minimal cut sets are determined considering the simultaneous outage of two components of the system, *i.e.* two generators, two transmission lines, or one generator and one transmission line. For each outage case, if there is loss of load at a bus, the two components on simultaneous outage form a second-order minimal cut set, if neither of them is a first-order minimal cut set. In Table 3.1, it is seen that there are 118 second-order minimal cut sets with either objectives, where both components are generators, 15 minimal cut sets where both components are transmission lines; and 59 with J_1 and 60 with J_2 second-order minimal cut sets of generator-line pairing. In the same way, the third-order minimal cut sets for the IEEE RTS are also determined, as shown in Table 3.1.

It is noted that the choice of the objective function has some Impact on the number of minimal cut sets, but whether this difference in minimal cut sets impacts the sizing and siting decisions of ER need to be examined, and is presented in the later sections.

Table 3.1: Base Case Minimal Cut Sets

Cut Set Order	**Component(s) on Outage**	**Number of Minimal Cut Sets**	
		J_1	J_2
1	Generator Only (1G)	3	3
	Line Only (1L)	None	None
2	Generators Only (2G)	118	118
	Lines Only (2L)	15	15
	One Generator + One Line (1G+1L)	59	60
3	Generators Only (3G)	454	454
	Lines Only (3L)	173	171
	One Generator + Two Lines (1G+2L)	234	338
	Two Generators + One Line (2G+1L)	427	436
	Total	**1483**	**1595**

Once the minimal cut sets are identified, the corresponding reliability indices can be determined, as discussed earlier. Table 3.2 presents a sample of minimal cut sets along with their outage probabilities considering J_1 objective only and the amount of load interrupted

at the affected buses. The outage probability of a minimal cut set is denoted by $p(\bar{C}_h)$.

For illustration, from Table 3.2, the third order minimal cut set {G3, G7, L10} only affects bus 4 and 8; the real power load curtailment at these buses are 0.012 p.u and 0.016 p.u., respectively, which denote the $LNSIs$ for this minimal cut set. The probability of the event that components G3, G7 and L10 are on outage simultaneously, is determined to be 5.27E-07. It should be noted that the minimal cut set {G3, G7, L10} is considered a nodal minimal cut set for bus 4 and 8 only and not for other buses.

Table 3.2: Sample of $\bar{C}_h$ and Nodal Reliability Indices with J_1

$\bar{C}_h$	$p(\bar{C}_h)$	$LNSI_{\bar{C}_h,i}$ $(p.u.)$				
		i=3	i=4	i=6	i=8	i=20
{G12, G31}	2.00E-03	0	0.405	0.624	0.317	0
{L2, L7}	8.77E-09	0.651	0	0	0	0
{G26, L11}	3.42E-06	0	0	0	0.136	0
{G1, G20, G29}	4.00E-05	0	0.169	0.008	0	0
{L2, L4, L14}	3.90E-12	0	0.115	0	0	0
{G31, L16, L17}	9.08E-12	0	0	0	0	0.113
{G3, G7, L10}	5.27E-07	0	0.012	0	0.016	0

Once the outage probabilities are obtained for each minimal cut set, the $LOLP_{Sys}$ can be determined using (2.7). In the IEEE RTS under study, the $LOLP_{Sys}$ for year-10, prior to installation of ERs, is found to be 0.5231 with both objective functions.

Computational Aspects

The considered test system is programmed and executed on a Dell PowerEdge R810 server, in GAMS environment [74], Windows 64-bit operating system, with 4 Intel-Xeon 1.87 GHz processors and 64 GB of RAM. The OPF is solved using the MINOS solver [74] which is suitable for non-linear programming (NLP) problems. The model and solver statistics are given in Table 3.3.

Table 3.3: Single OPF Solution Time for Different Outages

No. of Equations		239	
No. of Variables		339	
Component(s) on Outage	**Solution Time** *seconds*	**Component(s) on Outage**	**Solution Time** *seconds*
1G	0.369	3G	0.469
1L	0.361	3L	0.470
2G	0.458	1G + 2L	0.473
2L	0.460	2G + 1L	0.474
1G + 1L	0.464		

Table 3.4 presents the total number of possible outage combinations, the number of examined outage combinations, and the corresponding computing time for each cut set order considering the single OPF solution times given in Table 3.3. For example in Table 3.4, the case of three generator outage (3G) may occur in 4960 possible combinations of which only 457 combinations are examined after eliminating those cut sets which had one or more generators as part of lower order minimal cut sets. From Table 3.3 it is noted that the OPF with 3G outage requires 0.469 seconds of computing time, thus the total time required for this case is 3 minutes and 34.33 seconds. From Table 3.4 it is noted that the total time required to determine all minimal cut sets up to the third order, for the IEEE RTS is 5 hours, 28 minutes and 31.03 seconds. Since this is a planning study, carried out much in advance and does not affect the operational decisions, such computational times are generally acceptable.

3.4.2 ER Siting and Sizing

Using K-Means Clustering Technique

After obtaining all the values of load not served at each bus because of outage of minimal cut sets $\bar{C}_h$, $LNSI_{\bar{C}_h,i}$, and their outage probabilities $p(\bar{C}_h)_i$, the K-means clustering algorithm is applied to cluster these data points, $\mathrm{b}\big(p(\bar{C}_h)_i, LNSI_{\bar{C}_h,i}\big)$, at terminal year of planning

Table 3.4:
COMPUTATIONAL TIME FOR DETERMINING THE RELIABILITY INDICES

Cut Set Order	**Component(s) on Outage**	**Total Number of Possible Outage Combinations**	**Examined Outage Combinations**	**Computing Time**
1	1G	32	32	11.81 s
	1L	38	38	13.72 s
2	2G	496	406	3 m 5.9 s
	2L	703	703	5 m 23.38 s
	1G+1L	1216	1102	8 m 31.33 s
3	3G	4960	457	3 m 34.33 s
	3L	8436	8140	1 h 3 m 45.8 s
	1G+2L	22496	19952	2 h 37 m 17.3 s
	2G+1L	18848	10944	1 h 26 m 27.46 s
Total		**57,225**	**41,774**	**5 h 28 m 31.03 s**

(year-10) by initiating randomly chosen values of cluster means followed by measuring the distance between a data point and its cluster mean; then assigning each point to the cluster with the nearest mean and updating the mean until there is no further changes, as discussed in Section 3.3, Step-1 to Step-7.

In the IEEE RTS under study, there are a total of 2008 data points for $\mathrm{b}\Big(p(\bar{C}_h)_i, LNSI_{\bar{C}_h,i}\Big)$ with J_1 objective while 2132 data points with J_2. Table 3.5 and 3.6 presents the clusters obtained along with their means for the considered data set with J_1 and J_2, respectively. The best result of 31 and 33 clusters with J_1 and J_2, respectively, are obtained from multiple runs of different numbers of K.

Once clusters are formed as discussed before, Step-8 to Step-12 are carried out. First, the data points $\big(p(\bar{C}_h)_i, LNSI_{\bar{C}_h,i}\big)$ are re-assigned to their original buses, *e.g.* with J_1, bus-3 has 212 data points of $\mathrm{b}\big(p(\bar{C}_h)_3, LNSI_{\bar{C}_h,3}\big)$, bus-4 has 846 data points of $\mathrm{b}\big(p(\bar{C}_h)_4, LNSI_{\bar{C}_h,4}\big)$, ..., *etc.* This procedure is necessary to determine clusters within buses. As an example, Fig. 3.6 shows the plot of clusters of $\mathrm{b}\big(p(\bar{C}_h)_3, LNSI_{\bar{C}_h,3}\big)$ for bus-3. The next step is to calculate $EDNS_{a,i}$ for each cluster at a bus using (3.13). For each bus, the highest

Table 3.5: Clusters and their Means with J_1 (K-Means)

Cluster a	**Mean** me_a ($p.u.$) y-coordinates	**Cluster** a	**Mean** me_a ($p.u.$) y-coordinates	**Cluster** a	**Mean** me_a ($p.u.$) y-coordinates	**Cluster** a	**Mean** me_a ($p.u.$) y-coordinates
1	0.080114	9	0.252393	17	0.184263	25	0.035486
2	0.014614	10	3.33	18	0.128455	26	1.651769
3	0.005278	11	0.100806	19	3.17	27	0.373478
4	0.0485	12	0.171492	20	0.162506	28	0.054298
5	0.143074	13	1.00515	21	0.030593	29	0.086442
6	0.000591	14	0.569776	22	0.024432	30	0.0085
7	0.157269	15	0.21875	23	0.00241	31	0.072308
8	0.044594	16	0.211455	24	0.348667		

Table 3.6: Clusters and their Means with J_2 (K-Means)

Cluster a	**Mean** me_a ($p.u.$) y-coordinates	**Cluster** a	**Mean** me_a ($p.u.$) y-coordinates	**Cluster** a	**Mean** me_a ($p.u.$) y-coordinates	**Cluster** a	**Mean** me_a ($p.u.$) y-coordinates
1	0.1743	10	0.212	19	0.042886	28	0.018
2	0.170415	11	0.012194	20	0.816917	29	0.02063
3	0.160916	12	0.074597	21	1.156346	30	0.000211
4	0.371685	13	0.062022	22	0.5456	31	0.184345
5	2.91	14	0.052422	23	0.000874	32	0.135642
6	0.005167	15	0.007	24	0.032556	33	0.096671
7	0.008	16	0.252796	25	0.083333		
8	0.002364	17	1.7104	26	0.024679		
9	0.015297	18	0.009143	27	0.027747		

$EDNS_{a,i}$ is obtained. Finally, a list of significant cluster's $EDNS_{a,i}$ of all load buses in the system is created.

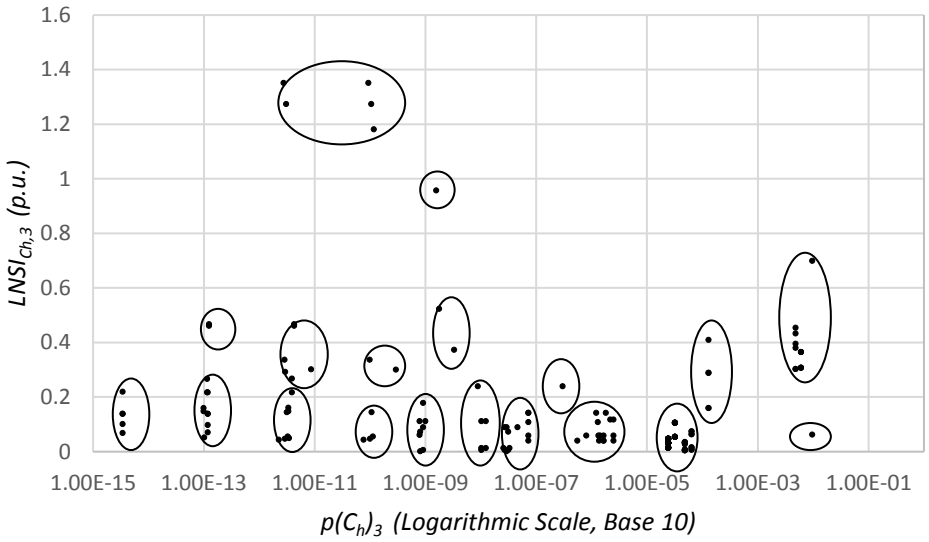

Figure 3.6. Clusters at bus-3 using K-means.

In Table 3.7, clusters with highest $EDNS_{a,i}$ at each bus are presented; and it is assumed that any value of $EDNS_{a,i}$ less than 0.0005 p.u is rejected. It can be observed that optimal ER locations are at buses 3, 4, 6, 8, 14, 20, 5, 9 and 7 with J_1 objective, and at buses 4, 3, 6, 8, 14, 20, 5, 9 and 7 with J_2 objective. The cluster means shown in Tables 3.5 and 3.6 for these selected clusters represents the ER size. A summary of the optimal siting and sizing of ERs, arranged in decreasing order of $EDNS$, is presented in Table 3.8. The ER sizes, as obtained from the K-means clustering technique are also noted in the table, for a base of 100 MW. One important observation from these results is that the choice of the objective function, J_1 or J_2, does not have any significant impact on the ER sizing or siting; the optimal sizing and siting decisions with the different objectives are very close to each other.

Table 3.7: Clusters with Highest $EDNS_{a,i}$ at a Bus (K-Means)

J_1			J_2		
Bus i	**Cluster** a	$EDNS_{a,i}$ $(p.u.)$	**Bus** i	**Cluster** a	$EDNS_{a,i}$ $(p.u.)$
3	14	0.1664	4	4	0.1315
4	24	0.1130	3	22	0.0866
6	14	0.0673	6	22	0.0619
8	15	0.0545	8	10	0.0551
14	24	0.0419	14	4	0.0419
20	24	0.0419	20	4	0.0419
5	4	0.0048	5	25	0.0048
9	9	0.0018	9	16	0.0019
7	11	0.0005	7	33	0.0005
1	16	EPS	13	5	EPS
2	17	EPS	18	17	EPS
19	26	EPS	1	10	EPS
18	10	EPS	2	31	EPS
15	19	EPS	19	17	EPS
16	13	EPS	15	5	EPS
10	16	EPS	10	17	EPS

*EPS: very small number

Table 3.8: Optimal Siting and Sizing of ERs in Order of EDNS (K-Means)

J_1		J_2	
Location (Bus)	**Size** (MW)	**Location** (Bus)	**Size** (MW)
3	56.98	4	37.17
4	34.87	3	54.56
6	56.98	6	54.56
8	21.88	8	21.20
14	34.87	14	37.17
20	34.87	20	37.17
5	4.85	5	8.33
9	25.24	9	25.28
7	10.08	7	9.67

Using Fuzzy C-Means Clustering Technique

The same exercise is repeated considering the algorithm presented in the Fuzzy C-means clustering technique in Section 3.3.2. Each data point of $\mathrm{b}\big(p(\bar{C}_h)_i, LNSI_{\bar{C}_h,i}\big)$, at year-10, in the Fuzzy C-means is assigned to the cluster with the highest degree of membership, as discussed in Section 3.3.2, Step-1 to Step-6. Table 3.9 and 3.10 presents the clusters obtained along with their means for the considered data set with J_1 and J_2, respectively. Step-8 to Step-12 are then carried out from the K-means clustering algorithm, discussed earlier, to re-assign the data points to their original buses to determine clusters within buses and to calculate $EDNS_{a,i}$ for each cluster.

Table 3.9: Clusters and their Means with J_1 (Fuzzy C-Means)

Cluster a	**Mean** me_a $(p.u.)$ y-coordinates	**Cluster** a	**Mean** me_a $(p.u.)$ y-coordinates	**Cluster** a	**Mean** me_a $(p.u.)$ y-coordinates	**Cluster** a	**Mean** me_a $(p.u.)$ y-coordinates
1	0.097582	9	0.30385	17	0.431666	25	0.230178
2	0.714782	10	0.073315	18	0.014341	26	0.181254
3	1.87251	11	0.239311	19	0.586471	27	0.171585
4	0.359726	12	0.141913	20	0.043758	28	0.161941
5	1.000265	13	0.404328	21	0.5114	29	0.202483
6	0.211279	14	0.003351	22	0.27871	30	0.330128
7	0.028165	15	0.085065	23	0.148604	31	0.112789
8	1.533465	16	0.130362	24	0.054797		

In Table 3.11, a list of significant cluster's $EDNS_{a,i}$ of all load buses in the RTS is presented. Table 3.12 presents the results of the optimal siting and sizing of ERs and it is noted that irrespective of the choice of J_1 and J_2 the results are very similar. Furthermore, it is noted from the results that the optimal size, site and year of installation of the ERs are very close to each other, and the choice of either K-Means or Fuzzy C-Means clustering technique has little impact on the ER selections.

Table 3.10: Clusters and their Means with J_2 (Fuzzy C-Means)

Cluster a	**Mean** me_a $(p.u.)$ y-coordinates	**Cluster** a	**Mean** me_a $(p.u.)$ y-coordinates	**Cluster** a	**Mean** me_a $(p.u.)$ y-coordinates	**Cluster** a	**Mean** me_a $(p.u.)$ y-coordinates
1	1.854702	10	0.239153	19	0.319092	28	0.073313
2	0.042614	11	0.097654	20	0.085274	29	0.161708
3	0.363865	12	0.203279	21	0.054268	30	0.02808
4	0.229292	13	0.130727	22	0.190865	31	0.419024
5	0.721446	14	0.63021	23	1.307943	32	0.211272
6	0.145245	15	0.180227	24	0.52684	33	0.003474
7	0.275155	16	0.334277	25	0.905804		
8	0.29552	17	0.171397	26	0.014641		
9	1.120767	18	0.4945	27	0.112557		

Table 3.11: Clusters with Highest $EDNS_{a,i}$ at a Bus (Fuzzy C-Means)

J_1			J_2		
Bus i	**Cluster** a	$EDNS_{a,i}$ $(p.u.)$	**Bus** i	**Cluster** a	$EDNS_{a,i}$ $(p.u.)$
3	2	0.1664	3	5	0.0866
4	30	0.0854	4	16	0.0844
6	19	0.0587	8	4	0.0550
8	25	0.0549	6	14	0.0544
14	4	0.0419	14	3	0.0419
20	4	0.0419	20	3	0.0419
5	24	0.0054	5	21	0.0054
9	11	0.0018	9	10	0.0019
7	31	0.0005	7	27	0.0005
1	29	EPS	13	1	EPS
2	29	EPS	18	1	EPS
19	3	EPS	1	12	EPS
18	3	EPS	2	22	EPS
15	3	EPS	19	1	EPS
16	5	EPS	15	1	EPS
10	6	EPS	10	1	EPS

*EPS: very small number

Table 3.12: Optimal Siting and Sizing of ERs in Order of EDNS (Fuzzy C-Means)

J_1		J_2	
Location (Bus)	**Size** (MW)	**Location** (Bus)	**Size** (MW)
3	71.48	3	72.14
4	33.01	4	33.43
6	58.65	8	22.93
8	23.02	6	63.02
14	35.97	14	36.39
20	35.97	20	36.39
5	5.48	5	5.43
9	23.93	9	23.92
7	11.28	7	11.26

3.4.3 Validation of Optimal ERs

In this validation exercise, nine ERs at the selected buses- 3, 4, 6, 8, 14, 20, 5, 9 and 7 are added to the system with their corresponding sizes as given in Table 3.8. It is assumed that the failure and repair rate of an ER are 0.005 per hour and 0.05 per hour, respectively. The unavailability of each ER is calculated using (2.16). The active and reactive power balance equations (3.3) and (3.4), respectively, are modified to include the power supplied by an ER at a bus (P_{ER_i} and Q_{ER_i}), and are optimization variables. The OPF model given by (3.1) - (3.10) now includes additional inequality constraints on active and reactive power generation limits of the ERs ($P_{ER_i}^{Min}, P_{ER_i}^{Max}$ and $Q_{ER_i}^{Min}, Q_{ER_i}^{Max}$), respectively.

The impact of the presence of ERs is observed in the formation of new combinations of minimal cut sets. Some of these new cut sets were previously of lower order, and have now changed to a higher order cut set and no longer leads to an interruption. For example, a simultaneous outage of {G1, G20, G29} does not cause a system failure anymore, because the cut set has changed from the third order to a higher order. These changes improve the system reliability since, when the cut set order increases, its unavailability reduces.

3.4.4 Optimal Year of Commissioning of ERs

Table 3.13 presents the optimal year of commissioning of the ERs, obtained using the proposed schematic of Fig. 3.4. The desired reliability target for the system ($LOLP_{targ}$) is set at 0.1562, which is the specified reliability level of the RTS at year-0. As the system load increases over the plan horizon, the $LOLP$ will increase beyond the system target level. ERs are commissioned at those specific years when the $LOLP$ is above the target level, in the order of $EDNS$ as given in Table 3.8 and Table 3.12 so as to bring the $LOLP$ below the system target level. This sequential process of addition of ERs is shown in Fig. 3.7. For the sake of brevity, this analysis is carried out with optimal ERs obtained from the K-means clustering technique only, however the approach is generic. It is noted that the year of installation is very similar for J_1 and J_2 except for one year.

Table 3.13: Optimal Year of Commissioning of ERs

Year	J_1		J_2	
	ER @Bus	**Size (MW)**	**ER @Bus**	**Size (MW)**
0	-	-	-	-
1	3	56.98	4	37.17
2	-	-	3	54.56
3	4	34.87	-	-
4	6	56.98	6	54.56
5	-	-	-	-
6	8	21.88	8	21.20
7	14	34.87	14	37.17
8	20	34.87	20	37.17
9	5, 9	4.85 + 25.24 = 30.09	5, 9	8.33 + 25.28 = 33.61
10	7	10.08	7	9.67
Total		**280.60**		**285.11**

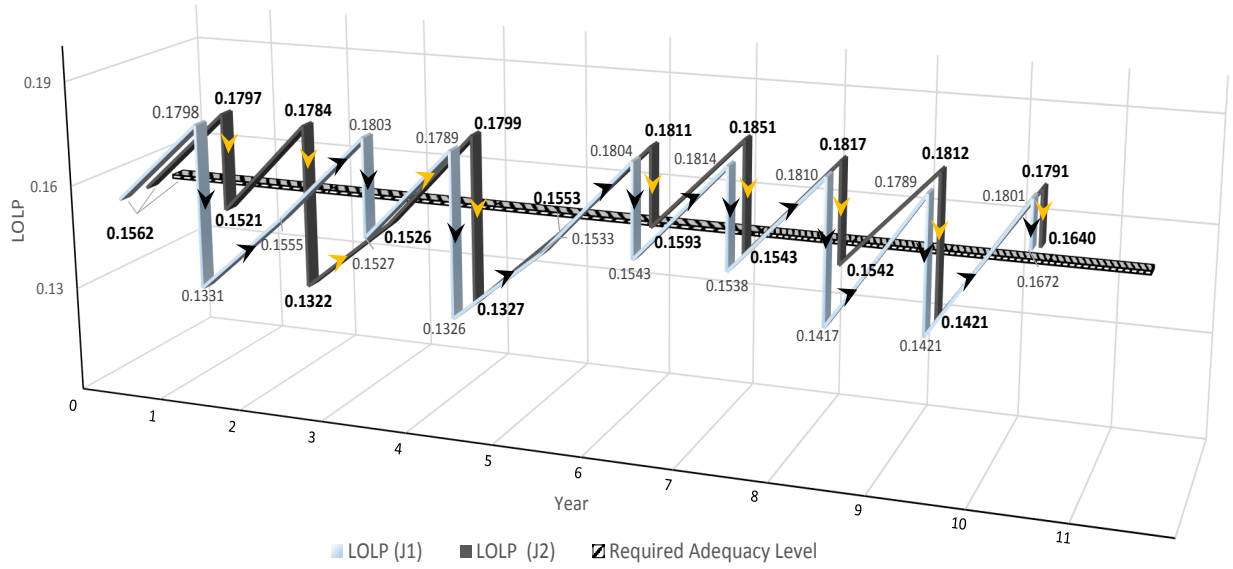

Figure 3.7. Optimal year of commissioning of ERs, siting and sizing determined by K-means clustering.

3.5 Some Important Comments

3.5.1 Effect of Cut Set Levels

As discussed earlier, once the outage probabilities of each minimal cut set are determined, the $LOLP_{Sys}$ can be obtained using (2.7). It can be noted from Table 3.14 that $LOLP_{Sys}$, for year-10 in the presence of ERs, converges to an equilibrium value with third order minimal cut sets. Beyond third order, the $LOLP_{Sys}$ does not change significantly but the computational burden can be very high. Therefore, in this work all analysis is carried out considering first, second and third order minimal cut sets only.

Table 3.14: $LOLP_{Sys}$ Considering Different Cut Set Levels at year-10

Cut Set Order	$LOLP_{Sys}$	
	J_1	J_2
1	0	0
2	0.14731	0.13291
3	0.16716	0.16400
4	0.17082	0.16721

3.5.2 Impact of Wind-Based ERs on Reliability

In this part of the study, it is assumed that generators G24 and G25, at bus 22 of the RTS are wind generators of 50 MW capacity, each. Furthermore, each wind-based ER is assumed to have an FOR of 0.5, as per [75]. In Table 3.15, the probability of outage corresponding to each cut set order and group are shown. Because of the high value of FOR of wind-based ERs, ranging from 0.5 to 0.8 [75], it is noted that $LOLP_{Sys}$ increases significantly when there are wind-based ERs in the system because of intermittent availability of wind. The $LOLP_{Sys}$, at year-0, was 0.1562 when only conventional generators are considered, while it is significantly increased to 0.2158 in the presence of wind-based ERs. The optimal siting, sizing and year of installation of ERs will also be affected consequently, although these have not been explicitly demonstrated in the studies presented, to limit the scope of discussions. This can considered as a future research issue.

Table 3.15: Comparison of System Reliability Considering Wind-Based ER (Year-0)

Cut Set Order	**Component(s) on Outage**	**No Wind-Based ER**		**With Wind-Based ER**	
		Number of Minimal Cut Sets	**Probability of Outage**	**Number of Minimal Cut Sets**	**Probability of Outage**
1	1G	-	-	-	-
	1L	-	-	-	-
2	2G	20	0.12	20	0.12
	2L	8	2.02E-6	8	2.02E-6
	1G + 1L	3	0.00011	3	0.00011
3	3G	327	0.03598	327	0.09557
	3L	67	7.60E-9	67	7.60E-9
	1G + 2L	54	6.83E-7	54	6.83E-7
	2G + 1L	106	0.00012	106	0.00012
		585	$LOLP_{Sys}$ **= 0.1562**	**585**	$LOLP_{Sys}$ **= 0.2158**

3.5.3 Some Comments on the Clustering Techniques

It should be noted that due to the sensitivity of the clustering techniques to the initial values of the means, all data points $\mathrm{b}\big(p(\bar{C}_h)_i, LNSI_{\bar{C}_h,i}\big)$ are aggregated at the beginning to ensure that a given cluster has the same mean across all buses. There is no general theoretical approach to find the optimal number of clusters; some researchers argue that it is beyond the scope of the theory of clustering algorithm [76, 77]. Researchers have either applied a simulation based approach where multiple runs considering different number of clusters are used to find the most suitable number, or some others have used a simple rule of thumb to set the number of clusters, where, Number of Clusters $=\sqrt{(n/2)}$, and n is the number of data points [78]. In this work, we have used the rule of thumb to determine the number of clusters. Furthermore, in the literature, some kind of indices referred to as the *cluster validity indices* have been reported which compare different clustering techniques and yield the best alternative [79]. However, these indices are not examined in this chapter and can be considered for future research.

3.6 Summary

This chapter presented a reliability analysis based framework for a composite power system to identify the optimal site, size and year of installation of ERs. The optimal size and sites for ERs were determined using the novel application of K-means clustering and Fuzzy C-means clustering of the bus-wise $LNSI$ indices. A novel, OPF based approach was used to compute the system minimal cut sets and hence the $LNSI$ indices; and in the OPF, two different objectives were considered to examine the differences on $LNSI$ indices. Thereafter, over a plan period of N years, a novel adequacy check algorithm, which starts from the plan terminal year and ends at the first year and hence determines the optimal year of commissioning of the ERs, was developed. This work simultaneously determined optimal size, site and year of installation of ERs using a reliability based criterion. Network constraints were imposed to guarantee acceptable reliability level. Results showed the improvements and the positive impact of the ERs on system reliability.

Chapter 4

Identification of Critical Components of Composite Power Systems Using System-Wide Minimal Cut Sets[‡]

4.1 Introduction

This chapter presents an OPF based method to determine the minimal cut sets of a composite power system and hence identify the critical components. In composite power systems, it is necessary to identify which components are more critical than others from a reliability stand point. For example, if *the impact of outage* of component 'a' is higher than that of component 'b', component 'a' has a higher "criticality index" than 'b', where *the impact of outage* is measured in terms of a given reliability index. Detecting critical components of the power system can help planners to make economic decisions on new investments in generation capacities and transmission lines upgrades, can help operators to ensure maintaining the delivery of electricity during system failure and disturbance events. The

[‡]Parts of this chapter have been published in: B. Lami and K. Bhattacharya, Identification of critical components of composite power systems using minimal cut sets, *in Proc. of Innovative Smart Grid Technologies (ISGT) Conference*, 2015, Washington D.C., USA, pp.1-5, Feb. 2015.

method presented provides important information on system planning, operation, maintenance and upgrades by ranking critical components of a composite power system. Each component is ranked based on minimal cut set outage probability and the consequent loss of load arising from outages of components belonging to a minimal cut set.

4.2 Determination of System Minimal Cut Sets

The concept of minimal cut sets can be used in the reliability and risk calculations for the system as a whole. The outage states of generators, transmission lines, or both, are considered within the OPF model to determine these cut sets. The algorithm to determine the minimal cut sets of a composite power system, up to the preset order, is shown in Fig. 4.1. The same objective function (3.2) to minimize the total load curtailment and its constraints, discussed in Chapter 3, Section 2, is used here. The step-wise procedure to determine the system minimal cut sets is as follows:

- Step-1: Select a cut set of first order, *i.e.*, each generator or each line is considered individually as a first order cut set.
- Step-2: Execute the OPF with this cut set on an outage.
- Step-3: If there is a loss of load at any bus ($\Delta Pd_i^{UNM} \neq 0$), then this cut set is a first-order minimal cut set for the whole system. Then,

  1. Calculate the probability of failure of this minimal cut set, $p(\bar{C}_h)$, using (2.6).
  2. Report the system LNSI.

  If there is no loss of load at any bus, then go to Step-2 with a new first-order cut set and check for loss of load at a bus. Continue until all first order cut sets are considered to be "on outage", and hence form lists of first-order system and nodal minimal cut sets.
- Step-4: Select a second order cut set, *i.e.*, a combination of two elements, which may be a generator-generator, generator-line, or line-line pair. Carry out Step-2 and Step-3 to determine the complete lists of second-order system minimal cut sets.

- Step-5: Continue Step-1 to Step-4 to determine higher-order combinations of outages of system components.

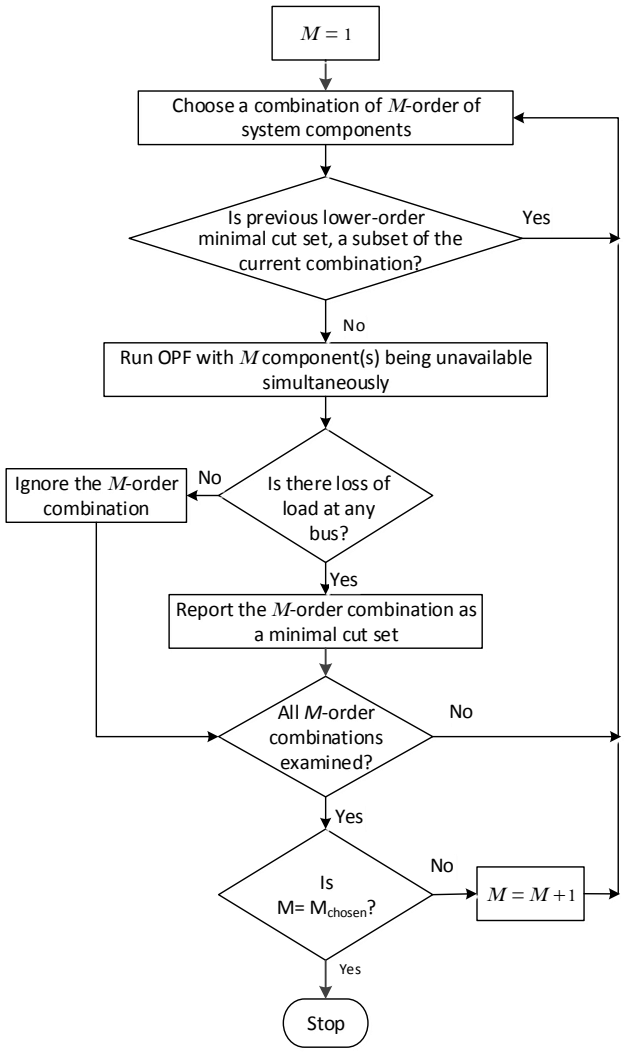

Figure 4.1: Schematic for determining system minimal cut sets.

4.3 Identifying Critical Components

Power systems comprise many types of components, such as transformers, lines, cables, generators, and loads that enable the system to function in a desired manner. The system is often subjected to abnormal effects, such as weather conditions, animals, human error, overload, and ageing that can cause failure of a component. Therefore, it is important in reliability assessment to identify components that can affect system safety.

The flow-chart of the proposed method to identify the critical components of a composite power system is described in Fig 4.2. The step-wise algorithm proceeds as follows:

- Step-1: Determine all minimal cut sets of the system, $(\bar{C}_h)$, as presented in Section 3.2, denoted as set $\{Z\}$.
- Step-2: Identify all minimal cut sets associated with cm, $(\bar{C}_h)_{cm}$, denoted as set $\{X_{cm}\}$.
- Step-3: Choose a minimal cut set $(\bar{C}_h)_{cm}$, $\forall\ (\bar{C}_h)_{cm} \in \{X_{cm}\}$ associated with component cm and execute the OPF with all elements of $(\bar{C}_h)_{cm}$ on outage.
- Step-4: Calculate the probability of failure of this minimal cut set, $p(\bar{C}_h)^t_{cm}$, by multiplying the probability of failure of each individual component, using (2.3) and (2.4), that construct this minimal cut set.
- Step-5: Estimate $LNSI_{\bar{C}_h,cm}$ associated with this minimal cut set.
- Step-6: Check for all minimal cut sets associated with cm by repeating Step-3 to Step-5.
- Step-7: Calculate Criticality Index (CR) for component cm as follows:

$$CR^t_{cm} = \sum_h p(\bar{C}_h)^t_{cm}.LNSI_{\bar{C}_h,cm} \tag{4.1}$$

- Step-8: Report frequency of occurrence of cm, f_{cm}, in $\{Z\}$.

The applied concept considers component cm is a trigger of an event if it is the last component, on a minimal cut set, to fail [28], *e.g.* consider the third order minimal cut set {G3, G7, L6} where the sequence of component outages is G3 followed by G7 then L6; the criticality index calculations is added to CR^t_{L6} but not to CR^t_{G3} or CR^t_{G7}.

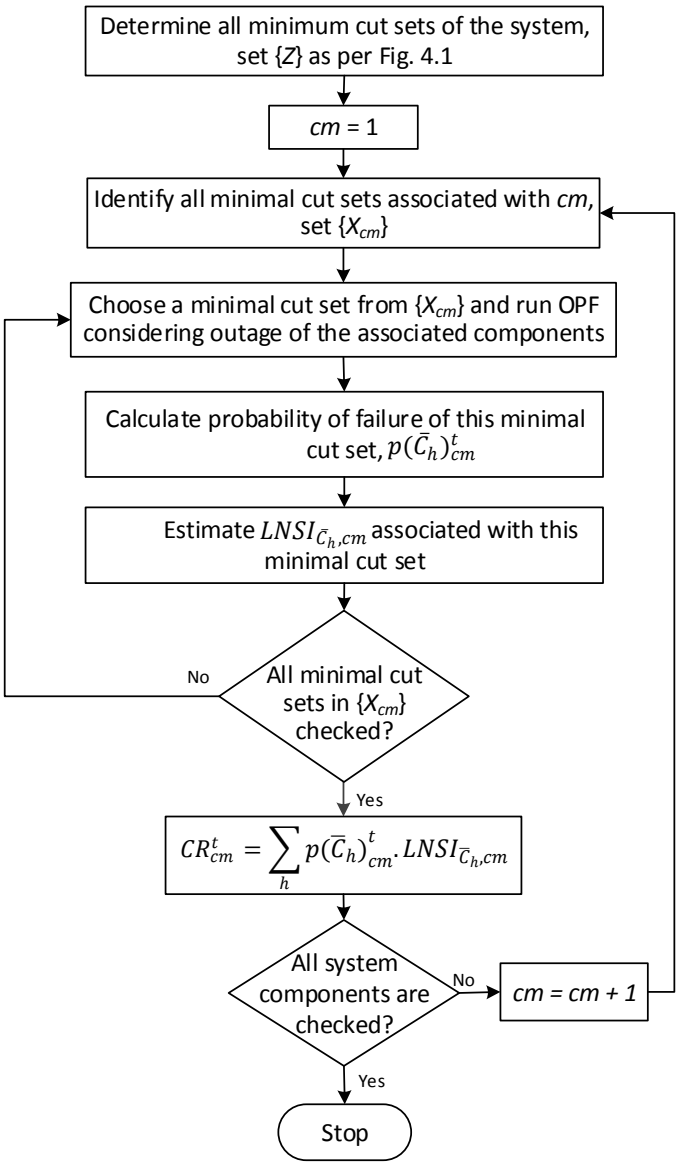

Figure 4.2: Schematic for determining critical components.

4.4 Case Studies: Analysis and Results

Studies are performed on two test case power systems, the 6-bus RBTS [80] shown in Fig. 4.3 and the 24-bus IEEE RTS [73] shown in Fig. 3.5 in Chapter-3. The proposed algorithm is programmed and executed in the GAMS environment [74]. In the RBTS there are 11 generators ranging from 5 MW to 40 MW in capacity, 6 buses, and 9 transmission lines. The system has an annual peak load of 185 MW, and the installed generation capacity is 240 MW. The transmission network voltage level is 230 kV. All per unit quantities refer to active power (MW), reactive power (Mvar) or complex power (MVA) with a base of 100 MVA. Relevant data of the RBTS is given in Appendix B.

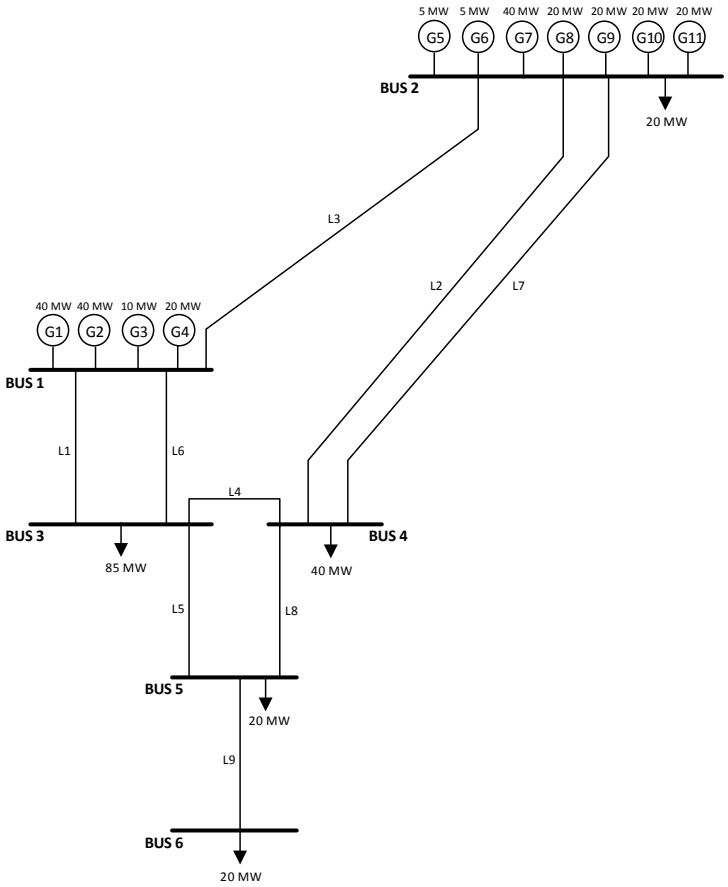

Figure 4.3: Roy Billinton Test System [80].

4.4.1 System Reliability and Risk Evaluation

A. RBTS

The system minimal cut sets are identified by using the method discussed in Section 3.2, and the results are presented in Table 4.1. The minimal cut sets are determined up to the third-order, in this research, to keep the computational burden within reasonable limits, and without any loss of generality.

The first-order minimal cut sets are determined considering a single component outage at a time, either a generator or a transmission line. For each outage case, if there is loss of load at a bus, the particular component on outage, becomes a first-order minimal cut set. As observed from Table 4.1, there is only one first-order minimal cut set in the RBTS which is line L9.

The second-order minimal cut sets are determined considering the simultaneous outage of two components of the system, *i.e.* two generators, two transmission lines, or one generator and one transmission line. For each outage case, if there is loss of load at a bus, the two components on simultaneous outage form a second-order minimal cut set, if neither of them is a first-order minimal cut set.

In Table 4.1, it is seen that there are 20 second-order minimal cut sets where both components are generators, 2 minimal cut sets where both components are transmission lines, and none second-order minimal cut sets of generator-line pairing. In the same way, the third-order minimal cut sets for the RBTS are also determined, and shown in Table 4.1.

In Table 4.2, the system reliability and operational risk corresponding to each cut set order and group are shown, where $p(\bar{C}_h)^{\infty}$ denote the steady-state probability of the outage of all minimal cut sets of a given order while $p(\bar{C}_h)^{10}$ is the system outage probabiltiy at time T=10 hrs, considering outage of all minimal cut sets of that order, obtained from (2.7). It can be seen from the table that the probability of failures progressively become low up to the third order so there is no need to test higher orders of minimal cut sets.

Table 4.1: System Minimal Cut Sets for RBTS

Cut Set Order	Cut Set Groups	Minimal Cut Sets {Z}
1	1 Generator	None
	1 Line	{L9}
2	2 Generators	{G1,G2},{G1,G3},{G1,G4},{G1,G7},{G1,G8},{G1,G9}, {G1,G10},{G1,G11},{G2,G3},{G2,G4},{G2,G7}, {G2,G8},{G2,G9},{G2,G10},{G2,G11},{G4,G7}, {G7,G8},{G7,G9},{G7,G10},{G7,G11}
	2 Lines	{L1,L6},{L5,L8}
	1 Gen, 1 Line	None
3	3 Generators	{G3,G5,G7},{G3,G6,G7},{G4,G8,G9},{G4,G8,G10}, {G4,G9,G10},{G4,G9,G11},{G4,G10,G11}, {G8,G9,G10},{G8,G9,G11},{G8,G10,G11}, {G9,G10,G11}
	3 Lines	{L1,L2,L7},{L2,L3,L7},{L2,L4,L5}, {L2,L6,L7},{L3,L4,L8},{L4,L5,L7}
	1 Gen, 2 Lines	{G1,L2,L7},{G2,L2,L7}
	2 Gens, 1 Line	{G3,G7,L1},{G3,G7,L6}

Table 4.2: System Reliability and Operational Risk for RBTS

Cut Set Order	Cut Set Groups	$p(\bar{C}_h)^{\infty}$	$p(\bar{C}_h)^{10}$
1	1 Generator	-	-
	1 Line	0.0011400	0.0007213
2	2 Generators	0.0100506	0.0003586
	2 Lines	4.222E-06	1.690E-06
	1 Generator, 1 Line	-	-
3	3 Generators	5.440E-05	3.070E-07
	3 Lines	2.770E-07	7.060E-08
	1 Generator, 2 Lines	1.926E-06	1.586E-07
	2 Generators, 1 Line	1.386E-06	2.784E-08
System LOLP (p_{sys}^{∞}) & Operational Risk (p_{sys}^{10})		0.0112529	0.0010822

Once the unavailabilities are obtained for each minimal cut set group, the system reliability and risk can be determined using (2.7). In the RBTS under study, the system reliability is found to be 0.0112529. The operational risk for a lead-time of 10 hours after the event, assuming that the system loads remain the same during this period is obtained to be 0.0010822. The same set of minimal cut sets are used for this purpose.

B. IEEE RTS

The same exercise is repeated for the IEEE RTS. In Table 4.3, it is seen that there is no first-order minimal cut set. There are 20 second-order minimal cut sets where both components are generators, 8 minimal cut sets where both components are transmission lines, and 3 second-order minimal cut sets of generator-line pairing. In the same way, the third-order minimal cut sets are also determined to be 327, 80, 54 and 106 when the three components on outage simultaneously are generators, transmission lines, one-generator-two-lines triad, and two-generator-one-line triad, respectively.

The system reliability and risk calculation are carried out for the IEEE RTS. The minimal cut set groups along with their corresponding outage probabilities at the steady-state and the lead-time of 10 hours after the event are determined to 0.1562166 and 0.001755074, respectively, as presented in Table 4.4.

4.4.2 Determining Critical Components

A. RBTS

Ranking calculations are performed on two component types, generators and lines. By using the procedure described in Section 4.2 and Fig. 4.2 on component G1 for the steady-state condition, the first row in Table 4.5 shows the complete list of the system minimal cut sets {Z}. The next row shows the set $\{X_{G1}\}$ of minimal cut sets associated with component G1. For each of these minimal cut sets, $p(\bar{C}_h)^{\infty}_{G1}$ and $LNSI_{\bar{C}_h,G1}$ are calculated.

Table 4.3: System Minimal Cut Sets for IEEE RTS

Cut Set Order	Cut Set Groups	Minimal Cut Sets {Z}
1	Generator Only (1G)	None
	Line Only (1L)	None
2	Generators Only (2G)	{GE12,GE22},{GE12,GE23},{GE12,GE32},{GE13,GE22},{GE13,GE23}, {GE13,GE32},{GE14,GE22},{GE14,GE23},{GE14,GE32},{GE20,GE22}, {GE20,GE23},{GE21,GE22},{GE21,GE23},{GE22,GE23},{GE22,GE30}, {GE22,GE31},{GE22,GE32},{GE23,GE30},{GE23,GE31},{GE23,GE32}
	Lines Only (2L)	{L2,L7},{L2,L27},{L3,L9},{L4,L8},{L5,L10},{L11,L13}, {L12,L13},{L19,L23}
	One Generator + One Line (1G+1L)	{GE22,L11},{GE23,L11},{GE32,L11}
3	Generators Only (3G)	{GE1,GE9,GE22},{GE1,GE9,GE23},{GE1,GE10,GE22},{GE1,GE10,GE23}, {GE1,GE11,GE22},{GE1,GE11,GE23},{GE1,GE20,GE32},{GE1,GE21,GE32}, {GE1,GE30,GE32},{GE1,GE31,GE32},{GE2,GE9,GE22},{GE2,GE9,GE23}, {GE2,GE10,GE22},{GE2,GE10,GE23},{GE2,GE11,GE22},{GE2,GE11,GE23}, {GE2,GE20,GE32},{GE2,GE21,GE32},{GE2,GE30,GE32},{GE2,GE31,GE32}, ...,{GE29,GE30,GE32},{GE29,GE31,GE32},{GE30,GE31,GE32}
	Lines Only (3L)	{L1,L4,L10},{L1,L6,L7},{L1,L6,L27},{L1,L8,L10},{L1,L10,L11}, {L1,L10,L14},{L1,L10,L15},{L3,L4,L5}, {L4,L5,L7},{L4,L5,L9}, {L4,L5,L13},{L4,L5,L14},{L4,L5,L15}, {L4,L5,L16},{L4,L5,L17}, {L4,L5,L18}, {L4,L5,L20}, {L4,L5,L21},{L4,L5,L22},{L4,L5,L25}, {L4,L5,L26},.....,{L25,L26,L28},{L29,L34,L35},{L29,L36,L37}
	One Generator + Two Lines (1G+2L)	{GE1,L6,L7},{GE1,L6,L27},{GE2,L6,L7},{GE2,L6,L27},{GE3,L6,L7}, {GE3,L6,L27},{GE4,L6,L7},{GE4,L6,L27},{GE5,L1,L10},{GE5,L6,L7}, {GE5,L6,L27},{GE6,L1,L10},{GE6,L6,L7},{GE6,L6,L27},{GE7,L1,L10}, {GE7,L6,L7},{GE7,L6,L27},{GE8,L1,L10},{GE8,L6,L7},{GE8,L6,L27}, ...,{GE32,L23,L29},{GE32,L24,L28},{GE32,L31,L38}
	Two Generators + One Line (2G+1L)	{GE9,GE10,L11},{GE9,GE10,L13},{GE9,GE11,L11},{GE9,GE11,L13}, {GE9,GE22,L7},{GE9,GE22,L17},{GE9,GE22,L27},{GE9,GE23,L7}, {GE9,GE23,L27},{GE10,GE11,L11},{GE10,GE11,L13},{GE10,GE22,L7}, {GE10,GE22,L17},{GE10,GE22,L27},{GE10,GE23,L7},{GE10,GE23,L27}, {GE11,GE22,L7},{GE11,GE22,L17}, {GE11,GE22,L27},{GE11,GE23,L7}, ...,{GE31,GE32,L30},GE {GE31,GE32,L31},{GE31,GE32,L38}

Table 4.4: System Reliability and Operational Risk for IEEE RTS

Cut Set Order	Cut Set Groups	$p(\bar{C}_h)^{\infty}$	$p(\bar{C}_h)^{10}$
1	1 Generator	-	-
	1 Line	-	-
2	2 Generators	0.12	0.00159648
	2 Lines	EPS	EPS
	1 Generator, 1 Line	0.00010955	EPS
3	3 Generators	0.035981	0.000150549
	3 Lines	EPS	EPS
	1 Generator, 2 Lines	EPS	EPS
	2 Generators, 1 Line	0.000123312	EPS
System LOLP (p^{∞}_{sys}) & Operational Risk (p^{10}_{sys})		0.1562166	0.001755074

*EPS: very small number

The criticality index for G1, CR^{∞}_{G1}, is found to be 6.58E-04, applying (4.1). The same exercise is repeated for all components at steady-state and T=10 hrs, and the criticality indices are determined for each component under study. Calculations are carried out on components if a single, double or triple outage occurs.

The list of system components are now ranked by Criticality Index as presented in Table 4.6. It can be observed from Fig. 4.3 that bus-6 is located far from the generation units and is connected to the system by a single line (L9). Although L9 seems to be the most critical component because of its location and its outage will cause a system failure, it is fourth in the ranking, under steady state condition, for its lower failure rate, which means L9 less likely to fail as compared to G1. However, the likelihood of failure during operation can increase, and can change the criticality of a component. As observed in Table 4.7, the rank of L9 jumps from fourth to first place.

G1 and G2 are considered the most critical components in the system because of their reliability characteristics, capacities and locations followed by G7 which has the same failure rate and capacity as G1 and G2 but less critical location.

Table 4.5: Determining Criticality Index for G1 at $t = \infty$, RBTS

Set {Z}	{L9},{G1,G2},{G1,G3},{G1,G4},{G1,G7},{G1,G8},{G1,G9},{G1,G10},{G1,G11},{G2,G3}, {G2,G4},{G2,G7},{G2,G8},{G2,G9},{G2,G10},{G2,G11},{G4,G7},{G7,G8},{G7,G9}, {G7,G10},{G7,G11},{L1,L6},{L5,L8},{G3,G5,G7},{G3,G6,G7},{G4,G8,G9},{G4,G8,G10}, {G4,G9,G10},{G4,G9,G11},{G4,G10,G11},{G8,G9,G10},{G8,G9,G11},{G8,G10,G11}, {G9,G10,G11},{L1,L2,L7},{L2,L3,L7},{L2,L4,L5},{L2,L6,L7},{L3,L4,L8},{L4,L5,L7}, {G1,L2,L7},{G2,L2,L7},{G1,L2,L7},{G2,L2,L7},{G3,G7,L1},{G3,G7,L6}			
Set $\{X_{cm}\}$ $cm = G1$	{G1,G2},{G1,G3},{G1,G4},{G1,G7},{G1,G8}, {G1,G9},{G1,G10},{G1,G11},{G1,L2,L7}			
$(\bar{C}_h)_{G1}$ $\forall\ \bar{C}_h \in \{X_{G1}\}$	$p(\bar{C}_h)^{\infty}_{G1}$ $\forall\ \bar{C}_h \in \{X_{G1}\}$	$LNSI_{\bar{C}_h,G1}$ (p.u.)	$p(\bar{C}_h)^{\infty}_{G1}.LNSI_{\bar{C}_h,G1}$ (p.u.)	CR^{∞}_{G1} (p.u.)
{G2, G1}	0.000894	0.292	2.6105E-04	
{G3, G1}	0.000602	0.0009	5.4180E-07	
{G4, G1}	0.0007488	0.097	7.2634E-05	
{G7, G1}	0.000602	0.276	1.6615E-04	
{G8, G1}	0.0004439	0.089	3.9507E-05	6.58E-04
{G9, G1}	0.0004439	0.089	3.9507E-05	
{G10, G1}	0.0004439	0.089	3.9507E-05	
{G11, G1}	0.0004439	0.089	3.9507E-05	
{L2,L7, G1}	9.631E-07	0.038	3.6598E-08	

B. IEEE RTS

The same exercise is repeated for the IEEE RTS considering the step-wise procedure for determining the critical components discussed in Section 4.2. Table 4.8, presents the procedures performed on G1. There 10 minimal cut sets associated with component G1 $\{X_{G1}\}$. For each of these minimal cut sets, $p(\bar{C}_h)^{\infty}_{G1}$ and $LNSI_{\bar{C}_h,G1}$ are and hence the criticality index for G1, CR^{∞}_{G1}, is found to be 0.0004655. The same exercise is repeated for all components at steady-state and T=10 hrs, and the criticality indices are obtained for each component under study.

The list of ranked components at steady-state and lead-time of 10 hours are presented in Tables 4.9 and 4.10, respectively. It can be observed from Fig. 3.5 that G22 and G23 are the most critical components in the system because of their capacity sizes and reliability

Table 4.6: Ranking of Components by Criticality Index at $t = \infty$, RBTS

cm	f_{cm}	CR^{∞}_{cm}	$Rank$	cm	f_{cm}	CR^{∞}_{cm}	$Rank$
G1	9	6.58E-04	1	G3	6	1.37E-06	11
G2	9	6.58E-04	2	L6	3	7.16E-07	12
G7	11	4.70E-04	3	L8	2	5.21E-07	13
L9	1	2.28E-04	4	L5	3	5.21E-07	14
G4	9	1.90E-04	5	L7	6	1.63E-07	15
G8	9	1.05E-04	6	G5	1	1.40E-07	16
G9	9	1.05E-04	7	G6	1	1.40E-07	17
G10	9	1.05E-04	8	L2	6	1.27E-07	18
G11	9	1.05E-04	9	L3	2	8.41E-08	19
L1	3	2.42E-05	10	L4	3	1.88E-09	20

Table 4.7: Ranking of Components by Criticality Index at $t = 10$ hr, RBTS

cm	f_{cm}	CR^{10}_{cm}	$Rank$	cm	f_{cm}	CR^{10}_{cm}	$Rank$
L9	1	0.00072	1	L6	3	2.9E-07	11
G1	9	2.5E-05	2	L5	3	2.8E-07	12
G2	9	2.5E-05	3	L8	2	2.1E-07	13
G7	11	1.4E-05	4	G3	6	4.7E-08	14
G4	9	7.4E-06	5	L7	6	2.9E-08	15
G8	9	3.4E-06	6	L2	6	2.6E-08	16
G9	9	3.4E-06	7	L3	2	2.1E-08	17
G10	9	3.4E-06	8	G5	1	8.9E-10	18
G11	9	3.4E-06	9	G6	1	8.9E-10	19
L1	3	6.3E-07	10	L4	3	4.8E-10	20

characteristics, followed by G32 which has a higher failure rate but less capacity.

It can observed from Fig.3.5 that although bus-7 is only connected to the system by line L11; the ranking of L11 is still twenty-second, which is not a very critical component in the system. The reason being the presence of three large generators with relatively low demand at the bus, and the low outage rate of L11. However, the likelihood of failure can increase at the operational stage and can change the criticality of a component.

Table 4.8: Determining Criticality Index for G1 at $t = \infty$, IEEE RTS

Set {Z}	{G12,G22},{G12,G23},{G12,G32},{G13,G22},{G13,G23},{G13,G32},{G14,G22}, {G14,G23},{G14,G32},{G20,G22},{G20,G23},{G21,G22},{G21,G23},{G22,G23},{G22,G30}, {G22,G31},{G22,G32},{L2,L7},{L2,L27},{L3,L9},{L4,L8},{L5,L10},{L11,L13},L {L12,L13}, {L19,L23},{G22,L11},{G23,L11},{G32,L11},{G1,G9,G22},{G1,G9,G23}, {G1,G10,G22},{G1,G10,G23},{G1,G11,G22},{G1,G11,G23},{G1,G20,G32}, {G1,G21,G32},{G1,G30,G32},{G1,G31,G32},{G2,G9,G22},{G2,G9,G23}, {G2,G10,G22},{G2,G10,G23},{G2,G11,G22},{G2,G11,G23},{G2,G20,G32}, {G2,G21,G32},{G2,G30,G32},{G2,G31,G32},{L1,L4,L10},{L1,L6,L7},{L1,L6,L27}, {L1,L8,L10},{L1,L10,L11},{L1,L10,L14},{L1,L10,L15},{L3,L4,L5},{L4,L5,L7}, {L4,L5,L9},{L4,L5,L13},{L4,L5,L14},{L4,L5,L15},{L4,L5,L16},{L4,L5,L17}, {L4,L5,L18},{L4,L5,L20},{L4,L5,L21},{L4,L5,L22},{L4,L5,L25}, {L4,L5,L26},{G1,L6,L7}{G1,L6,L27},{G2,L6,L7},{G2,L6,L27},{G3,L6,L7}, ……,{GE31,GE32,L30},{GE31,GE32,L31},{GE31,GE32,L38}			
Set $\{X_{cm}\}$ $cm = G1$	{G1,G9,G22},{G1,G10,G22},{G1,G10,G22},{G1,G10,G23},{G1,G11,G22}, {G1,G11,G23},{G1,G20,G32},{G1,G21,G32},{G1,G30,G32},{G1,G31,G32}			
$(\bar{C}_h)_{G1}$ $\forall\ \bar{C}_h \in \{X_{G1}\}$	$p(\bar{C}_h)^{\infty}_{G1}$ $\forall\ \bar{C}_h \in \{X_{G1}\}$	$LNSI_{\bar{C}_h,G1}$ (p.u.)	$p(\bar{C}_h)^{\infty}_{G1}.LNSI_{\bar{C}_h,G1}$ (p.u.)	CR^{∞}_{G1} (p.u.)
{G9,G22,G1}	0.00048	0.09505	0.000045624	
{G9,G23,G1}	0.00048	0.07604	0.000036499	
{G10,G22,G1}	0.00048	0.07604	0.000036499	
{G10,G23,G1}	0.00048	0.09505	0.000045624	
{G11,G22,G1}	0.00048	0.09505	0.000045624	0.0004655
{G11,G23,G1}	0.00048	0.07604	0.000036499	
{G20,G32,G1}	0.00032	0.157	0.00005024	
{G21,G32,G1}	0.00032	0.163	0.00005216	
{G30,G32,G1}	0.00032	0.182	0.00005824	
{G31,G32,G1}	0.00032	0.182	0.00005824	

Table 4.9: Ranking List of Components Importance at $t = \infty$, IEEE RTS

cm	f_{cm}	CR^{∞}_{cm}	$Rank$	cm	f_{cm}	CR^{∞}_{cm}	$Rank$	cm	f_{cm}	CR^{∞}_{cm}	$Rank$	cm	f_{cm}	CR^{∞}_{cm}	$Rank$
G22	100	0.088003	1	G2	10	0.000466	19	L19	3	EPS	37	L36	1	EPS	55
G23	100	0.086602	2	G5	10	0.000466	20	L8	2	EPS	38	L34	1	EPS	56
G32	121	0.049186	3	G6	10	0.000466	21	L4	22	EPS	39	L16	22	EPS	57
G12	18	0.012247	4	L11	9	5.87E-05	22	L13	14	EPS	40	L17	19	EPS	58
G13	18	0.012247	5	G24	18	5.57E-05	23	L9	9	EPS	41	L14	9	EPS	59
G14	18	0.012126	6	G25	18	5.57E-05	24	L3	4	EPS	42	L15	8	EPS	60
G20	39	0.005689	7	G26	18	5.57E-05	25	L2	3	EPS	43	L28	4	EPS	61
G21	39	0.005667	8	G27	18	5.57E-05	26	L27	22	EPS	44	L18	1	EPS	62
G30	39	0.005377	9	G28	18	5.57E-05	27	L7	22	EPS	45	L20	1	EPS	63
G31	39	0.005369	10	G29	18	5.57E-05	28	L12	2	EPS	46	L35	1	EPS	64
G9	53	0.002383	11	G15	10	2.93E-05	29	L6	15	EPS	47	L37	1	EPS	65
G10	53	0.002383	12	G16	10	2.93E-05	30	L24	3	EPS	48	L30	0	0	66
G11	53	0.002365	13	G17	10	2.93E-05	31	L1	7	EPS	49	L31	0	0	67
G7	34	0.000768	14	G18	10	2.93E-05	32	L29	7	EPS	50	L32	0	0	68
G8	34	0.000768	15	G19	10	2.93E-05	33	L21	2	EPS	51	L33	0	0	69
G3	34	0.000767	16	L5	26	EPS	34	L22	2	EPS	52	L38	0	0	70
G4	34	0.000767	17	L10	8	EPS	35	L25	2	EPS	53				
G1	10	0.000466	18	L23	5	EPS	36	L26	2	EPS	54				

*EPS: very small number

Table 4.10: Ranking List of Components Importance at $t = 10$, IEEE RTS

cm	f_{cm}	CR^{∞}_{cm}	$Rank$	cm	f_{cm}	CR^{∞}_{cm}	$Rank$	cm	f_{cm}	CR^{∞}_{cm}	$Rank$	cm	f_{cm}	CR^{∞}_{cm}	$Rank$
G22	100	0.000745	1	G1	10	1.71E-06	19	G19	10	EPS	37	L34	1	EPS	55
G23	100	0.000727	2	G2	10	1.71E-06	20	L4	22	EPS	38	L1	7	EPS	56
G32	121	0.000429	3	G5	10	1.71E-06	21	L8	2	EPS	39	L16	22	EPS	57
G12	18	0.000176	4	G6	10	1.71E-06	22	L13	14	EPS	40	L17	19	EPS	58
G13	18	0.000176	5	G24	18	EPS	23	L9	9	EPS	41	L14	9	EPS	59
G14	18	0.000175	6	G25	18	EPS	24	L3	4	EPS	42	L15	8	EPS	60
G20	39	7.88E-05	7	G26	18	EPS	25	L2	3	EPS	43	L28	4	EPS	61
G21	39	7.83E-05	8	G27	18	EPS	26	L27	22	EPS	44	L18	1	EPS	62
G30	39	7.28E-05	9	G28	18	EPS	27	L7	22	EPS	45	L20	1	EPS	63
G31	39	7.27E-05	10	G29	18	EPS	28	L12	2	EPS	46	L35	1	EPS	64
G9	53	8.21E-06	11	L23	5	EPS	29	L24	3	EPS	47	L37	1	EPS	65
G10	53	8.21E-06	12	L19	3	EPS	30	L6	15	EPS	48	L30	0	0	66
G11	53	8.09E-06	13	L5	26	EPS	31	L29	7	EPS	49	L31	0	0	67
G7	34	3.07E-06	14	L10	8	EPS	32	L21	2	EPS	50	L32	0	0	68
G8	34	3.07E-06	15	G15	10	EPS	33	L22	2	EPS	51	L33	0	0	69
G3	34	3.07E-06	16	G16	10	EPS	34	L25	2	EPS	52	L38	0	0	70
G4	34	3.07E-06	17	G17	10	EPS	35	L26	2	EPS	53				
L11	9	2.87E-06	18	G18	10	EPS	36	L36	1	EPS	54				

*EPS: very small number

4.5 Validation of Components' Criticality

In this validation exercise, carried out on the IEEE RTS at the steady-state condition, four components G22, G13, G31 and L11 are arbitrary selected. The OPF is executed with one of these components on outage at a time. The nodal and system LOLP is then calculated and compared to the base case with no component on outage. It can be observed from Fig. 4.4 and Table 4.11, that the novel OPF based procedure proposed to compute the nodal and system minimal cut sets for composite power systems, not only provides information on system and nodal reliability and risk indices, but in the process, can also give a sense of identifying of critical components and rank their importance in the system without the need of testing each component individually and therefore reduces the computational time.

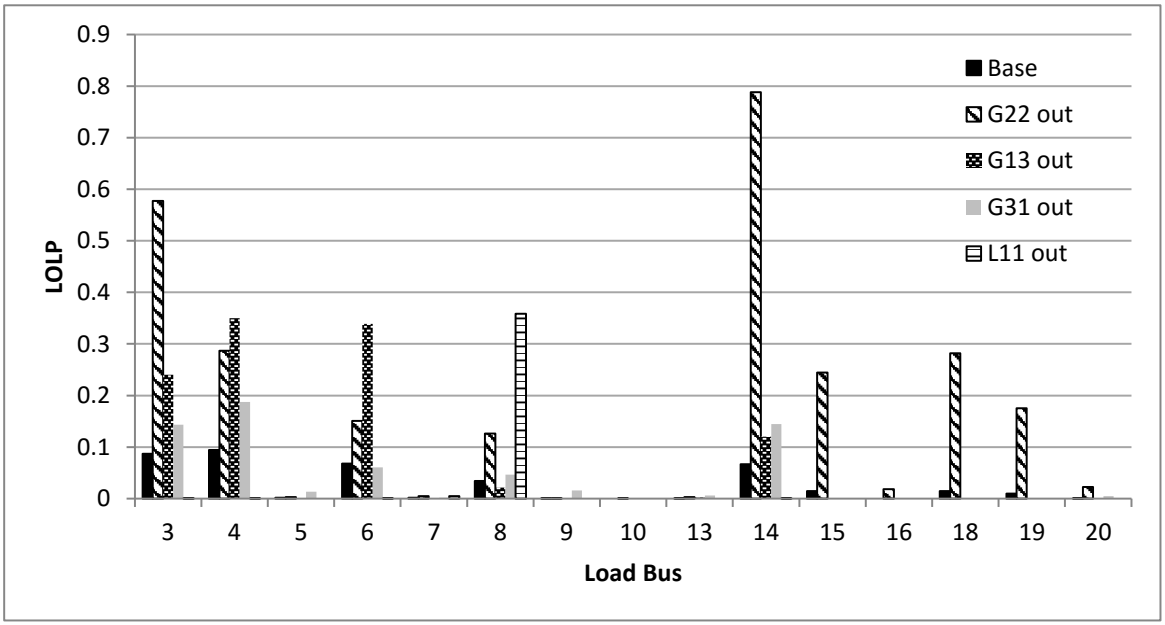

Figure 4.4: Nodal LOLP at Different Outages for IEEE RTS at $t = \infty$.

Table 4.11: Ranking List of Components Importance at $t = \infty$, IEEE RTS

Bus	LOLP				
	Base	G22 out	G13 out	G31 out	L11 out
3	0.087241	0.577139	0.240016	0.143444	6.87E-06
4	0.094343	0.286786	0.350166	0.187727	7.14E-07
5	0.001601	0.002767	0.00024	0.013389	1.46E-07
6	0.068153	0.150971	0.338983	0.060883	1.36E-06
7	0.001608	0.0048	0.001318	0.001751	0.0048
8	0.034262	0.126447	0.021162	0.046394	0.358526
9	0.000128	7.36E-05	1.18E-07	0.015741	3.62E-08
10	0	0.000105	1.06E-08	0.000637	2.99E-13
13	0.000125	0.002954	0.0025	0.006191	0
14	0.066775	0.788178	0.120008	0.144579	0.000128
15	0.0144	0.244473	0	0	0
16	0	0.018122	0	6.40E-05	0
18	0.014403	0.28192	0	5.18E-05	0
19	0.009603	0.174989	2.75E-10	0.000524	1.75E-10
20	0.000128	0.022687	2.27E-08	0.004984	7.77E-11
System	0.15621282	0.979131	0.359964	0.312021	0.242223

4.6 Summary

In this chapter, the concept of minimal cut sets was applied to identify critical components in the composite power system. The proposed method, applied to the 6-bus RBTS and the 24-bus IEEE RTS involved solving an appropriate OPF to obtain the system minimal cut sets under outage condition of generators, transmission lines, or both. Once the component unavailabilities were calculated using failure and repair rate data, the minimal cut set probabilities were determined, which were then used to evaluate component Criticality Indices. The proposed method provided a ranking of components' criticality and this information is important in decision making pertaining to maintenance scheduling, generator investments and line upgrading.

Chapter 5

Impact of EV Charging Loads and Demand Response on Composite Reliability Assessment and Critical Component Identification[‡]

5.1 Introduction

This chapter presents a reliability assessment framework for composite power systems taking into account both uncontrolled and smart charging PEV loads as well as DR options and determines the minimal cut sets for the system. Various combinations of shares of uncontrolled and smart charging PEVs are examined to determine the system adequacy indices. Furthermore, this is extended to include the identification of critical components

[‡]Parts of this chapter have been submitted as a paper for review in: B. Lami, A. B. Humayd and K. Bhattacharya, "Impact of EV Charging Loads and DR on Composite System Reliability and Critical Component Identification," *IEEE Transactions on Power Systems.*

[*]An earlier versions of this work was published in: B. Lami, A. B. Humayd and K. Bhattacharya, "Adequacy Assessment of Power Systems with PEV Charging Loads Considering Customer Behaviour," *in Proc. of IEEE PES General Meeting, Boston, MA, USA,* pp. 1-5, July. 2016.

of the system in the presence of PEV loads and DR.

5.2 System Models Including PEV Loads and DR for Reliability Assessment

5.2.1 Uncontrolled PEV Charging Load Model

Using driver behaviour, vehicle type and charging level information, the uncontrolled PEV charging load profiles at each bus can be developed and added to the nominal load profile, for use in the reliability model.

First, the probability density functions (pdf) of PEV driving pattern parameters, namely daily mileage driven and home arrival times are extracted using the NHTS data [38]. Thereafter, the SOC and the charging duration, T^D, of each vehicle in the fleet is calculated from the mileage driven data (D^{km}), generated using the pdf of the daily mileage, the driving range in the electrical mode (AER), the SOC^{min} and depth of discharge (DOD) of the vehicle as follows:

$$SOC = \begin{cases} SOC^{min} + (1 - \frac{D^{km}}{AER})DOD & D^{km} \leq AER, \\ SOC^{min} & D^{km} > AER. \end{cases} \tag{5.1}$$

T^D for each vehicle in the fleet is estimated from the power drawn at a given charging level (P^{ChL}), the charging efficiency (η), the SOC of the vehicle, and the battery capacity, B^{Cap}.

$$T^D = \frac{(1 - SOC)B^{Cap}}{P^{ChL}\,\eta}. \tag{5.2}$$

The starting time of charging can be modelled considering two realistic scenarios to mimic the behaviour of PEV customers, and hence assess the impact of the charging load, arising there from, on system reliability, as discussed below:

- *Arrive and Plug* (A&P) - it is assumed that customers will start charging their

vehicles immediately after the last trip to home.

- *Time of Use* (TOU) Price Based - the PEV drivers are assumed to respond to TOU price, starting to change at the onset of the off-peak price at 7 PM. The starting time of charging follows a Poisson distribution where the charging delay, γ, obtained considering Ontario TOU price. For example, for on-peak arrivals, γ is the wait time from their arrival to the onset of off-peak TOU price, while for off-peak arrivals, $\gamma =$ 0.1 hour.

Finally, the uncontrolled charging profile can be constructed using determined parameters, *i.e.* charging duration and starting time of charging, for each vehicle in the fleet.

5.2.2 Smart-OPF Considering PEVs and DR

The objective function aims to minimize the total load curtailment, as given below:

$$J = \sum_{i=1}^{N} \sum_{hr=1}^{24} Pd_{i,hr}^{UNM} \tag{5.3}$$

subject to the following constraints:

1. *Active and Reactive Power Balance*: is ensured by the power flow equations, which include Pd^{UNM} and Qd^{UNM}, the real and reactive power load curtailment variables, respectively, that may arise from the outages of various components.

$$\begin{aligned} Pg_{i,hr} - Pd_{i,hr} - \Delta PD_{i,hr}^{UP} + \Delta PD_{i,hr}^{DN} + Pd_{i,hr}^{UNM} - \sum_{c} \sum_{cl} P_{i,hr,c,cl}^{EV\_S} - P_{i,hr}^{PEV\_Unc} \\ = \sum_{j=1}^{N} \sum_{hr=1}^{24} |V_{i,hr}||V_{j,hr}||Y_{ij}|cos(\theta_{ij,hr} + \delta_{j,hr} - \delta_{i,hr}), \end{aligned} \tag{5.4}$$

$$Qg_{i,hr} - Qd_{i,hr} + Qd^{UNM}_{i,hr} = -\sum_{j=1}^{N}\sum_{hr=1}^{24}|V_{i,hr}||V_{j,hr}||Y_{ij}|sin(\theta_{ij,hr} + \delta_{j,hr} - \delta_{i,hr}) \quad (5.5)$$

where

$$Qd^{UNM}_{i,hr} = Pd^{UNM}_{i,hr}tan[cos^{-1}(pf)]. \quad (5.6)$$

$Qd^{UNM}_{i,hr}$ is the relief in reactive power associated with $Pd^{UNM}_{i,hr}$, and depends on the load power factors pf [81].

2. *Smart Charging Constraints*: These constraints ensure that the total energy required by PEVs of class c is equal to the daily charging energy drawn from the grid and that the maximum power drawn by PEVs is specified by the charging level.

$$\sum_{hr=1}^{24} P^{EV\_S}_{i,hr,c,cl} = \beta N^{EV}_{i,c,cl}E_c \qquad \forall\ i,c,cl, \quad (5.7)$$

$$P^{EV\_S}_{i,hr,c,cl} \leq \beta N^{EV}_{i,c,cl}P_{cl} \qquad \forall\ i,hr,c,cl, \quad (5.8)$$

3. *DR Constraints*: Theses constrains ensure the maximum and minimum allowable demand to be shifted from hour to hour, which are limited by B_{UP} and B_{DN}.

$$\sum_{hr=1}^{24} \Delta PD^{UP}_{i,hr} = \sum_{hr=1}^{24} \Delta PD^{DN}_{i,hr}, \quad (5.9)$$

$$\Delta PD^{UP}_{i,hr} \leq B_{UP}.Pd_{i,hr}, \quad (5.10)$$

$$\Delta PD^{DN}_{i,hr} \leq B_{DN}.Pd_{i,hr}. \quad (5.11)$$

Balancing the demand variations during the day from shifting to another day is defined by (5.9). Equations (5.10) and (5.11) are the maximum shiftable demand variation upward and downward.

4. *Limits on Load Curtailment*: This constraint adapts (adjusts) the loss of generation

that may occur from the outages of various components.

$$0 \leq Pd_{i,hr}^{UNM} \leq Pd_{i,hr}. \tag{5.12}$$

In addition, the model also considers the limits on bus voltages, active and reactive power generations, and transmission line capacities.

5.3 Composite Reliability Assessment and Critical Components

Failure of a component can be due to various reasons such as system overload, ageing of components, human error, weather, *etc.* Detecting the critical components of the system can help planners make decisions on new investments, and operators to maintain a secure supply during contingencies. Fig. 5.1 presents a detailed schematic of the proposed method to determine the critical components of a composite power system. The procedure begins with determining the system minimal cut sets ($\bar{C}_h$) at peak load (Fig. 5.1 (Part-I)), and is based on [82] which can be summarized as follows: select a cut set of order M, and execute the Smart-OPF, discussed in Section II-B, with all components of this cut set on outage. If there is a loss of load at any bus ($Pd_{i,hr}^{UNM} \neq 0$) then this cut set is a minimal cut set of order M. Repeat this procedure for all possible M^{th} order cut sets, and up to the desired order of M. Thereafter, as shown in Fig. 5.1 (Part-II), the minimal cut sets associated with a given component cm, $(\bar{C}_h)_{cm}$, denoted as set $\{X_{cm}\}$ are identified. Considering a specific minimal cut set from $\{X_{cm}\}$, execute the Smart-OPF again, with all components of the cut set on outage and hence calculate the probability of failure of this minimal cut set, $p(\bar{C}_h)_{cm}$, by multiplying the probability of failure of each cm that construct this minimal cut set. Estimate $LNSI_{\bar{C}_h,cm}$ associated with this minimal cut set and report the frequency of occurrence of the component f_{cm}. Check for all minimal cut sets associated with cm by repeating this procedure. Thereafter, the criticality index for

component cm is calculated as follows:

$$CR_{cm} = \sum_{h} p(\bar{C}_h)_{cm}.LNSI_{\bar{C}_h,cm}. \tag{5.13}$$

CR_{cm} is the EDNS for the component cm.

5.4 Case Studies and Assumptions

The main focus of this chapter is to evaluate the impact of PEV charging demand on system adequacy, considering different shares of uncontrolled and smart charging PEVs and different levels of DR. To this effect, several case studies are constructed adopting the two uncontrolled charging strategies (a) A&P and (b) TOU price based.

The proposed framework is tested on the IEEE RTS, Fig. 3.5, [73]. The considered PEVs are from eleven commonly found makes, based on their sales, and covers 95% of the total number of PEVs sold in the US between 2010 to 2015 [83]. These PEVs are grouped into four major classes, plug-in hybrid electric vehicle-I (PHEV), PHEV-II, battery electric vehicle-I (BEV) and BEV-II, with their parametric details provided in Table 5.1. The NHTS 2009 data [38] has been considered to simulate driver behaviour. The charging efficiency is assumed to be 90% [84–86], and two different charging levels are considered, Level-1 (1.44 kW) and Level-2 (7.2 kW), with a share of 65% and 35%, respectively [87]. The number of houses at a bus is calculated assuming that 15% of the total load is residential and the hourly load of a typical house is 2.08 kW [88]. It is assumed that 28% of the houses have electric cars [89], the number of vehicles per house is 2, and that PEV charging occurs only at home. For battery life consideration, it is assumed the battery depth of charge is 70%.

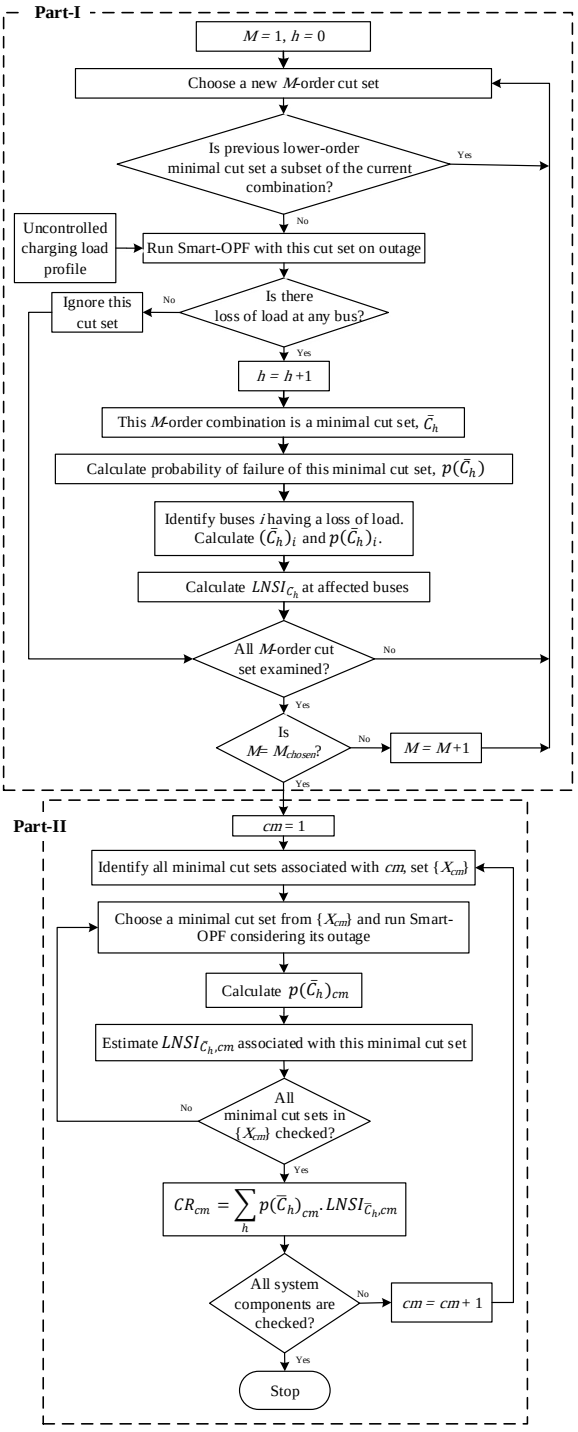

Figure 5.1: Schematic for determining composite system reliability indices and critical components.

Table 5.1:
PEV Classes Considered For Studies

	Market Share	Battery Capacity Range (kWh)	AER (km)	Weighted Average Battery Size (kWh)	Weighted Average AER (km)
PHEV-I	26%	4.4-7.6	18-32	5.76	24.03
PHEV-II	24%	18.4	85	18.40	85
BEV-I	34%	14-24	100-135	21.89	124.03
BEV-II	16%	85	426	85.00	426

The daily mileage driven and home arrival time data of the vehicle classes selected, are processed for developing in the pdfs in Fig. 5.2.

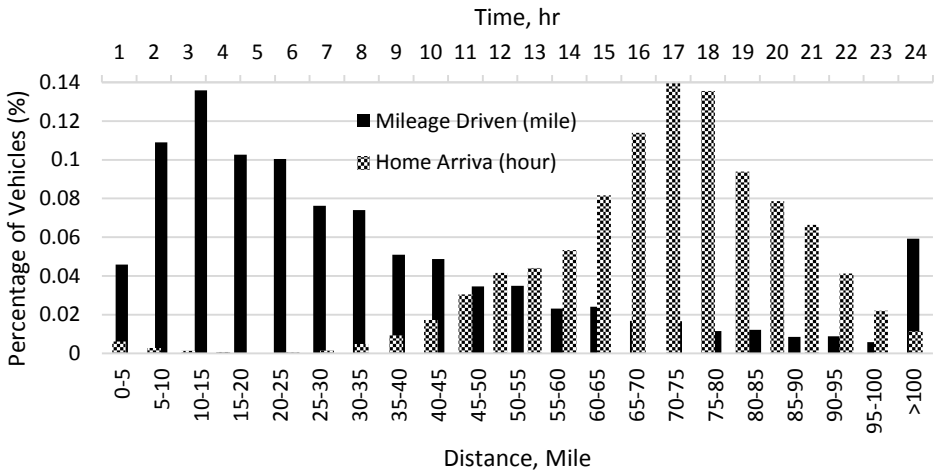

Figure 5.2. Mileage driven and home arrival pdf of PEVs.

5.5 Results And Discussions

5.5.1 Determining Reliability Indices in the Presence of PEVs

The 24 hour load profiles with 100% smart charging, and when the A&P based and TOU price based uncontrolled charging strategies account for 100% of the PEV charging load, are shown in Fig. 5.3. These are obtained from the Smart-OPF model, but without considering any outages, to examine the impact of smart charging *vis-à-vis* uncontrolled charging. It is noted that TOU price based uncontrolled charging results in more severe peak loading as compared to A&P based, while smart charging is able to control the load profile significantly, and the resulting profile is almost same as the base load profile.

The system minimal cut sets are identified using the method discussed in Section 5.2.2, up to the second-order, in order to keep the computational burden within reasonable limits, but without any loss of generality.

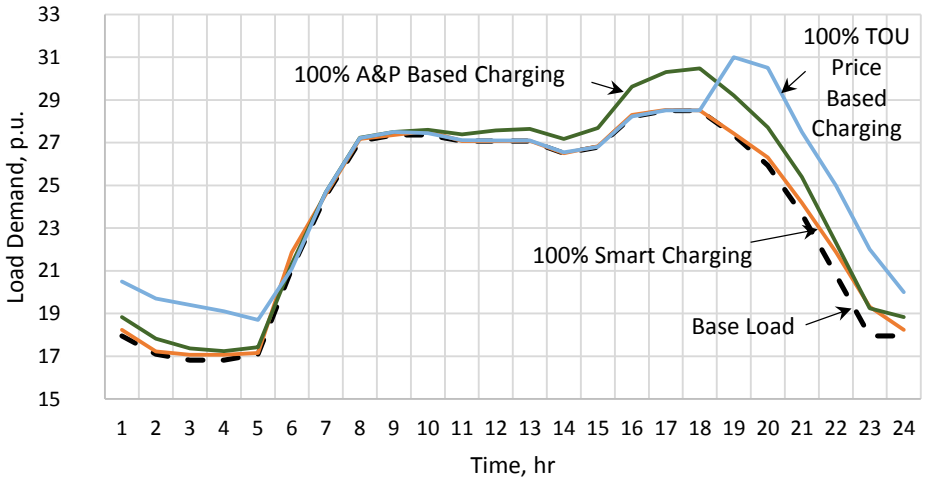

Figure 5.3. Load profiles for different charging shares, no DR.

Once the minimal cut sets are identified along with their outage probabilities, the corresponding reliability indices are determined, as discussed in Section 5.3. Fig.5.4 and Fig. 5.5 presents the hourly variation in LOLP and EDNS for different shares of uncontrolled and smart charging, without DR. It is noted that the reliability indices are worse during

hours 15-19, and significantly impacted by the share of uncontrolled charging. As this share decreases, and replaced by smart charging, the reliability is improved.

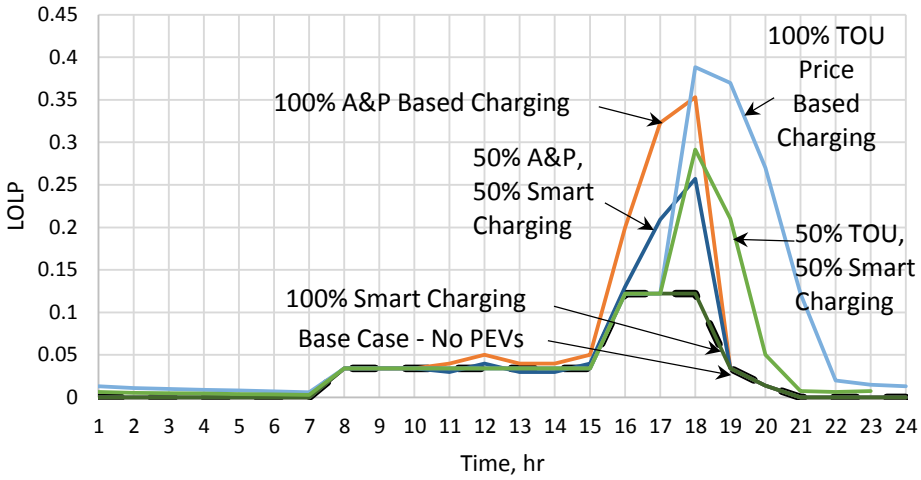

Figure 5.4. Hourly LOLP for different charging shares, no DR.

Table 5.2 presents the reliability indices for no DR, and with varying shares of uncontrolled versus smart charging of PEVs. These results are obtained by neglecting ΔPD^{UP} and ΔPD^{DN} in (5.4) and excluding the constraints (5.9) - (5.11) from the Smart-OPF model. It is noted that the reliability is worse affected with 100% uncontrolled charging and improves as smart charging penetration increases. Interestingly, the 100% smart charging case is able to provide the same level of reliability as with the case of no PEV loads.

The reliability indices for TOU price based uncontrolled charging are worse compared to the A&P based charging, since all PEVs react on the price signal at the same time. It can be seen from Table 5.2 that the $LOLP_{sys}$ is higher when considering TOU price based uncontrolled charging. However, it may be noted that TOU price can be appropriately adjusted by the utility to regulate the uncontrolled charging demand and hence can dampen the adverse impact on the system.

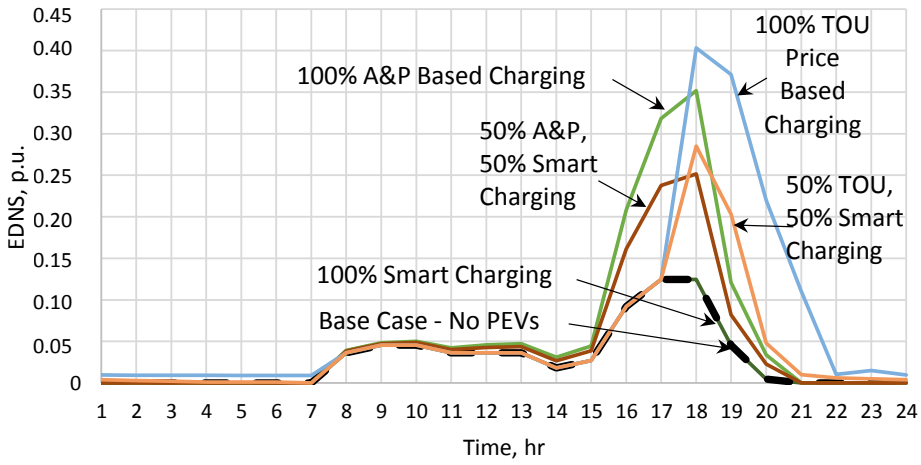

Figure 5.5. Hourly EDNS for different charging shares, no DR.

Table 5.2:
System Reliability Indices without DR

PEV Penetration (%)		A&P Based Charging			TOU Price Based Charging		
Uncontrolled	Smart	$LOLP_{Sys}$ at Peak	$LOLE$ (hr/day)	$EENS$ (p.u/day)	$LOLP_{Sys}$ at Peak	$LOLE$ (hr/day)	$EENS$ (p.u./day)
No PEV		0.1221	0.6864	0.6725	0.12211	0.6864	0.6725
100%	0%	0.3531	1.5536	1.6773	0.38837	1.6948	1.7596
90%	10%	0.3531	1.4262	1.6091	0.37078	1.5985	1.6779
80%	20%	0.3371	1.3656	1.5375	0.35675	1.3833	1.6111
70%	30%	0.2948	1.2995	1.4474	0.31144	1.3421	1.4951
60%	40%	0.2791	1.26	1.3811	0.30511	1.3102	1.4285
50%	50%	0.2571	1.0585	1.2134	0.26145	123.52	1.3302
40%	60%	0.2011	0.9365	1.0811	0.19857	0.9939	1.1009
30%	70%	0.1801	0.8675	0.9624	0.18912	0.8944	0.9958
20%	80%	0.1641	0.8264	0.8520	0.17232	0.8522	0.9082
10%	90%	0.1491	0.7254	0.7542	0.15422	0.7902	0.7945
0%	100%	0.1221	0.6864	0.6725	0.1221	0.6864	0.6725

5.5.2 Impact of PEV Charging and DR on Reliability

In this section, the DR option is introduced by including ΔPD^{UP} and ΔPD^{DN} in (5.4) and the constraints (5.9) - (5.11) in the Smart-OPF model. The purpose is to investigate the role of DR in assisting the system reliability. To this effect, two different values of B_{UP} and B_{DN} of 5% and 10% are considered.

The impact of DR on the charging of PEVs is shown in Fig. 5.6(a) and Fig. 5.6(b) without considering any outage. It is noted that if there is no DR, the desired adequacy level in the presence of PEVs, of $LOLP_{Sys} = 0.1221$, is only attained with 100% smart charging which is quite impractical to achieve in the near-term. Therefore, to maintain the desired adequacy level, DR is a viable option, and the impact of the demand participating in DR programs, *i.e.* the values of B_{UP} and B_{DN}, on system reliability need be investigated.

Comparing the plots in Fig. 5.6(a) and Fig. 5.6(b) with those in Fig. 5.3, it is noted that DR significantly dampens the peak load, to the order of about 200 MW, in the case of 100% A&P based PEV charging.

The same exercise in determining the minimal cut sets and the reliability indices is repeated considering DR. From Table 5.2 and 5.3, it is noted that for the cases with no PEV, $LOLP_{Sys}$ improved from 0.1221 (without DR) to 0.034 with 5% DR and to 0.014 with 10% DR.

When PEVs are considered and DR = 5%, it is noted from Table 5.3 that the value of $LOLP_{Sys}$ is high (=0.18) with 100% uncontrolled charging. As the smart charging share increases, $LOLP_{Sys}$ decreases, and with 30% smart charging, the designed adequacy level is achieved. It is noted that DR can significantly improve the reliability indices; when DR increases to 10% for both A&P based charging and TOU price based charging, the value of $LOLP_{Sys}$ is below the designed LOLP of 0.1221, even with 100% uncontrolled charging.

Fig. 5.7 and Fig. 5.8 presents the hourly variation of $LOLP_{Sys}$ and $EDNS$ for various shares of PEV smart charging, with 5% and 10% DR, respectively. It is noted from the figures that the DR has a significant impact on both the indices and can play a significant role in reliability enhancement.

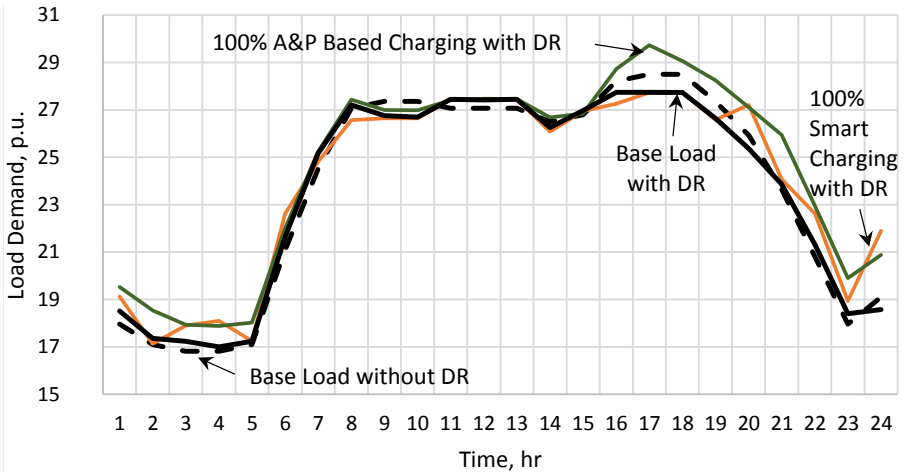

(a) DR = 5%

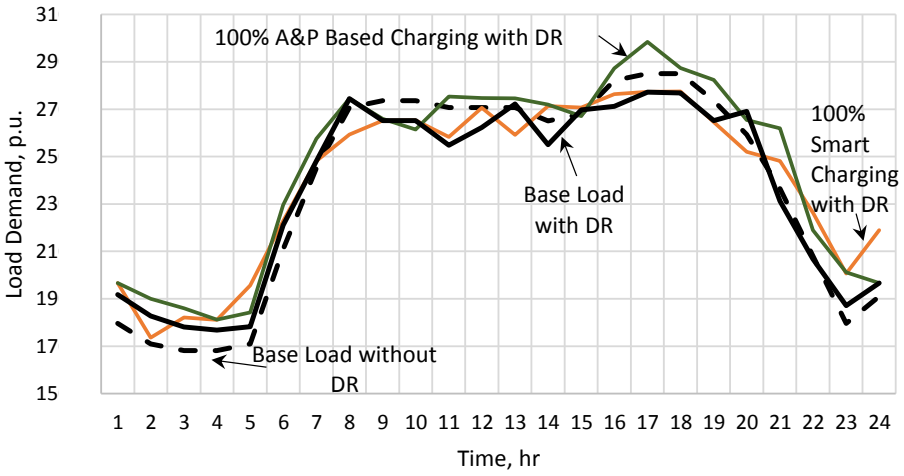

(b) DR = 10%

Figure 5.6. Load profiles for different charging shares, with DR.

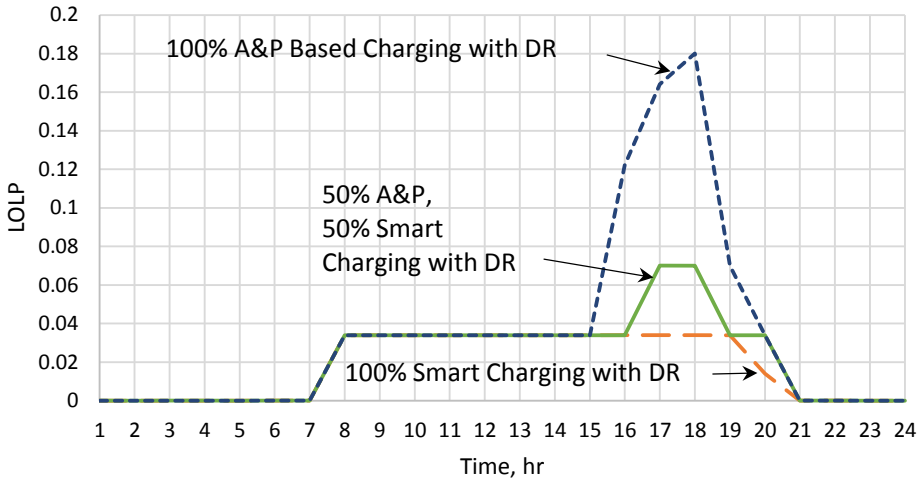

(a) DR = 5%

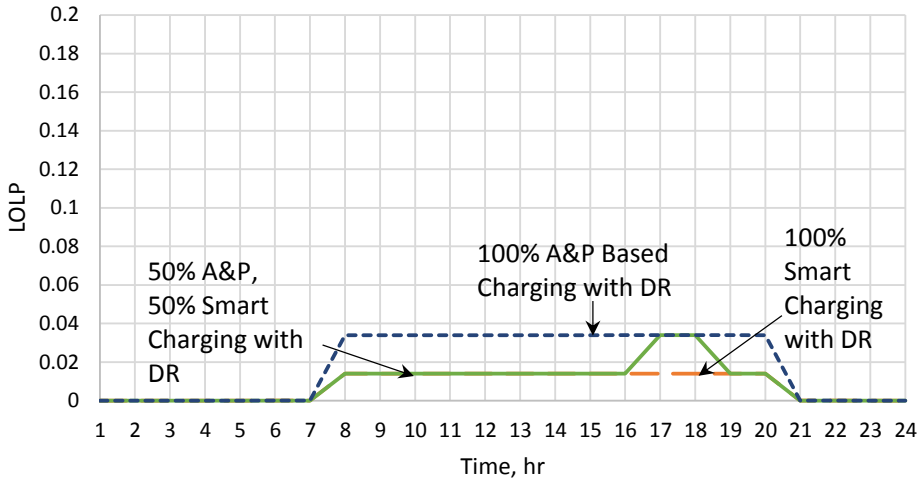

(b) DR = 10%

Figure 5.7. Hourly LOLP for different charging shares, with DR.

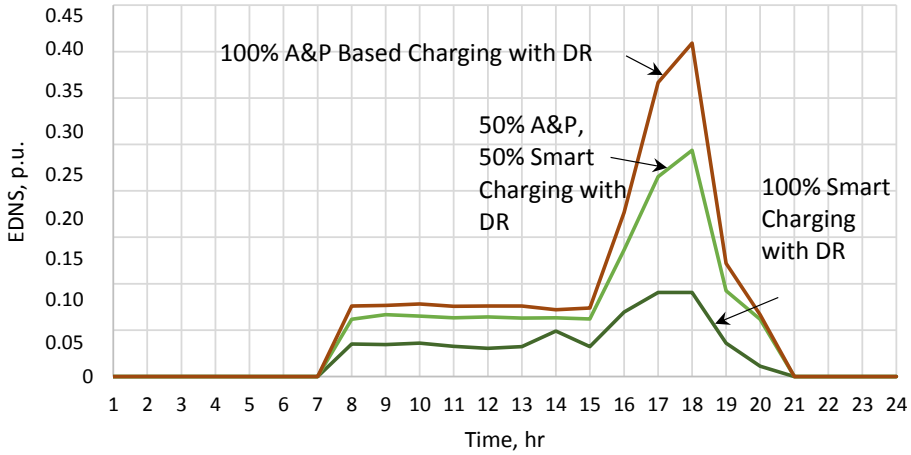

(a) DR = 5%

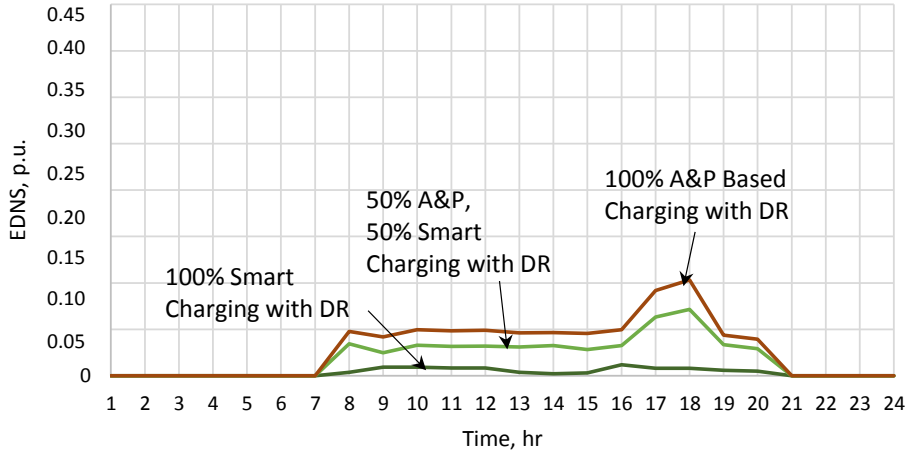

(b) DR = 10%

Figure 5.8. Hourly EDNS for different charging shares, with DR.

Table 5.3:
System Reliability Indices with DR

PEV Penetration (%)		A&P Based Charging						TOU Price Based Charging		
		5% DR			10% DR			10% DR		
Uncontrolled	Smart	$LOLP_{Sys}$ at Peak	$LOLE$ (hr/day)	$EENS$ (p.u./day)	$LOLP_{Sys}$ at Peak	$LOLE$ (hr/day)	$EENS$ (p.u./day)	$LOLP_{Sys}$ at Peak	$LOLE$ (hr/day)	$EENS$ (p.u./day)
No PEV		0.034	0.4221	0.2247	0.014	0.182	0.0345	0.014	0.182	0.0345
100%	0%	0.18	0.842	0.8549	0.034	0.442	0.372	0.034	0.476	0.386
90%	10%	0.164	0.723	0.7486	0.034	0.442	0.327	0.034	0.456	0.337
80%	20%	0.134	0.666	0.6582	0.034	0.442	0.281	0.034	0.456	0.289
70%	30%	0.122	0.654	0.5783	0.034	0.442	0.272	0.034	0.442	0.272
60%	40%	0.122	0.586	0.5037	0.034	0.442	0.191	0.034	0.442	0.191
50%	50%	0.07	0.514	0.4441	0.034	0.292	0.146	0.034	0.292	0.146
40%	60%	0.07	0.514	0.3904	0.034	0.222	0.117	0.034	0.222	0.117
30%	70%	0.034	0.442	0.3430	0.034	0.222	0.0918	0.014	0.222	0.0918
20%	80%	0.034	0.442	0.3036	0.014	0.182	0.0717	0.014	0.182	0.0717
10%	90%	0.034	0.442	0.2641	0.014	0.182	0.0531	0.014	0.182	0.0531
0%	100%	0.034	0.442	0.2317	0.014	0.182	0.0345	0.014	0.182	0.0345

Fig. 5.9 presents a comparison of $LOLP_{Sys}$ for various shares of PEV smart charging penetration, *vis-à-vis*, the contribution of DR participation. It is noted that without DR, the system reliability exceeds the level specified by the planner, with penetration of PEV charging loads, unless 100% smart charging is used. With DR = 5%, and A&P based uncontrolled charging, the share of smart charging need be at least 30% to ensure system LOLP below the desired level. With DR = 10%, $LOLP_{Sys}$ is always below the desired level, for any mix of uncontrolled and smart charging loads.

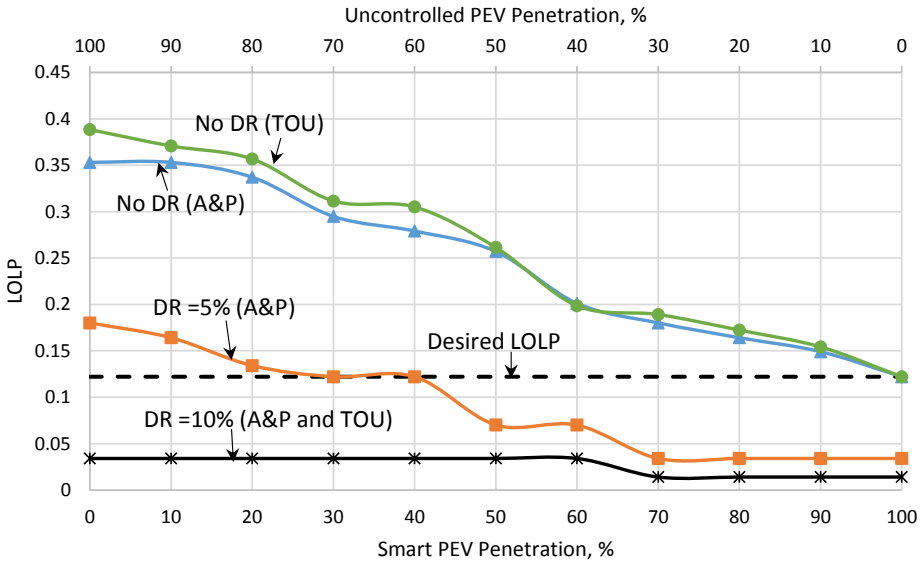

Figure 5.9. Comparison of system LOLP.

5.5.3 Effect of PEV on Components Criticality

All the minimal cut sets are identified for the peak hour (hour-18) with their corresponding $p(\bar{C}_h)$ and $LNSI_{\bar{C}_h}$ and grouped with associated component cm; 32 groups for generators and 38 groups for lines.

For each of these minimal cut sets associated with a cm, $p(\bar{C}_h)_{cm}$ and $LNSI_{\bar{C}_h,cm}$ are determined, and the criticality index for a cm, CR_{cm}, is calculated, as given in (5.13). The criticality index is determined for each component under study, for the base case, where there is no PEV charging load or DR; various shares of A&P based PEV charging and smart charging; and various shares of A&P based PEV charging with smart charging and DR option. The list of system components ranked by criticality index is presented in Table 5.4. Components with very low values of CR_{cm} are not mentioned in the ranking list. Generators G22 and G23 are found to be the most critical components in the system because of their reliability characteristics, capacities and locations.

In the Base Case, without PEVs or DR, there are 10 components listed with the criticality index in decreasing order; these are noted to be all generators. In the case of A&P

uncontrolled charging with smart charging, Line-11 also appears in the list of critical components for 100% or 50% uncontrolled charging; while the list with 100% smart charging is exactly same as the Base Case.

When DR is introduced in the presence of A&P uncontrolled and smart charging, the list of critical components is significantly curtailed, only a few components are now critical, their CR_{cm} values are much reduced, for all combinations of uncontrolled and smart charging as seen in Table 5.4.

Table 5.4:
Ranking of Components by their Criticality

	Base Case			A&P Based Charging + Smart Charging									A&P Based Charging + Smart Charging + DR								
	(No PEV, No DR)			0% + 100%			50% + 50%			100% + 0%			0% + 100% + 10%			50% + 50% + 10%			100% + 0% + 10%		
Rank	cm	f_{cm}	CR_{cm}	cm	f_{cm}	CR_{cm}	cm	f_{cm}	CR_{cm}	cm	f_{cm}	CR_{cm}	cm	f_{cm}	CR_{cm}	cm	f_{cm}	CR_{cm}	cm	f_{cm}	CR_{cm}
1	G22	10	0.08004	G22	10	0.08004	G22	27	0.15792	G22	1	0.301	G22	1	0.00331	G22	2	0.02014	G22	3	0.04077
2	G23	10	0.07931	G23	10	0.07931	G23	23	0.15658	G23	1	0.2987	G23	1	0.00331	G23	2	0.02	G23	3	0.04059
3	G32	6	0.04552	G32	6	0.04552	G32	17	0.09011	G32	1	0.1446				G32	2	0.00823	G32	3	0.02614
4	G12	3	0.00993	G12	3	0.00993	G12	3	0.02547	G12	7	0.16421				L11	1	0.00011	L11	4	0.00017
5	G13	3	0.00993	G13	3	0.00993	G13	3	0.02547	G13	7	0.16421									
6	G14	3	0.00993	G14	3	0.00993	G14	3	0.02547	G14	7	0.16421									
7	G20	2	0.00324	G20	2	0.00324	G20	3	0.01514	G21	4	0.05164									
8	G21	2	0.00321	G21	2	0.00321	G21	3	0.01512	G20	4	0.05137									
9	G30	2	0.00286	G30	2	0.00286	G30	3	0.01482	G30	4	0.05001									
10	G31	2	0.00286	G31	2	0.00286	G31	3	0.01482	G31	4	0.05001									
11							L11	4	0.00015	L11	8	0.00078									

5.6 Summary

This chapter has presented a reliability analysis framework for a composite power system considering PEV customer charging behavior in order to study the impact of PEVs on the grid. A Smart-OPF model was peoposed to compute the system minimal cut sets for a 24-hour load demand, and subsequently the daily system reliability indices were obtained. Different vehicle types, charging levels, penetration levels, and charging scenarios were examined. Results showed that PEVs charged in uncontrolled mode would negatively impact system reliability, while smart charging can significantly alleviate their impact. In addition, it was found that TOU electricity pricing had a severe impact on system reliability as compared to A&P based uncontrolled charging. Therefore, TOU price periods need be adjusted to mitigate the impact of PEV charging loads. A novel procedure to determine the critical components in composite power systems in the presence of PEV charging loads and DR was proposed. The method provided a ranking of components by their criticality, that would pertaining to system operations and planning.

Chapter 6

Conclusions, Contributions and Future Work

6.1 Summary

Reliability evaluation plays an important role in system analysis, design, upgrades, and operations, especially in composite power systems. This research presents a comprehensive framework for composite power systems to assess the reliability from uncertain events. The concept of minimal cut sets is applied to evaluate two sets of indices, at the system level and nodal level. System-wide indices can be utilized by both planners and operators to determine the likelihood of interruption of supply, while nodal indices provide useful information on the most important nodes during system disturbances. The challenge of using analytical methods in reliability evaluation of composite power systems is the large computational burden involved, to examine all the possible outage events. Once the component failure probability is calculated using the data of the failure and repair rates, the minimal cut set evaluation is implemented.

In Chapter 2, a brief background on some basic definitions, reliability measures and adequacy indices, and basic approaches to reliability evaluation of the power system, was

described. Thereafter, the description and applications of ERs, DR, and PEVs were presented, followed by a brief introduction to clustering techniques.

Chapter 3 presented novel clustering techniques based approaches to determine the optimal location, size and year of installation of ERs in composite power system. The K-means clustering and Fuzzy C-means clustering techniques were applied to the set of reliability indices, LNSIs, which were determined using nodal minimal cut sets. Once the optimal sizes and locations of ERs were obtained, the earliest year of penetration was determined using an adequacy check algorithm. Studies were carried out considering the 24-bus IEEE RTS.

In Chapter 4, a novel method to detect the critical components in a composite power system was presented, and the method was illustrated by application to the 6-bus RBTS and to the 24-bus IEEE RTS. Studies were carried out evaluating system reliability under steady state conditions, and assessing the operational risks in real-time system operations. The objective was to identify the critical components in order to help planners to make economic decisions on new investments in generation capacities and transmission lines upgrades, also to help operators maintain the delivery of electricity during system failure and disturbance events.

In Chapter 5, a novel framework to evaluate the impact of PEV charging loads on composite power system reliability was presented. A Smart-OPF model combined with a minimum cut set approach was proposed to evaluate the system reliability indices, examining various combinations of shares of uncontrolled and smart charging PEVs. DR was included in the proposed procedure and its impact on system reliability indices was studied. Finally, the procedure to determine the critical components of the power system in the presence of PEV loads and DR was proposed. Detailed studies considering the IEEE RTS, demonstrating the applicability of the proposed technique, were presented.

The main conclusions of the presented work are:

- The findings of *nodal minimal cut sets* provide a better understanding of the reliability of serving load at a specific bus, while *system minimal cut sets* provide useful

information for both planners and operators to determine the likelihood of interruption of supply.

- System/bus reliability does not change significantly with higher order minimal cut set beyond third order; however, the computational burden can be very high. Therefore, third order minimal cut sets are sufficient for this purpose of these studies.

- The choice of either the K-Means or Fuzzy C-Means clustering technique has little impact on the selection of ERs, and their optimal size, site and year of installation are very close to each other.

- The impact of the presence of ERs is observed in the formation of new combinations of minimal cut sets. Some of these new cut sets were previously of lower order, and have changed to a higher order cut set, and no longer leads to an interruption. These changes improve the system reliability, since, when the cut set order increases, its unavailability reduces.

- The selection of critical components depends on the nature of the problem, *i.g.*, whether it is a planning problem or an operational issue; the likelihood of failure can be different at the steady-state condition and in the operational stage, and can change the criticality of a component.

- It is viable to have DR as a practical option to dampen the adverse impact of the PEV charging loads on system reliability. Whereas for 10% DR, the system reliability is always below the desired level set by system planners, for any mix of uncontrolled and smart charging loads. With 5% DR, the share of smart charging need be at least 30% to ensure system reliability is below the desired level.

6.2 Research Contributions

The main contributions of the research presented in this thesis can be summarized as follows:

- A novel OPF based procedure was proposed to compute the nodal minimal cut sets for composite power systems, since these identify the subset of cut sets that were associated with the loss of load at a specific bus. Using the nodal minimal cut sets, the nodal LNSI indices were hence determined. This information is very useful to system planners and operators as it provides an insight into the reliability of serving the load at a specific location.

- For the first time, the K-means and the Fuzzy C-means clustering techniques were applied to identify critical reliability clusters in composite power systems. Hence, the sizing and siting of ERs that should be in place in the composite system, in the terminal year were determined. Furthermore, the impact of the choice of an appropriate clustering technique has been discussed. Two different OPF objectives were considered to examine how the solution of minimal cut sets and hence the optimal ER plan was impacted.

- A novel adequacy check algorithm was proposed, that was applied sequentially over the plan period, starting from the first year to determine the earliest year of penetration of ERs, to satisfy the system adequacy constraints and achieving a target reliability level over a long-term plan.

- A quantitative method, using system minimal cut sets that introduced a priority list of critical components in the power system, was developed. The critical components were ranked in order of the impact caused by their outage, to system reliability, for different combinations of outage scenarios under steady-state conditions and short-term operations. From these studies, useful information could be provided to the transmission system operator and system planner, for decision-making pertaining to operational planning, strategic maintenance planning and investment planning.

- A novel Smart-OPF model was developed to determine the minimal cut sets considering the uncontrolled and smart charging PEV loads. The uncontrolled PEV charging load profile at each system bus was obtained using a data analysis technique with real mobility data. Using these minimal cut sets, the composite system reliability in-

dices of the power system, in the presence of PEV loads, were determined for various degrees of smart charging penetration.

- The impact of DR on composite system adequacy by damping the peak load in the presence of PEV loads was considered for the first time by including it in the Smart-OPF.

- Determining the critical components in composite power systems in the presence of PEV charging loads and DR was proposed, providing a ranking list of components by their criticality, that would pertaining to system operations and planning.

6.3 Future Work

Based on the work presented in this thesis, future research may explore the following issues:

- The decision of new addition of ERs with regard to the choice of ER technology and their associated costs can be taken into account. The optimal sizing and siting of ERs based on nodal reliability can be extended to include the cost of investments. The model can also include the expected cost of interruption of customers over the planning horizon.

- A value based reliability planning model can be developed that takes into account the expected cost of interruption of various system components based on their criticality indices and cost of component upgrades, and hence integrate these information in a system planning environment to determine the most beneficial component upgrade and timing of installation. The objective of the value-based reliability planning model will be to create a balance between the cost of improving system reliability with the cost of system upgrades. Various other factors such as operation cost, loss cost, capital investment cost, components aging, outage duration, seasonal outage rates and types of customers can also be considered.

- The proposed reliability framework can be extended to incorporate reliability models for intermittent generators, in particular renewable-based ERs. In the present work only dispatchable ER units were considered to examine and assess the reliability of the power system following uncertain events. The power output from renewable ER is typically intermittent and uncertain and is highly dependent on external characteristics such as wind speed, solar radiation, *etc.*, at a particular site. In order to consider such ER units in reliability problem, it will be necessary to consider uncertainties in the proposed framework. This can be done by improving the present framework to include dependent outages, such as fluctuating weather and derated generator unit outages, in reliability calculations.

References

[1] G. J. Anders and A. Vaccaro, *Innovations in Power Systems Reliability*. New York, USA: Springer, 2011.

[2] D. Cheng, "Integrated system model reliability evaluation and prediction for electrical power systems: Graph trace analysis based solutions," Ph.D. dissertation, 2009.

[3] Plug'n Drive, "Electric Car Incentives." [Online]. Available: http://www.plugndrive.ca/

[4] Y. Liu and C. Singh, "Reliability evaluation of composite power systems using Markov cut-set method," *IEEE Transactions on Power Systems*, vol. 25, no. 2, pp. 777–785, 2010.

[5] A. Leite da Silva, A. Cassula, R. Billinton, and L. Manso, "Integrated reliability evaluation of generation, transmission and distribution systems," *IEE Proceedings-Generation, Transmission and Distribution*, vol. 149, no. 1, pp. 1–6, Jan 2002.

[6] Y. Feng, W. Wu, B. Zhang, and W. Li, "Power system operation risk assessment using credibility theory," *IEEE Transactions on Power Systems*, vol. 23, no. 3, pp. 1309–1318, 2008.

[7] W. Li, J. Zhou, K. Xie, and X. Xiong, "Power system risk assessment using a hybrid method of fuzzy set and monte carlo simulation," *IEEE Transactions on Power Systems*, vol. 23, no. 2, pp. 336–343, 2008.

[8] M. Bollen, L. Wallin, T. Ohnstad, and L. Bertling, "On operational risk assessment in transmission systems - weather impact and illustrative example," in *Proceedings of the 10th International Conference on Probabilistic Methods Applied to Power Systems, 2008. (PMAPS '08.)*, 2008, pp. 1–6.

[9] M. Kirthiga, S. Daniel, and S. Gurunathan, "A methodology for transforming an existing distribution network into a sustainable autonomous micro-grid," *IEEE Transactions on Sustainable Energy*, vol. 4, no. 1, pp. 31–41, Jan 2013.

[10] J. Mitra, M. Vallem, and S. Patra, "A probabilistic search method for optimal resource deployment in a microgrid," in *International Conference on Probabilistic Methods Applied to Power Systems, 2006. (PMAPS '06.)*, June 2006, pp. 1–6.

[11] A. Leite da Silva, L. Nascimento, M. da Rosa, D. Issicaba, and J. Peas Lopes, "Distributed energy resources impact on distribution system reliability under load transfer restrictions," *IEEE Transactions on Smart Grid*, vol. 3, no. 4, pp. 2048–2055, Dec 2012.

[12] A. Kwasinski, V. Krishnamurthy, J. Song, and R. Sharma, "Availability evaluation of micro-grids for resistant power supply during natural disasters," *IEEE Transactions on Smart Grid*, vol. 3, no. 4, pp. 2007–2018, Dec 2012.

[13] R. Billinton and R. Karki, "Maintaining supply reliability of small isolated power systems using renewable energy," *IEE Proceedings- Generation, Transmission and Distribution*, vol. 148, no. 6, pp. 530–534, Nov 2001.

[14] A. Leite da Silva, L. Manso, W. Sales, S. Flavio, G. Anders, and L. de Resende, "Chronological power flow for planning transmission systems considering intermittent sources," *IEEE Transactions on Power Systems*, vol. 27, no. 4, pp. 2314–2322, Nov 2012.

[15] H. Hedayati, S. Nabaviniaki, and A. Akbarimajd, "A method for placement of dg units in distribution networks," *IEEE Transactions on Power Delivery*, vol. 23, no. 3, pp. 1620–1628, July 2008.

[16] W. Muneer, K. Bhattacharya, and C. Canizares, "Large-scale solar pv investment models, tools, and analysis: The ontario case," *IEEE Transactions on Power Systems*, vol. 26, Nov 2011.

[17] I. Das, K. Bhattacharya, and C. Canizares, "Optimal incentive design for targeted penetration of renewable energy sources," *IEEE Transactions on Sustainable Energy*, vol. 5, no. 4, pp. 1213–1225, Oct 2014.

[18] P. Jirutitijaroen and C. Singh, "Reliability constrained multi-area adequacy planning using stochastic programming with sample-average approximations," *IEEE Transactions on Power Systems*, vol. 23, no. 2, pp. 504–513, May 2008.

[19] E. Preston, W. Grady, and M. Baughman, "A new planning model for assessing the effects of transmission capacity constraints on the reliability of generation supply for large nonequivalenced electric networks," *IEEE Transactions on Power Systems*, vol. 12, no. 3, pp. 1367–1373, Aug 1997.

[20] J. Aghaei, N. Amjady, A. Baharvandi, and M.-A. Akbari, "Generation and transmission expansion planning: Milp-based probabilistic model," *IEEE Transactions on Power Systems*, vol. 29, no. 4, pp. 1592–1601, 2014.

[21] A. Mehrtash, P. Wang, and L. Goel, "Reliability evaluation of restructured power systems using a novel optimal power-flow-based approach," *IET Generation, Transmission Distribution*, vol. 7, no. 2, pp. 192–199, Feb 2013.

[22] P. Jirutitijaroen and C. Singh, "Comparative study of system-wide reliability-constrained generation expansion problem," in *Third International Conference on Electric Utility Deregulation and Restructuring and Power Technologies, 2008. DRPT 2008.*, April 2008, pp. 675–678.

[23] R. Billinton and R. N. Allan, *Reliability Evaluation of Power Systems*. New York, USA: Plenum Press, 1996.

[24] R. Karki, P. Hu, and R. Billinton, "A simplified wind power generation model for reliability evaluation," *IEEE Transactions on Energy Conversion*, vol. 21, no. 2, pp. 533–540, June 2006.

[25] Z. W. Birnbaum, *On the Importance of Different Components in a Multicomponent System. In P. R. Krishnaiah (Editor), Multivariate Analysis-II,.* New York, USA: Academic Press, 1969.

[26] P. Hilber and L. Bertling, "Monetary importance of component reliability in electrical networks for maintenance optimization," in *International Conference on Probabilistic Methods Applied to Power Systems, 2004. (PMAPS '04.)*, Sept 2004, pp. 150–155.

[27] ——, "Component reliability importance indices for electrical networks," in *IEEE Intl. Power Engineering Conference, 2007 (IPEC 2007)*, Dec 2007, pp. 257–263.

[28] J. Setreus, P. Hilber, S. Arnborg, and N. Taylor, "Identifying critical components for transmission system reliability," *IEEE Transactions on Power Systems*, vol. 27, no. 4, pp. 2106–2115, Nov 2012.

[29] J. F. Espiritu, D. W. Coit, and U. Prakash, "Component criticality importance measures for the power industry," *Electric Power Systems Research*, vol. 77, no. 56, pp. 407 – 420, 2007. [Online]. Available: //www.sciencedirect.com/science/article/pii/S037877960600099X

[30] F. Pourahmadi, M. Fotuhi-Firuzabad, and P. Dehghanian, "Identification of critical components in power systems: A game theory application," in *2016 IEEE Industry Applications Society Annual Meeting*, Oct 2016, pp. 1–6.

[31] G. Vancells, S. Herraiz, J. Meléndez, and A. Ferreira, "Analysis of importance of components in power systems using time sequential simulation," in *International Conference on Renewable Energies and Power Quality*, 2013.

[32] J. Tan and L. Wang, "Adequacy assessment of power distribution network with large fleets of PHEVs considering condition-dependent transformer faults," *IEEE Transactions on Smart Grid*, vol. PP, no. 99, pp. 1–1, 2016.

[33] A. Dubey and S. Santoso, "Electric vehicle charging on residential distribution systems: Impacts and mitigations," *IEEE Access*, vol. 3, pp. 1871–1893, 2015.

[34] Z. Liu, D. Wang, H. Jia, N. Djilali, and W. Zhang, "Aggregation and bidirectional charging power control of plug-in hybrid electric vehicles: Generation system adequacy analysis," *IEEE Transactions on Sustainable Energy*, vol. 6, no. 2, pp. 325–335, April 2015.

[35] K. Hou, X. Xu, H. Jia, X. Yu, T. Jiang, B. Shu, and K. Zhang, "A reliability assessment approach for integrated transportation and electrical power systems incorporating electric vehicles," *IEEE Transactions on Smart Grid*, vol. PP, no. 99, pp. 1–1, 2016.

[36] C. Liu, J. Wang, A. Botterud, Y. Zhou, and A. Vyas, "Assessment of impacts of phev charging patterns on wind-thermal scheduling by stochastic unit commitment," *IEEE Transactions on Smart Grid*, vol. 3, no. 2, pp. 675–683, June 2012.

[37] L. Cheng, Y. Chang, J. Lin, and C. Singh, "Power system reliability assessment with electric vehicle integration using battery exchange mode," *IEEE Transactions on Sustainable Energy*, vol. 4, no. 4, pp. 1034–1042, Oct 2013.

[38] U.S. Department of Transportation, Federal Highway Administration. (2015) National Household Travel Survey 2009. [Online]. Available: http://nhts.ornl.gov

[39] G. Allen and W. Setiawan, "Draft assessment of the real-world impacts of commingling california phase 3 reformulated gasoline," *California Environmental Protection Agency*, 2002.

[40] R. Green, L. Wang, M. Alam, and S. Depuru, "Evaluating the impact of plug-in hybrid electric vehicles on composite power system reliability," in *2011 North American Power Symposium (NAPS)*, Aug 2011, pp. 1–7.

[41] D. Boi and M. Panto, "Impact of electric-drive vehicles on power system reliability," *Energy*, vol. 83, pp. 511 – 520, 2015. [Online]. Available: http://www.sciencedirect.com/science/article/pii/S0360544215002108

[42] R. Billinton and R. N. Allan, *Reliability Evaluation of Engineering Systems: Concepts and Techniques*. Plenum Press, 1992.

[43] North American Electric Reliability Corporation (NERC), "Reliability assessment guidebook." [Online]. Available: http://www.nerc.com/comm/PC/Reliability%20Assessment%20Subcommittee%20RAS%20DL/Reliability%20Assessment%20Guidebook/Reliability%20Assessment%20Guidebook%203%201%20Final.pdf

[44] R. Billinton, R. N. Allan, and L. Salvaderi, "Applied reliability assessment in electric power systems," 1991.

[45] R. Billinton and R. N. Allan, "Power-system reliability in perspective," *Electronics & Power*, vol. 30, no. 3, pp. 231–236, 1984.

[46] C. Singh, "Markov cut-set approach for the reliability evaluation of transmission and distribution systems," *IEEE Transactions on Power Apparatus and Systems*, vol. PAS-100, no. 6, pp. 2719–2725, 1981.

[47] J. MacQueen *et al.*, "Some methods for classification and analysis of multivariate observations," in *Proceedings of the fifth Berkeley symposium on mathematical statistics and probability*, vol. 1, no. 14. California, USA, 1967, pp. 281–297.

[48] L. Anstine, R. Burke, J. Casey, R. Holgate, R. John, and H. Stewart, "Application of probability methods to the determination of spinning reserve requirements for the pennsylvania-new jersey-maryland interconnection," *IEEE Transactions on Power Apparatus and Systems*, vol. 82, no. 68, pp. 726–735, Oct 1963.

[49] APM Bulk Power Indices Task Force, "Bulk power system reliability criteria and indices-trends and future needs," *IEEE Transactions on Power Systems*, vol. 9, no. 1, pp. 181–190, Feb 1994.

[50] C. Singh and R. Billinton, *System Reliability Modeling and Evaluation*. London, UK: Hutchinson Educational, 1997.

[51] D. Gaver, F. E. Montmeat, and A. Patton, "Power system reliability I-measures of reliability and methods of calculation," *IEEE Transactions on Power Apparatus and Systems*, vol. 83, no. 7, pp. 727–737, July 1964.

[52] Z. G. Todd, "A probability method for transmission and distribution outage calculations," *IEEE Transactions on Power Apparatus and Systems*, vol. 83, no. 7, pp. 695–701, July 1964.

[53] Federal Energy Management Program, "Using distributed energy resources: A how-to guide for federal facility managers." [Online]. Available: http://www.nrel.gov/docs/fy02osti/31570.pdf

[54] P. McLean-Conner, *Energy Efficiency - Principles and Practices*. PennWell Books, Oklahoma, USA, 2009.

[55] I. D. de Cerio Mendaza, I. G. Szczesny, J. R. Pillai, and B. Bak-Jensen, "Demand response control in low voltage grids for technical and commercial aggregation services," *IEEE Transactions on Smart Grid*, vol. 7, no. 6, pp. 2771–2780, Nov 2016.

[56] R. Yu, W. Zhong, S. Xie, C. Yuen, S. Gjessing, and Y. Zhang, "Balancing power demand through EV mobility in vehicle-to-grid mobile energy networks," *IEEE Transactions on Industrial Informatics*, vol. 12, no. 1, pp. 79–90, Feb 2016.

[57] Ontario Ministry of Transportation, "Electric Vehicles." [Online]. Available: http://www.mto.gov.on.ca

[58] U. Department of Energy, "Vehicle Technologies Program." [Online]. Available: http://www.afdc.energy.gov/pdfs/52723.pdf

[59] R. Garcia-Valle and J. A. P. Lopes, *Electric vehicle integration into modern power networks*. Springer Science & Business Media New York, 2013.

[60] P. Steinbach, M. Tan and V. Kumar, *Introduction To Data Mining*. New Jersey, USA: Pearson Education, 2005.

[61] H.-T. Yang, S. C. Chen, and P. C. Peng, "Genetic K-means-algorithm-based classification of direct load-control curves," *IEE Proceedings- Generation, Transmission and Distribution*, vol. 152, no. 4, pp. 489–495, July 2005.

[62] V. Figueiredo, F. Rodrigues, Z. Vale, and J. Gouveia, "An electric energy consumer characterization framework based on data mining techniques," *IEEE Transactions on Power Systems*, vol. 20, no. 2, pp. 596–602, May 2005.

[63] W. Li, J. Zhou, X. Xiong, and J. Lu, "A statistic-fuzzy technique for clustering load curves," *IEEE Transactions on Power Systems*, vol. 22, no. 2, pp. 890–891, May 2007.

[64] A. Nizar, Z. Dong, and Y. Wang, "Power utility nontechnical loss analysis with extreme learning machine method," *IEEE Transactions on Power Systems*, vol. 23, no. 3, pp. 946–955, Aug 2008.

[65] S. Verdu, M. Garcia, C. Senabre, A. Marin, and F. Franco, "Classification, filtering, and identification of electrical customer load patterns through the use of self-organizing maps," *IEEE Transactions on Power Systems*, vol. 21, no. 4, pp. 1672–1682, Nov 2006.

[66] T. Zhang, G. Zhang, J. Lu, X. Feng, and W. Yang, "A new index and classification approach for load pattern analysis of large electricity customers," *IEEE Transactions on Power Systems*, vol. 27, no. 1, pp. 153–160, Feb 2012.

[67] G. Chicco, O.-M. Ionel, and R. Porumb, "Electrical load pattern grouping based on centroid model with ant colony clustering," *IEEE Transactions on Power Systems*, vol. 28, no. 2, pp. 1706–1715, May 2013.

[68] J. C. Dunn, "A fuzzy relative of the isodata process and its use in detecting compact well-separated clusters," 1973.

[69] F. Höppner, *Fuzzy cluster analysis: methods for classification, data analysis and image recognition.* John Wiley & Sons, 1999.

[70] J. C. Bezdek, *Pattern recognition with fuzzy objective function algorithms.* Springer Science & Business Media, 2013.

[71] K. Honda, H. Ichihashi, and S. Miyamoto, *Algorithms for Fuzzy Clustering Methods in C-Means Clustering with Applications*. Springer-Verlag, Berlin Heidelberg, 2008.

[72] M. Xu, S. Luo, and J. S. Jin, "Affective content detection by using timing features and fuzzy clustering," in *Advances in Multimedia Information Processing-PCM 2008*. Springer, 2008, pp. 685–692.

[73] RTS Task Force on Application of Probability Methods, "IEEE Reliability Test System," *IEEE Transactions on Power Apparatus and Systems*, vol. PAS-98, Nov 1979.

[74] G. D. Corporation, "General Algebraic Modeling System (GAMS), software." [Online]. Available: http://www.gams.com.

[75] M. Milligan and K. Porter, "The capacity value of wind in the united states: Methods and implementation," *The Electricity Journal*, vol. 19, no. 2, pp. 91–99, 2006.

[76] M. Matteucci. "A Tutorial on Clustering Algorithms." URL http://home.deib.polimi.it/matteucc/Clustering/tutorial_html/kmeans.

[77] B. Mirkin, *Clustering: A Data Recovery Approach*. CRC Press, 2012.

[78] J. Kent, J. Bibby, and K. Mardia, *Multivariate Analysis (Probability and Mathematical Statistics)*. Elsevier Amsterdam, 2006.

[79] F. Kovács, C. Legány, and A. Babos, "Cluster validity measurement techniques," in *6th International symposium of hungarian researchers on computational intelligence*. Citeseer, 2005.

[80] R. Billinton, S. Kumar, N. Chowdhury, K. Chu, K. Debnath, L. Goel, E. Khan, P. Kos, G. Nourbakhsh, and J. Oteng-Adjei, "A reliability test system for educational purposes-basic data," *IEEE Transactions on Power Systems*, vol. 4, no. 3, pp. 1238–1244, Aug 1989.

[81] L. A. Tuan and K. Bhattacharya, "Competitive framework for procurement of interruptible load services," *IEEE Transactions on Power Systems*, vol. 18, no. 2, pp. 889–897, May 2003.

[82] B. Lami and K. Bhattacharya, "Clustering technique applied to nodal reliability indices for optimal planning of energy resources," *IEEE Transactions on Power Systems*, vol. 31, no. 6, pp. 4679–4690, Nov 2016.

[83] U.S. Department of Energy. (2015) U.S. PEV sales by model. [Online]. Available: http://www.afdc.energy.gov/data/

[84] M. S. ElNozahy and M. M. A. Salama, "A comprehensive study of the impacts of PHEVs on residential distribution networks," *IEEE Transactions on Sustainable Energy*, vol. 5, no. 1, pp. 332–342, 2014.

[85] J. de Hoog, T. Alpcan, M. Brazil, D. A. Thomas, and I. Mareels, "Optimal charging of electric vehicles taking distribution network constraints into account," *IEEE Transactions on Power Systems*, vol. 30, no. 1, pp. 365–375, Jan 2015.

[86] M. Ansari, A. T. Al-Awami, M. A. Abido, and E. Sortomme, "Optimal charging strategies for unidirectional vehicle-to-grid using fuzzy uncertainties," in *2014 IEEE PES T D Conference and Exposition*, April 2014, pp. 1–5.

[87] J. Axsen, H. J. Bailey, and G. Kamiya, "The Canadian plug-in electric vehicle survey (CPEVS 2013): Anticipating purchase, use, and grid interactions in British Columbia," 2013.

[88] I. Sharma, C. Canizares, and K. Bhattacharya, "Smart charging of PEVs penetrating into residential distribution systems," *IEEE Trans. Smart Grid*, vol. 5, no. 3, pp. 1196–1209, May 2014.

[89] M. ElNozahy and M. Salama, "Studying the feasibility of charging plug-in hybrid electric vehicles using photovoltaic electricity in residential distribution systems," *Electric Power Systems Research*, vol. 110, pp. 133–143, 2014.

Appendices

Appendix A

IEEE Reliability Test System Data

Table A1:
Generating Unit Location and Capability [73]

Generator Number	Bus	PGmax MW	Qmax MVAr	Qmin MVAr
1	1	20	10	0
2	1	20	10	0
3	1	76	30	25
4	1	76	30	25
5	2	20	10	0
6	2	20	10	0
7	2	76	30	25
8	2	76	30	25
9	7	100	60	0
10	7	100	60	0
11	7	100	60	0
12	13	197	80	0
13	13	197	80	0
14	13	197	80	0
15	15	12	6	0
16	15	12	6	0
17	15	12	6	0
18	15	12	6	0
19	15	12	6	0
20	15	155	80	50
21	16	155	80	50
22	18	400	200	50
23	21	400	200	50
24	22	50	16	10
25	22	50	16	10
26	22	50	16	10
27	22	50	16	10
28	22	50	16	10
29	22	50	16	10
30	23	155	80	50
31	23	155	80	50
32	23	350	150	25

Table A2:
Voltage Correction Devices [73]

Device	Bus	MVAr Capability
Synchronous Condenser	14	50 Reactive 200 Capacitive
Reactor	6	100 Reactive

Table A3:
Generator Reliability Data [73]

Unit Size (MW)	Unit Type	MTTF (Hour)	MTTR (Hour)	Forced Outage Rate
12	Oil/Steam	2940	60	0.02
20	Oil/CT	450	50	0.1
50	Hydro	1980	20	0.01
76	Coal/Steam	1960	40	0.02
100	Oil/Steam	1200	50	0.04
155	Coal/Steam	960	40	0.04
197	Oil/Steam	950	50	0.05
350	Coal/Steam	1150	100	0.08
400	Nuclear	1100	150	0.12

** MTTF = mean time to failure = λ^{-1}
MTTR = mean time to repair = μ^{-1}
Forced Outage Rate = MTTR / (MTTF + MTTR)

Table A4:
Bus Load Data [73]

Bus Number	Load	
	MW	MVAr
1	108	22
2	97	20
3	180	37
4	74	15
5	71	14
6	136	28
7	125	25
8	171	35
9	175	36
10	195	40
13	265	54
14	194	39
15	317	64
16	100	20
18	333	68
19	181	37
20	128	26
Total	2850	580

Table A5:
Hourly Peak Load in Percent of Daily Peak [73]

	Winter Weeks 1-8 & 44-52		Summer Weeks 18-30		Spring/Fall Weeks 9-17 & 31-43	
Hour	Weekday	Weekend	Weekday	Weekend	Weekday	Weekend
12-1am	67	78	64	74	63	75
1-2	63	72	60	70	62	73
2-3	60	68	58	66	60	69
3-4	59	66	56	65	58	66
4-5	59	64	56	64	59	65
5-6	60	65	58	62	65	65
6-7	74	66	64	62	72	68
7-8	86	70	76	66	85	74
8-9	95	80	87	81	95	83
9-10	96	88	95	86	99	89
10-11	96	90	99	91	100	92
11-Noon	95	91	100	93	99	94
Noon-1pm	95	90	99	93	93	91
1-2	95	88	100	92	92	90
2-3	93	87	100	91	90	90
3-4	94	87	97	91	88	86
4-5	99	91	96	92	90	85
5-6	100	100	96	94	92	88
6-7	100	99	93	95	96	92
7-8	96	97	92	95	98	100
8-9	91	94	92	100	96	97
9-10	83	92	93	93	90	95
10-11	73	87	87	88	80	90
11-12	63	81	72	80	70	85

Table A6:
Transmission Line Length, Reliability, Impedance, and Rating Data [73]

Line Number	From Bus	To Bus	Length (mile)	λ (1/yr)	MTTR (hours)	Impedance P.U. /100 MVA Base R	X	B	Normal Rating (MVA)
1	1	2	3	0.24	16	0.003	0.014	0.461	175
2	1	3	55	0.51	10	0.055	0.211	0.057	175
3	1	5	22	0.33	10	0.022	0.085	0.023	175
4	2	4	33	0.39	10	0.033	0.127	0.034	175
5	2	6	50	0.48	10	0.05	0.192	0.052	175
6	3	9	31	0.38	10	0.031	0.119	0.032	175
7	3	24	0	0.02	768	0.002	0.084	0	400
8	4	9	27	0.36	10	0.027	0.104	0.028	175
9	5	10	23	0.34	10	0.023	0.088	0.024	175
10	6	10	16	0.33	35	0.014	0.061	2.459	175
11	7	8	16	0.3	10	0.016	0.061	0.017	175
12	8	9	43	0.44	10	0.042	0.161	0.044	175
13	8	10	43	0.44	10	0.043	0.165	0.045	175
14	9	11	0	0.02	768	0.043	0.165	0.045	175
15	9	12	0	0.02	768	0.002	0.084	0	400
16	10	11	0	0.02	768	0.002	0.084	0	400
17	10	12	0	0.02	768	0.002	0.084	0	400
18	11	13	33	0.4	11	0.006	0.048	0.1	500
19	11	14	29	0.39	11	0.005	0.042	0.088	500
20	12	13	33	0.4	11	0.006	0.048	0.1	500
21	12	23	67	0.52	11	0.012	0.097	0.203	500
22	13	23	60	0.49	11	0.011	0.087	0.182	500
23	14	16	27	0.38	11	0.005	0.059	0.082	500
24	15	16	12	0.33	11	0.002	0.017	0.036	500
25	15	21	34	0.41	11	0.006	0.049	0.103	500
26	15	21	34	0.41	11	0.006	0.049	0.103	500
27	15	24	36	0.41	11	0.007	0.052	0.109	500
28	16	17	18	0.35	11	0.003	0.026	0.055	500
29	16	19	16	0.34	11	0.003	0.023	0.049	500
30	17	18	10	0.32	11	0.002	0.014	0.03	500
31	17	22	73	0.54	11	0.014	0.105	0.221	500
32	18	21	18	0.35	11	0.003	0.026	0.055	500
33	18	21	18	0.35	11	0.003	0.026	0.055	500
34	19	20	27.5	0.38	11	0.005	0.04	0.083	500
35	19	20	27.5	0.38	11	0.005	0.04	0.083	500
36	20	23	15	0.34	11	0.003	0.022	0.046	500
37	20	23	15	0.34	11	0.003	0.022	0.046	500
38	21	22	47	0.45	11	0.009	0.068	0.142	500

Appendix B

Roy Billinton Test System Data

Table B1:
Generating Unit Location, Capability and Type [80]

Generator Number	Bus	PGmax MW	Qmax MVAr	Qmin MVAr	Type
1	1	40	17	-15	Thermal
2	1	40	17	-15	Thermal
3	1	10	7	0	Thermal
4	1	20	12	-7	Thermal
5	2	5	5	0	Hydro
6	2	5	5	0	Hydro
7	2	40	17	-15	Hydro
8	2	20	12	-7	Hydro
9	2	20	12	-7	Hydro
10	2	20	12	-7	Hydro
11	2	20	12	-7	Hydro

Table B2:
Generating Unit Reliability Data [80]

Unit Size (MW)	Unit Type	No. of Units	MTTF (Hour)	MTTR (Hour)	Forced Outage Rate
5	Hydro	2	4380	45	0.01
10	Theraml	1	2190	45	0.02
20	Hydro	4	3650	55	0.015
20	Theraml	1	1752	45	0.025
40	Hydro	1	2920	60	0.02
40	Theraml	2	1460	45	0.03

Table B3:
Bus Load Data [80]

Bus Number	Load MW
1	0
2	20
3	85
4	40
5	20
6	20
Total	185

**Unity power factor is assumed. At 0.98 power factor, the reactive load Mvar requirements at each bus is 20% of the corresponding MW load.

Table B4:
Transmission Line Length, Reliability, Impedance, and Rating Data [80]

Line Number	From Bus	To Bus	Length (KM)	λ (per year)	MTTR (hours)	Impedance P.U. /100 MVA Base			Current Rating (p.u.)
						R	X	B/2	
1	1	3	75	1.5	10	0.0342	0.18	0.0106	0.85
2	2	4	250	5	10	0.114	0.6	0.0352	0.71
3	1	2	200	4	10	0.0912	0.48	0.0282	0.71
4	3	4	50	1	10	0.0228	0.12	0.0071	0.71
5	3	5	50	1	10	0.0228	0.12	0.0071	0.71
6	1	3	75	1.5	10	0.0342	0.18	0.0106	0.85
7	2	4	250	5	10	0.114	0.6	0.0352	0.71
8	4	5	50	1	10	0.0228	0.12	0.0071	0.71
9	5	6	50	1	10	0.0228	0.12	0.0071	0.71

**100 MVA base
230 kV base